

Atmospheric Oxidation of Selected Alcohols and Esters

Thesis submitted to the Faculty of Chemistry
The Bergische Universität – Gesamthochschule Wuppertal
for the Degree of Doctor of Science
(Dr. rer. nat.)

by
Fabrizia Cavalli

December 2000

The work described in this thesis was carried out in the Department of Physical Chemistry, the Bergische Universität – Gesamthochschule Wuppertal, under the scientific supervision of Prof. Dr. K. H. Becker, during the period of September, 1997 – December, 2000.

Referee: Prof. Dr. K. H. Becker

Co-referee: Prof. Dr. E. H. Fink

ai miei genitori

I would like to express my sincere thanks to Prof. Dr. K. H. Becker for the opportunity of doing this Ph.D. in his research group and for the supervision of this work.

I thank Prof. Dr. E. H. Fink for agreeing to co-referee the thesis and his many useful comments.

My thanks are also due to Dr. I. Barnes who not only helped me to understand at least a part of the vast domain of the atmospheric chemistry but also followed with particular care my scientific work and gave me every encouragement at all times.

I wish to thank all my colleagues and the technical staff of this group; especially, Dr. T. Maurer must be singled out for a particular mention for the helpful discussions and for the suggestions and comments on several aspects of this work.

Finally, I gratefully acknowledge the European Commission for funding, in part, my research within the framework of the Environmental and Climate Programme by a Marie Curie Research Training Grant.

Abstract

Alcohols and esters are oxygenated volatile organic compounds of commercial interest as potential replacements for traditional solvents and fuel additives; their increased use will lead to an increased release into the atmosphere where these compounds will contribute to the formation of photochemical air pollution. Consequently, detailed knowledge of their chemical behaviour in the atmosphere is required to assess possible implications of their widespread application.

Relative rate coefficients were measured for the gas-phase reactions of hydroxyl radicals and chlorine atoms with selected alcohols, esters and carbonyl oxidation products. At room temperature and atmospheric pressure, the following rate coefficients (in $\text{cm}^3 \text{molecule}^{-1} \text{s}^{-1}$) were obtained:

	k_{OH}	k_{Cl}
1-butanol	$(8.28 \pm 0.85) \cdot 10^{-12}$	–
1-pentanol	$(1.11 \pm 0.11) \cdot 10^{-11}$	–
methyl propionate	$(9.29 \pm 1.13) \cdot 10^{-13}$	$(1.51 \pm 0.22) \cdot 10^{-11}$
dimethyl succinate	$(1.95 \pm 0.27) \cdot 10^{-12}$	$(6.79 \pm 0.93) \cdot 10^{-12}$
dimethyl glutarate	$(2.18 \pm 0.30) \cdot 10^{-12}$	$(1.90 \pm 0.33) \cdot 10^{-11}$
dimethyl adipate	$(3.73 \pm 0.59) \cdot 10^{-12}$	$(6.08 \pm 0.86) \cdot 10^{-11}$
propionic formic	–	$(2.89 \pm 0.35) \cdot 10^{-12}$
propionic acid	–	$(4.72 \pm 0.62) \cdot 10^{-12}$
methyl pyruvate	–	$(4.99 \pm 0.96) \cdot 10^{-13}$

Product investigations were performed on the gas-phase oxidation of the two alcohols, 1-butanol and 1-pentanol, in the large-volume outdoor photoreactor *EUPHORE* in Valencia, Spain, with analyses by *in situ* Fourier transform infrared (FTIR) absorption spectroscopy, gas chromatography with photo-ionisation detection (GC-PID) and with high performance liquid chromatography (HPLC). The OH initiated oxidation of 1-butanol in 1 bar of synthetic air in the presence of nitrogen monoxide led to the formation of butanal, propanal, ethanal, formaldehyde and 4-hydroxy-2-butanone with molar yields of 0.518 ± 0.071 , 0.234 ± 0.035 , 0.127 ± 0.022 , 0.434 ± 0.024 and 0.050 ± 0.010 , respectively. The OH initiated oxidation of 1-pentanol in 1 bar of synthetic air in the presence of nitrogen monoxide led to the formation of pentanal, butanal, propanal, ethanal and formaldehyde with molar yields of 0.405 ± 0.082 ,

0.161 ± 0.037, 0.081 ± 0.019, 0.181 ± 0.042 and 0.251 ± 0.013, respectively. Further, the results support the possible formation of 5-hydroxy-2-pentanone, and residual IR absorptions indicated the possible presence of compounds such as 3-hydroxy-propanal as product of the reaction system.

Cl atom initiated product studies were performed, in the presence of NO_x, on methyl propionate and dimethyl succinate in a laboratory reaction vessel in Wuppertal, using FTIR analyses; this approach was necessary to conveniently emulate the OH radical chemistry since these compounds react very slowly with OH radicals. The products formed in the Cl atom initiated oxidation of methyl propionate and their molar yields were: propionic formic anhydride 0.099 ± 0.019; propionic acid 0.139 ± 0.027; carbon monoxide 0.132 ± 0.026; methyl pyruvate 0.289 ± 0.057; ethanal 0.077 ± 0.015; methoxy formyl peroxy nitrate 0.083 ± 0.016; methyl glyoxylate 0.111 ± 0.022. The products formed in the Cl atom initiated oxidation of dimethyl succinate and their molar yields were: succinic formic anhydride 0.341 ± 0.068; *mono*-methyl succinate 0.447 ± 0.111; carbon monoxide 0.307 ± 0.061; dimethyl oxaloacetate 0.176 ± 0.044; and methoxy formyl peroxy nitrate 0.032-0.084.

The product studies allowed the construction of detailed photooxidation mechanisms for the selected oxygenated compounds required for atmospheric modelling.

Contents

1	INTRODUCTION.....	1
1.1	Oxygenated volatile organic compounds.....	1
1.2	State of the art.....	4
1.3	Compounds investigated.....	6
1.4	Aim of the work.....	7
2	EXPERIMENTAL.....	9
2.1	Reaction chambers.....	9
2.1.1	Description of 405 <i>l</i> reactor.....	9
2.1.2	Description of 480 <i>l</i> reactor.....	10
2.1.3	Description of the European photoreactor <i>EUPHORE</i>	11
2.2	Procedure and analysis at the Wuppertal laboratory.....	13
2.2.1	General.....	13
2.2.2	Relative rate method.....	14
2.2.3	Product analysis.....	16
2.3	<i>EUPHORE</i> -experiments.....	18
3	KINETIC STUDY.....	23
3.1	Hydroxyl radical reaction rate coefficients.....	23
3.1.1	Results.....	23
3.1.2	Discussion.....	25
3.2	Chlorine atom reaction rate coefficients.....	31
3.2.1	Results.....	31
3.2.2	Discussion.....	33
4	ATMOSPHERIC OXIDATION OF ALCOHOLS.....	35
4.1	General mechanistic considerations on the degradation of primary alcohols.....	35
4.2	Atmospheric degradation of 1-pentanol.....	39
4.2.1	Results.....	39
4.2.2	Discussion: mechanistic considerations based on <i>SAR</i> and the product yield data.....	43
4.3	Atmospheric degradation of 1-butanol.....	51
4.3.1	Results.....	51
4.3.2	Discussion: mechanistic considerations based on <i>SAR</i> and the product yield data.....	54

5	ATMOSPHERIC OXIDATION OF ESTERS	59
5.1	General mechanistic considerations on the degradation of esters	59
5.2	Atmospheric degradation of methyl propionate.....	63
5.2.1	Results.....	63
5.2.2	Discussion	67
5.3	Atmospheric degradation of dimethyl succinate.....	73
5.3.1	Results.....	73
5.3.2	Discussion	76
6	FUNCTIONAL GROUP REACTIVITY	81
6.1	Alcohol.....	81
6.2	Ester.....	85
7	ATMOSPHERIC IMPLICATIONS	89
8	SUMMARY	95
	ANNEX A ABBREVIATIONS.....	99
	ANNEX B EXPERIMENTAL PARAMETERS.....	101
	ANNEX C ABSORPTION CROSS SECTIONS.....	107
	ANNEX D SYNTHESSES.....	111
	ANNEX E CHEMICALS and GASES	117
	BIBLIOGRAPHY	119

Chapter 1

Introduction

1.1 Oxygenated volatile organic compounds

Tropospheric air pollution has a long and storied history. From at least the 13th century up to the mid-20th century, documented air pollution problems were primarily associated with high concentrations of sulphur dioxide and soot particles. These problems are often dubbed “London smog” because of a severe episode in that city in 1952. However, with the discovery of photochemical air pollution in the Los Angeles area in the mid-1940s, increasing concentrations of ozone and other photochemical oxidants and their associated impacts on human health, plant growth and materials have become a major issue world-wide [1, 2, 3]. Ozone exposures can induce alterations in the mechanical function of the lungs and structural injuries of bronchial tissue resulting in acute and chronic respiratory diseases [2]. Ozone can also enter plant leaves and react with important chemical moieties of the vegetable cells inhibiting photosynthetic activity and allocation and translocation of sucrose from shoots to the roots. Because of these biochemical and physiological effects, it can reduce biomass and the yield of vegetation and cause visible injuries [3].

The term “photochemical” air pollution reflects the essential role of solar radiation in driving atmospheric chemistry: at the Earth’s surface, radiation of 290 nm and greater induces a complex chemistry involving volatile organic compounds (VOC) and nitric oxide ($\text{NO}_x = \text{NO} + \text{NO}_2$) which leads to the formation of ozone and a variety of additional oxidising species, for example peroxy acetyl nitrate, referred to as photochemical oxidants [4, 5]. With respect to the European scale, road transport and solvent use are by far the most important source categories of anthropogenic nonmethane VOC (NMVOC) emissions [6]. Fossil fuel combustion, mainly road transport, and biomass burning represent the major emission sources of anthropogenic NO_x [6]. It is obvious that the overall emissions of these substances are not distributed evenly over Europe and show different trends. In Germany, for example, while the NMVOC emissions from road traffic have been considerably reduced over the last ten years through legal regulations on exhaust gas composition and the substitution of two stroke vehicles with

more modern models equipped with three-way catalysts, only a limited reduction has been achieved in the NMVOC emissions from solvent use [7]. In general, the growth in solvent demand has stabilised and it is unlikely that solvent use will decline appreciably due to industrial growth in Europe. Thus, solvent use remains one of the most important sources of NMVOC emissions. Solvents and solvent-containing products find a broad range of applications in industry as well as in business and private households [8]. Paints, paint strippers, printing inks, adhesives and coating agents contain solvents in different mixtures with the solvent comprising in some cases a relatively high percentage of the content. Furthermore, solvents are utilised for degreasing metals, dry cleaning textiles as well as extracting agents, media in chemical reactions and raw materials for pharmaceutical preparations. Being volatile substances, solvents may be released during their various applications into the atmosphere and thereby create a significant impact on photochemical ozone formation.

The “traditional” classes of solvents are chlorinated hydrocarbons, aromatic hydrocarbons and unsubstituted hydrocarbons. Although chlorofluorocarbons, CFCs, are considered to have a low photochemical reactivity, some are responsible for the depletion of ozone in the stratosphere (i.e. 1,1,1-trichloroethane and the chlorofluorocarbon CFC-113 [9, 10, 11]), while others such as tetra- and trichloroethylene and tetra- and trichloromethane are considered to be potential carcinogenic species [12]. Aromatic hydrocarbons appear to have high ozone formation potentials [13] and also lead to the generation of ring-opening products which show high mutagenity and carcinogenity [14]. Finally, unsubstituted hydrocarbons besides their relatively low toxicity have a significant ozone forming potential [13].

International and European measures have, therefore, been adopted to regulate and reduce in stages solvent emissions by restricting the use of or by phasing out the production, as in the case of CFC solvents [15]. Solvent-containing coating systems are to be replaced, where technically possible, by environmental-friendly alternatives such as waterborne paints; introduction of best practice and pollutant-abatement technology in manufacturing processes is also expected to positively contribute to a decrease in VOC emissions. Furthermore, it has been internationally recognised that a switch from chlorocarbon, aromatic and unsubstituted hydrocarbon based solvents to oxygen-containing compounds, OVOC: oxygenated volatile organic compounds, is beneficial because the latter generally combine lower toxicity and reduced ozone formation potentials with better dissolution properties. Table 1.1 summarises the development in solvents consumption during the last 20 years in Western Europe [8].

Table 1.1: Development of consumption of solvents in Western Europe (as percentage of total) [8].

Category	1980	1986	1990	1995	2000
Oxygen-containing solvents	36.5	45	51	58	65
Aliphatics	28.5	22	20.5	19	18
Aromatics	20.5	20	19	17	15.5
Chlorinated hydrocarbons	14.5	13	9.5	6	1.5
Total consumption 10 ⁶ t	5.1	4.75	4.7	4.15	3.3

All the largest producers of solvents both in the US and world-wide (Shell Chemicals, DuPont, Union Carbide and Dow) are investigating the possibility to widen the current application fields of oxygenated compounds in an attempt to replace traditional solvents and are testing, in terms of chemical and physical properties, the possible introduction of new solvent types such as bi- or polyfunctional oxygen-containing compounds. Thus, it seems that replacement of many existing solvents will occur in the near future and that esters, alcohols, ketones and ethers will constitute significant proportion of these future solvents.

A similar tendency is to be found in the automotive and petroleum industry where a large research effort has taken place over the past decade to develop new, oxygenated, low reactivity gasoline formulations for spark ignited engines in automobiles and light duty trucks. Highly branched ethers (i.e. methyl *tert*-butyl ether, ethyl *tert*-butyl ether and *tert*-amyl methyl ether) and alcohols are used, in large volumes, as additives in gasoline fuels since they improve the octane ratio of the formulation, reduce the aromatic compound content and lower tailpipe emissions of CO and the fuel's Reid vapour pressure. In the United States this change in fuel composition has been pushed by the 1990 Clean Air Act Amendments in certain areas of the state. While limited quantities have been used in gasoline in California since the 1970s, methyl *tert*-butyl ether, MTBE, became the oxygenated of choice for refiners in 1992 due to its favourable properties of blending and low cost. Potential and documented contamination of groundwater and surface water sources by MTBE [16, 17] and health effects from inhaling gas fumes [18] have become a cause of major concern and increasing controversy. MTBE emerges as a compound of considerable interest because of its presence at relatively high concentrations in some urban air, low Henry's law constant (3.8 M atm^{-1} , at 15 °C), low partitioning to soil organic matter and resistance to degradation in the subsurface [19]. Finally, US Environmental Protection Agency has classified MTBE as a potential human carcinogen [18]. These factors

have caused widespread public health concern, and therefore, California legislature required the use of MTBE to be banned beyond 2003 [20].

Oxygenated organic compounds including ethers, alcohols and esters are also currently being investigated as attractive alternative diesel fuels and fuel components since they combine acceptable fuel properties (i.e. high cetane number and low self-ignition temperature) with low exhaust emissions (particulate and NO_x) and reduced combustion noise. Finally, the already wide use of oxygenated organic compounds as solvents as well as fuels additives will probably increase in the future making their release into the atmosphere an important environmental consideration.

In order to avoid past mistakes and to obtain the maximum benefit from a switch to oxygenated compounds, reliable information on the chemical and physical properties of individual compounds and their technical performances should not be the only criteria for the selection of the alternative solvents and/or additives; the ability to affect human health and the behaviour in the environment of the possible candidates represent equally crucial aspects to be investigated before the wider use of these compounds.

1.2 State of the art

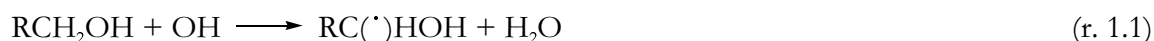
Volatile organic compounds present in the atmosphere can undergo photolysis and chemical reactions with hydroxyl radicals, nitrate radicals and ozone, with the OH radical reaction being an important, and often dominant, atmospheric loss process [21]. Kinetic data and mechanistic information on the atmospheric degradation of individual compounds are, therefore, essential components in any attempts to reliably assess the possible contribution of these substances to photochemical air pollution in urban and regional areas. Despite their importance, the atmospheric lifetime and fate of alcohols and esters have received relatively little attention.

During the last years, kinetic data have been determined for the reaction of OH radicals with both alcohols and esters [22, 23, 24, 25, 26, 27] since such reactions constitute important steps in the oxidation of these compounds in the atmosphere and in combustion systems. These kinetic studies have provided estimates of the tropospheric lifetimes of alcohols and esters. The tropospheric lifetime of a chemical determines the relative importance of its transport and thereby the geographical scale of its potential atmospheric impacts i.e. local, regional or global. The results of the many kinetic studies [22, 23, 24, 25, 26, 27] have extended the database for the reactions of OH radicals with alcohols and esters allowing refinements in the structure-reactivity relationships developed by Atkinson and Kwok [28, 29] to predict rate coefficients

for the gas-phase reactions of OH radicals with organic compounds. While an accurate assessment of reaction kinetics is essential, a complete understanding of tropospheric processes also requires detailed product analyses of the complex chemical systems.

The atmospheric chemistry of primary alcohols and methyl esters is, to date, relatively poorly understood. The major uncertainties in the photo-degradation mechanisms of alcohols and esters which affect the final product distributions include i) the effect of the functional groups –OH and –C(O)O– in increasing or lessening the reactivity of the various sites of the molecule towards OH radicals; ii) the relative importance of the competing reaction pathways of the alkoxy radical intermediates, i.e. reaction with oxygen, thermal decomposition and isomerisation. In the case of esters, OH radical reactions are relatively slow, making studies of their degradation products difficult; thus, reactions with chlorine atoms are often employed as a surrogate to mimic the OH radical induced oxidation of such oxygenated compounds. In general, Cl atoms and OH radicals have similar modes of attack in their reaction with organic compounds, attack by Cl being more rapid but slightly less selective than that by OH. Nevertheless, the subsequent chemistry is the same. This implies that the fate of the different alkoxy radicals formed in the OH radical initiated atmospheric degradation of esters can also be accurately determined in studies of Cl reactions with esters, but the final product distribution will be somewhat different.

From the product studies currently available in the literature [30, 31, 32, 33, 34] on the atmospheric oxidation of alcohols it is known that the OH radical reaction proceeds mainly by H-atom abstraction from the C–H bond of the –CH₂OH group with the resulting α hydroxy alkyl radical reacting with O₂ to form the corresponding carbonyl.



The relative importance of the OH attack at the other sites of the molecule and the fate of the alkoxy radical intermediates depend on the chain length of the alcohol and on the position of the various –CH– groups respect to the –OH functional group.

It is presently difficult to extrapolate, from the few published product studies on esters [35, 36, 37, 38, 39], characteristic mechanistic behaviour patterns for these compounds. However, it appears that alkoxy radicals of structure CH₃C(O)OCH(O \cdot)R undergo an “ α ester” rearrangement reaction involving migration of the H-atom on the alkoxy carbon to the oxygen

atom in the C=O group through a five-membered transition state, resulting in the formation of an acid and the acyl radical, RCO. This rearrangement is unique to esters and represents an additional possible competing reaction pathway which must be incorporated into chemical mechanisms for the tropospheric degradation of these compounds.

1.3 Compounds investigated

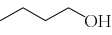

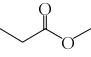
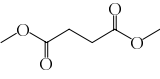
In this work the atmospheric oxidation of two selected alcohols and two selected esters has been investigated (Table 1.2). The alcohols 1-butanol and 1-pentanol find a variety of applications within the chemical industry: a potential increase of their use as solvents is currently under discussion. 1-Butanol is used principally in the field of surface coating either directly as a solvent or converted into derivatives, which then serve as solvents or monomer components. It is an excellent thinner and useful for regulating the viscosity and improving the flow properties of varnishes. 1-Butanol has also numerous applications in plastics and textile sectors and in the manufacture of butylamines. 1-Pentanol, a high volume chemical with a production exceeding 1 million pounds annually (in the U. S.) is particularly useful as a solvent in the reaction of substituted diamines with diisocyanates and for the production of sulphurised olefins and polyacrylates. 1-Pentanol is also employed as an extracting agent (in the purification of phosphoric acid and the separation of strontium chloride from aqueous metal chloride solutions) and as a starting material for the production of lubricant additives and for auxiliaries in flotation. Furthermore, 1-pentanol finds an important application in the pharmaceutical industry as a starting material for several syntheses and in the production of several esters that are applied in different fields.

Similarly, prompted by the need for more environmentally compatible solvents there is commercial interest in the use of esters such as methyl propionate and dibasic esters as replacements for traditional solvents. Because of their highly lipophilic and hydrophobic nature, esters are widely used as solvents, extractants and diluents. On account of their pleasant and usually fruity odour, they find important application in the manufacture of fragrances, foods, cosmetics and soaps. [Note that esters are also formed as intermediate species during the tropospheric degradation reactions of VOCs such as ethers [40, 41, 42]].

Particular attention merit dibasic esters (DBE) such as dimethyl succinate, dimethyl glutarate and dimethyl adipate. DBEs are important high-boiling, oxygenated solvents in the coatings industry: their high solvent power, excellent flow properties, low cost and toxicity have given paint and coatings companies the incentive to use them in their formulations. DBEs can be

used to replace methylene chloride in consumer and industrial paints removers and their high flash point and low volatility make DBEs an ideal replacement for acetone. Further, they are employed in a wide range of other applications such as plasticisers and as building blocks for a variety of polyesters and polymers.

Table 1.2: Chemical physical properties of the investigated compounds [43].

Substance	1-butanol	1-pentanol	methyl propionate	DBE-4
structure				
molecular weight (g/mol)	74.13	88.15	88.11	146.14
melting point (°C)	-89.5	-108.4	-88	18-19
boiling point (°C)	117.5	137.9	79.7	200
flash point (°C)	35	32	6	85
density (g/ml)	0.81	0.815	0.915	1.117

In conclusion, the alcohols and esters described above, which combine satisfactory technical performances in chemical industry applications with low costs and low health risks appear to be valuable candidates for replacing traditional solvents. The potential of an increased usage of alcohols and esters introduces a general need to map out their oxidation mechanisms and necessitates a better understanding of the environmental impacts of these species since they will eventually be released into the atmosphere.

1.4 Aim of the work

The purpose of this work was to provide a scientific evaluation of the atmospheric fate of the following oxygenated volatile organic compounds: 1-butanol, 1-pentanol, methyl propionate and dimethyl succinate (DBE-4).

The programme involved measuring the rate coefficients for the hydroxyl radical reactions of the two alcohols and selected esters including besides methyl propionate and dimethyl succinate also dimethyl glutarate (DBE-5) and dimethyl adipate (DBE-6). Laboratory chamber investigations (at the University of Wuppertal) and outdoor chamber studies (at the *EUPHORE* facility in Valencia/Spain) were performed to identify the oxidation products formed from the reaction of OH radicals with these OVOCs and to define then their atmospheric degradation mechanisms. In the case of esters, particularly slow OH radical

reactions prevented accurate product studies, then chlorine atom reactions were employed as a surrogate to mimic their OH radical induced atmospheric oxidation. The knowledge of the oxidation mechanisms obtained for the selected OVOCs were then used to identify characteristics in their atmospheric chemistry and to formulate generalised degradation mechanism for these two classes of compounds, alcohols and esters.

The chemical mechanisms proposed in this work should be incorporated in chemical/transport models to obtain for these OVOCs estimates of their ozone formation potentials and their ability to generate other photooxidants. The information could eventually serve as a basis for decision making concerning the widespread implementation of these compounds in various applications.

Chapter 2

Experimental

2.1 Reaction chambers

2.1.1 Description of 405 ℓ reactor

The majority of the experiments performed in this work were carried out in a 405 ℓ reaction chamber. The reactor consists of a pyrex cylindrical glass vessel with a length of 1.5 m and a diameter of 60 cm closed, at both ends, by Teflon coated aluminium end flanges. Integrated on one of the metal flanges are ports for the inlet of the reactants into the chamber and for the collection of samples for further analytical analysis. Other inlet and outlet ports and accessories, like a magnetic coupled Teflon mixing fan and a capacitance manometer (Membranovac MV 110 S2), are located on the opposite flange. The experimental set-up is shown schematically in Figure 2.1.

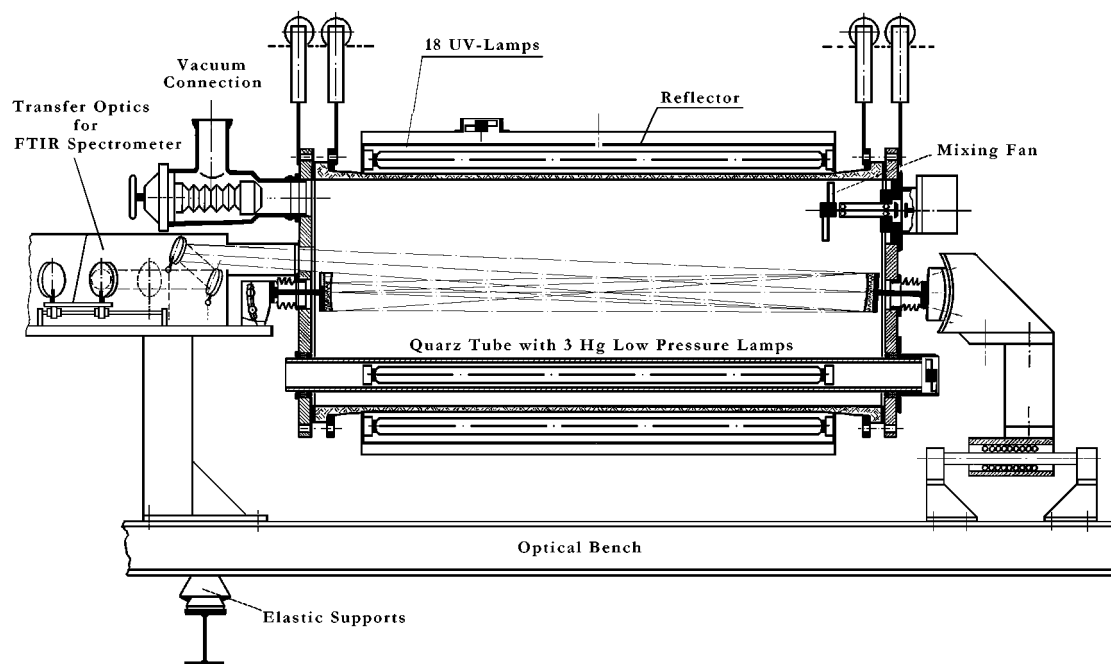


Figure 2.1: Schematic diagram of the 405 ℓ reaction chamber.

The reactor is equipped with 18 fluorescent lamps (Philips TLA 40W/05; $300 \leq \lambda \leq 450$ nm, $\lambda_{\max} = 360$ nm) arranged concentrically around the outside of the chamber and with 3 low pressure mercury vapour lamps (Philips TUV 40W; main emission at $\lambda_{\max} = 254$ nm) contained inside a quartz glass tube (1.6 m length, 10 cm dia.) mounted centrally inside the chamber between the end flanges. Both types of lamps were used as photolysis sources. In order to maintain the reactor at room temperature during the photolysis of reaction mixtures, the lamps are cooled by flowing ambient air through the lamp housing units of the system. The pumping system of the reactor consisted of a Balzer turbo-molecular pump, model WZ 500, backed by a Leybold double stage rotary fore pump, D 40 B model, providing a vacuum of ca. 10^{-4} mbar. A White mirror system (base path length 1.4 m) mounted inside the reactor and coupled, by an external mirror system, to a Fourier Transform-Spectrometer (Nicolet Magna 550) enables the *in situ* monitoring of both reactants and products by long path infrared absorption using a total path length of 50.4 m and a resolution of 1 cm^{-1} . The spectrometer is equipped with a globar as IR source and with a MCT-detector (mercury/cadmium/tellurium detector) cooled to 77 K with liquid nitrogen. The spectrometer and the external transfer optics (covered with a protective box) are permanently purged with dry air to remove water vapour. The spectrometer is directly controlled by the software OMNIC, provided by Nicolet, running on a personal computer where raw data are stored.

2.1.2 Description of 480 ℓ reactor

The experiments to determine the rate coefficients for the reaction of OH radicals with 1-butanol and 1-pentanol were carried out in a 480 ℓ reaction chamber which has many construction similarities with the 405 ℓ reactor described in paragraph 2.1.1. The chamber consists of a cylindrical Duran glass vessel (3 m length, 45 cm dia.) closed at both ends by Teflon coated aluminium end flanges. The experimental set-up is shown schematically in Figure 2.2.

Integrated on the metal flanges are ports for the inlet of reactants into the chamber and for the collection of samples from the reaction mixtures for further analysis. Other accessories, like a mixing fan to ensure homogeneity of the reaction mixtures and a capacitance manometer, are also located on the flanges. Arranged concentrically around the outside of the reactor are 32 superactinic fluorescent lamps (Philips TLA 40W/05, $300 \leq \lambda \leq 450$ nm, $\lambda_{\max} = 360$ nm). The vacuum (ca. 10^{-3} mbar) is maintained by means of a Leybold turbo-molecular pump, model RUVAC WZ 151 ($500 \text{ m}^3/\text{h}$), backed by a Leybold double stage rotary fore pump, model D 40 B ($200 \text{ m}^3/\text{h}$).

The chamber is equipped with 3 build-in White mirror systems which were, usually, operated at a total path length of 51.6 m, 28.8 m and 28.0 m for the acquisition of IR, VIS and UV spectra, respectively.

Analysis of reactants and products were made, during the experiments performed in this work, by *in situ* FTIR long path spectroscopy using a resolution of 1 cm^{-1} . The FTIR spectrometer (Nicolet Magna 520) and the transfer mirror system are covered with a protective box and are permanently purged with dry air to remove water vapour. The spectrometer is directly controlled by the software OMNIC, provided by Nicolet, running on a personal computer where raw data as well as processed data are stored.

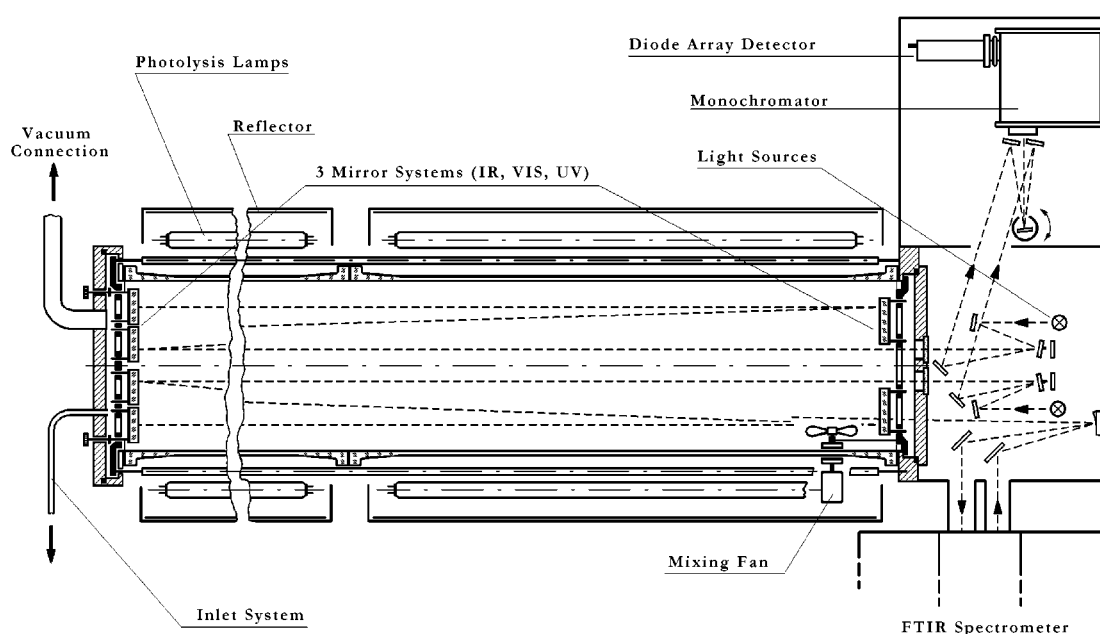


Figure 2.2: Schematic diagram of the 480 l reaction chamber.

2.1.3 Description of the European photoreactor *EUPHORE*

Investigations on the degradation mechanism of 1-butanol and 1-pentanol were performed in the European Photoreactor *EUPHORE*, which is a part of the Centro de Estudios Ambientales del Mediterraneo (CEAM) in Valencia/Spain.

The facility consists of two identical half spherical fluorine-ethene-propene (FEP, Du Pont) foil chambers mounted on aluminium floor panels covered with FEP foil (Figure 2.3).

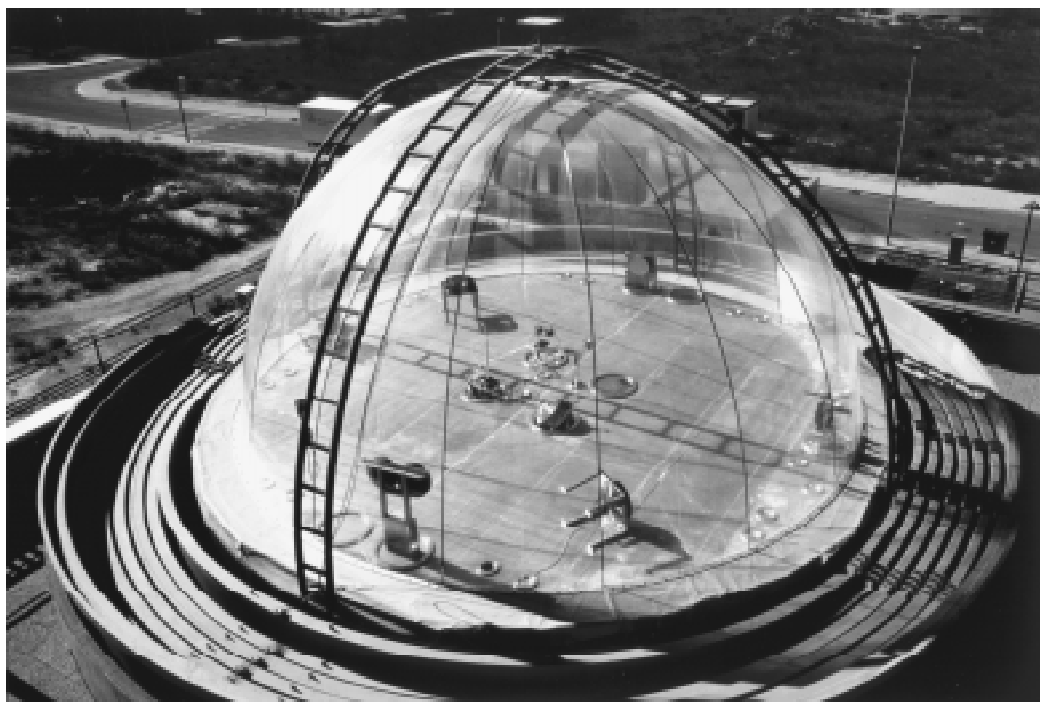


Figure 2.3: The *EUPHORE* photoreactor.

The FEP foil transmits 85-90% of the light with wavelengths from > 500 to 320 nm, dropping to 75% transmission at the atmospheric threshold of 290 nm. Each chamber has a volume of ca. 195 m³ and a diameter of 9.2 m and is protected by a light-tight housing which can be opened, exposing the photoreactor contents to sunlight, thereby initiating the photooxidation of the reaction mixtures. To avoid unwanted heating of the chambers, the floor panels are connected to a refrigerating system (cooling capacity of 0.75 kW/m²) allowing realistic atmospheric temperature conditions to be maintained even during long-term irradiations. The temperature in the chambers is measured with two thermocouples PT-100, one measuring the floor temperature and one measuring the temperature of the chamber air. An air-drying and purification system supplies the chamber with oil vapour, hydrocarbon and NO_y-free dry air. The air is dried in absorption dryers (Zander, Type HEA 1400) reaching a dew point of -50 °C and a reduced content of CO₂; with help of a special charcoal adsorber, NO_x is eliminated and oil vapour and non-methane hydrocarbons are reduced to ≤ 0.3 µg/m³. In order to mix the reactants, two mixing fans with an air throughput of 4000 m³/h each are installed in the chamber.

The chamber, used for the experiments performed in this work, is equipped with many different analytical and *in situ* measurement techniques, but only those used during the campaign of March 1999 (1-pentanol oxidation) and March 2000 (1-butanol oxidation) are

here described; a more detailed description of the European Photoreactor *EUPHORE* can be found in the literature [44].

An FTIR spectrometer (NICOLET Magna 550, MCT detector, 1 cm^{-1} resolution) coupled to a White mirror system (base length 8.17 m, total optical path length 553.5 m) was used to monitor reactants and products. The mirrors, mounted at the periphery of the chamber, have a diameter of 406 mm and, to improve their reflectivity in the infrared range, are gold coated. The reactant mixtures were also analysed by gas chromatography with photo-ionisation detection (GC-PID). Gas samples were automatically collected from the chamber every 10-15 min and introduced, via a heated sampling loop of 2 ml capacity, onto a DB624 column at $80\text{ }^{\circ}\text{C}$ (J & W Scientific, 30m, $1\mu\text{m}$) mounted in a Fisons GC 8000 instrument. In addition, carbonyl compounds were sampled from the chamber using solid phase 2,4-dinitrophenyl hydrazone (DNPH)-Silica cartridges. Hydrazones, formed by derivatization, were separated and quantitatively measured by HPLC (Hewlett Packard Model 1050, UV detector).

Two instruments, both using a chemiluminescence detection method, were employed for NO_x measurement: an Eco Physics CLD 770 AL NO_x monitor with photolytic converter PLC 760 and a measurement range of 50 ppt-500 ppb; and a Monitor Labs ML9841A NO_x monitor with a catalytic converter and a measurement range of 1 ppb-20 ppm. Measurement of ozone was made in the range of 1 ppb-2 ppm using an ozone monitor (Monitor Labs ML 9810) with UV absorption detection. The solar light intensity was measured in the chamber with a spectral radiometer (scanning double monochromator Bentham TM300) and filterband radiometers were used to measure the photolysis frequencies of $J(\text{O}^1\text{D})$ and $J(\text{NO}_2)$ during the days of the experiments. The NO_x , ozone concentration, temperature and radiation measurements data were collected and saved by a data acquisition system.

2.2 Procedure and analysis at the Wuppertal laboratory

2.2.1 General

The compounds under investigation were introduced into the evacuated chamber: gas and liquid substances were injected, by means of syringes (gas-tight syringes and microliter syringes), either directly into the reactor or in a stream of gas; in the case of substances with high boiling points, the inlet port to the reactor was also heated. Solid compounds were placed in a glass bulb attached to the injection port of the chamber, they were then heated and flushed into the reaction chamber with diluent gas. The typical initial concentration of the reactants, in the reaction chambers, were 10-15 ppm. The reaction chamber was subsequently filled to

(1000 ± 50) mbar with synthetic air [all the experiments were performed within this pressure range]. Before commencing a measurement, the reaction mixture was kept in the dark for approximately 5 min to allow thorough mixing of the reactants and thermal equilibrium to be established. The experiments were carried out at (298 ± 5) K, where the indicated interval covers the temperature span of all experiments performed in this work.

FTIR spectra were recorded regularly over the wavelength range 690-4000 cm⁻¹ with a resolution of 1 cm⁻¹. After acquiring a few spectra of the mixture in dark, the photooxidation was initiated by switching on the lamps, the number and the type of the lamps employed differed for the individual experiments according to the required conditions. The integration time of each spectrum and the interval between two spectra were chosen to give 10-20 measurement points over the duration of the experiment.

The photolysis of methyl nitrite in synthetic air was used as the hydroxyl radical source; nitric oxide, NO, was added to the reaction mixture to compensate its loss by the reaction with peroxy radicals formed in photooxidation systems and to suppress the formation of ozone and hence of nitrate radicals:

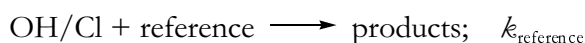
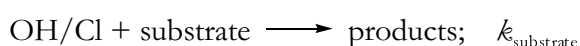


Chlorine atoms were generated by the photolysis of molecular chlorine:



2.2.2 Relative rate method

The rate coefficients for the reactions of OH radicals and Cl atoms with the investigated oxygenated compounds were determined using a relative rate method in which the relative disappearance rates of the substrate and of a reference compound, whose rate coefficient with OH radicals or with Cl atoms is reliably known [45, 46], are monitored parallel in the presence of OH radicals or Cl atoms:



Providing that the substrate and the reference are removed solely by reaction with the OH radicals, or Cl atoms then:

$$\ln \left\{ \frac{[\text{substrate}]_{t_0}}{[\text{substrate}]_t} \right\} = \frac{k_{\text{substrate}}}{k_{\text{reference}}} \ln \left\{ \frac{[\text{reference}]_{t_0}}{[\text{reference}]_t} \right\} \quad (\text{I})$$

where $[\text{substrate}]_{t_0}$ and $[\text{reference}]_{t_0}$ are the concentrations of the substrate and the reference compound, respectively, at time t_0 ; $[\text{substrate}]_t$ and $[\text{reference}]_t$ are the corresponding concentrations at time t ; $k_{\text{substrate}}$ and $k_{\text{reference}}$ are the rate coefficients for the reaction with OH radicals/Cl atoms of the substrate and the reference compound, respectively. Thus, the concentrations of the substrate and the reference as a function of reaction time, plotted as given by Eq. I, can be used to derive the rate coefficient ratio $k_{\text{substrate}}/k_{\text{reference}}$. Plots of $\ln \left\{ \frac{[\text{substrate}]_{t_0}}{[\text{substrate}]_t} \right\}$ versus $\ln \left\{ \frac{[\text{reference}]_{t_0}}{[\text{reference}]_t} \right\}$ should give straight lines with slopes $k_{\text{substrate}}/k_{\text{reference}}$ and zero intercept. If the value of the rate coefficient of the reference $k_{\text{reference}}$ is known, then $k_{\text{substrate}}$ can be obtained. Under the experimental conditions, the substrate and/or the reference can additionally undergo photodissociation and may also be lost to the chamber surface. The photostability of each substrate was established by irradiation of substrate-air mixtures in the absence of a radical precursor for a time period longer than that employed in the kinetic experiments. Dark experiments of the substrate-reference-air mixtures were also carried out to investigate the possibility of adsorption on the wall of the chamber. Photolysis and wall loss rate, if any, could then be compared to the extent of the reaction with the radical of interest over the time scale of the experiment. Normally, the references employed did not photolyse and their wall losses were found to be very low, often below the detection limit. For some of the oxygenated compounds investigated in this work the wall losses were relatively high and non-negligible on the time scale of the experiments. Taking into account this first-order process, Eq. I can be rearranged to give [45]:

$$\ln \left\{ \frac{[\text{substrate}]_{t_0}}{[\text{substrate}]_t} \right\} - k_{\text{substrate}}^{\text{loss}} \times t = \frac{k_{\text{substrate}}}{k_{\text{reference}}} \ln \left\{ \frac{[\text{reference}]_{t_0}}{[\text{reference}]_t} \right\} \quad (\text{II})$$

where t is the reaction time and $k_{\text{substrate}}^{\text{loss}}$ is the wall loss rate of the substrate.

The errors of the rate coefficients determined in this work are given as twice the standard deviation of the linear regression of the data plotted according to Eq. I or Eq. II plus an

additional 10% uncertainty due to the potential systematic errors associated with the value of the reference rate coefficient.

The rate coefficients were, typically, measured relative to two different references, thus, the final values of the rate coefficients are averages of those determined using the two different reference compounds together with error limits which encompass the extremes of the individual determinations.

2.2.3 Product analysis

Product studies were carried out mainly in the 405 ℓ reactor, described in paragraph 2.1.1, using FTIR spectroscopy. Substrates and products were, first of all, identified by comparison of the infrared spectra of the reaction mixture with those of authentic samples (reference spectra); the analysis of the complex spectra proceeded, then, by successively subtracting the characteristic absorptions of identified compounds with the use of calibrated spectra. The known concentration of the reference spectra and the subtraction factors allowed the concentration of each identified compound to be determined. The molar formation yield of each product was, then, derived by plotting the amount of the product formed against the amount of the substrate consumed (e.g. Figure 2.4).

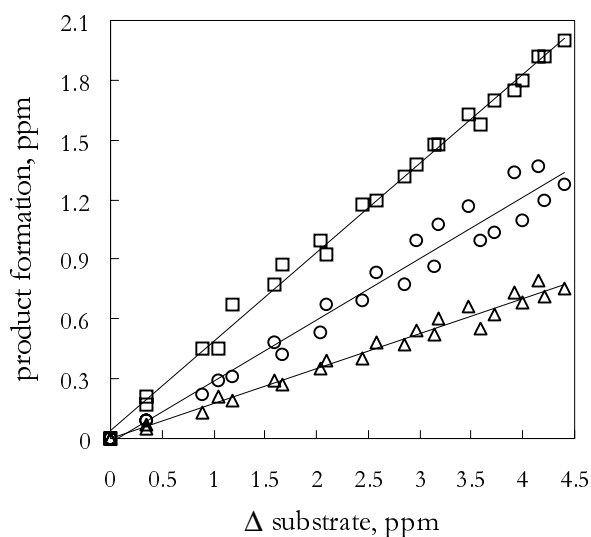


Figure 2.4: Determination of the molar formation yields of *mono*-methyl succinate (squares), carbon monoxide (circles) and dimethyl oxaloacetate (triangles) formed from the reaction of dimethyl succinate with Cl atoms. See text.

Least-square analysis of these data led to product formation yields. The indicated error of the product formation yields is twice the standard deviation of the linear regression combined with overall uncertainties in the concentration of the reference spectra and in the subtraction factors.

For some of the identified products, plots of their concentration against the amounts of substrate consumed showed curvature, strongly supporting that secondary reactions of these primary products occurred during the time period of the experiments.

In order to derive the formation yields of these products, their measured concentrations had to be corrected for further reactions, in particular for the reaction with OH radicals. Corrections were performed using Eq. III which is described in detail in [47]:

$$F = \frac{k_{\text{sub}} - k_{\text{prod}}}{k_{\text{sub}}} \times \frac{1 - \frac{[\text{substrate}]_t}{[\text{substrate}]_{t_0}}}{\left(\frac{[\text{substrate}]_t}{[\text{substrate}]_{t_0}} \right)^{\frac{k_{\text{prod}}}{k_{\text{sub}}}} - \frac{[\text{substrate}]_t}{[\text{substrate}]_{t_0}}} \quad (\text{III})$$

where F is the multiplicative correction factor, k_{sub} and k_{prod} are the OH reaction rate coefficients of the substrate and the product, respectively, and $[\text{substrate}]_{t_0}$ and $[\text{substrate}]_t$ are the concentrations of the substrate at time t_0 and t , respectively. The corrected product concentrations, $F \times [\text{product}]_t^{\text{meas}}$, were then plotted against the amount of the substrate consumed to derive molar product formation yield, as above described (e.g. Figure 2.5).

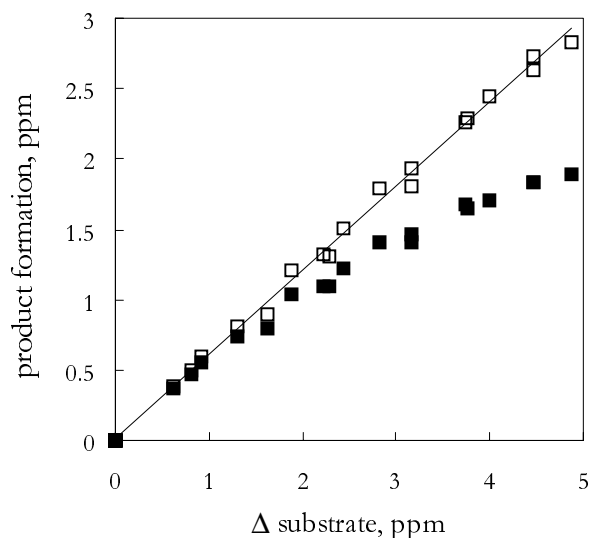


Figure 2.5: Determination of the molar formation yield of butanal formed from the reaction of 1-butanol with OH radicals: the measured concentrations of butanal (■) have been corrected (□) for secondary loss processes. See text.

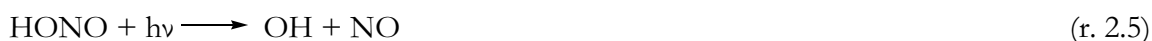
In the case of C_1 - and C_2 -primary products, secondary formation and removal processes occurring in the system under the experimental conditions employed rendered the procedure for the correction of the measured concentrations difficult. Therefore, the molar formation yield of the products was derived from the uncorrected concentrations plotted against the

consumption of the substrate in the early stage of the reaction, when the secondary processes can largely be neglected.

2.3 *EUPHORE*-experiments

The product investigations on the OH initiated oxidation of 1-pentanol and 1-butanol were carried out in March 1999 and March 2000, respectively, in smog chamber *B* of the European photoreactor facility in Valencia (Spain).

Prior to an experiment, the chamber valve, kept opened during the night allowing purified air to be flushed through the chamber, was closed and the chamber was filled to ca. 0.1-0.2 mbar over atmospheric pressure. In order to characterise the initial conditions of the clean chamber, a FTIR background spectrum, derived from 575 co-added spectra (575 scans corresponding to 15 min), and a GC-PID background chromatogram were acquired; ozone and NO_x background concentrations were also measured. In the experiments performed on the degradation mechanisms of the two alcohols, OH radicals were produced by the photolysis of HONO:



HONO, synthesised as described in Annex D, was first introduced into the chamber in an air stream for about 30 min. During the addition, the NO_x concentration was measured by the Eco Physics and the Monitor Labs NO_x monitors, which allowed the HONO concentration in the chamber to be estimated: in the absence of any VOC, the Eco Physics instrument provides, as NO₂ signal, the sum of the NO₂ and HONO concentration and the Monitor Labs instrument, as NO₂ signal, the actual NO₂ concentration. Typical initial concentration of HONO as well as of NO and NO₂ were 40-80 ppb (see Annex D).

After addition of HONO, the substrates, 1-butanol or 1-pentanol, were added to the chamber by gently heating the required amount in a stream of air entering the chamber. The typical initial concentrations of 1-butanol and 1-pentanol were approximately 400-800 ppb. To compensate for the consumption of HONO during the 2-5 h duration of the experiments, addition of HONO was repeated twice during the course of the experiments to maintain the level of OH radicals and also the conversion of RO₂· to RO· via RO₂· + NO reactions.

During the experiments, the chamber was continuously refilled with clean air, to compensate for pressure losses due to small leaks and sampling. SF₆, sulphur hexafluoride, was added to the reaction mixture in order to determine the dilution rate of the mixture since SF₆ is

unreactive and stable at ambient temperatures to all radical processes and is not photolysed by sunlight. After allowing for mixing of the reactants, photooxidation was initiated by opening the light-tight protective housing of the chamber and exposing the photoreactor contents to sunlight.

During the experiments 15-30 spectra were recorded, typically a spectrum was collected every 10 min, each with an integration time of 3-5 min; gas samples of the reaction mixtures were collected for GC-PID and HPLC analysis every 10 min and every 20 min, respectively. The intensity of the sunlight, temperature, ozone and NO_x concentration were continuously monitored by a data acquisition computer and stored in digital format for further processing. During the experiments, the analysis of the alcohol and carbonyl products were principally performed by gas chromatography with photo-ionisation detection (GC-PID) since this analytical technique provided a better separation of the aldehydic products than that offered by FTIR, allowing a more accurate identification and quantification of the reaction products. Calibration experiments were, therefore, carried out to derive the GC-PID response factors and repeated in each campaign to check for possible changes due to variation in the intensity of the photo-ionisation source. Weighed amounts of a compound were introduced into the chamber and the concentration determined by FTIR reference spectra and by the HPLC response factor obtained with authentic standards. The measured concentration divided by the area of the corresponding GC peak gives the GC-PID response factor for that compound.

In order to derive molar formation yields of the oxidation products, secondary loss processes of both substrates and products had to be taken into account.

The dilution rate of the chamber was determined from the SF₆ decay monitored during the experiments, by integrating its intense infrared band between 935-955 cm⁻¹; this first order loss process can be described as follows:

$$\ln([\text{SF}_6]_0/[\text{SF}_6]_t) = k_D \times t \quad (\text{IV})$$

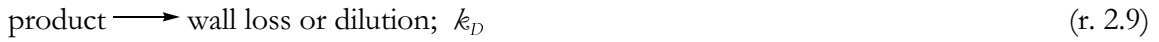
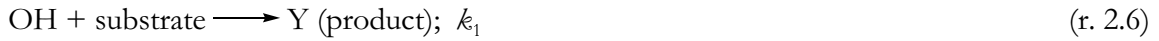
where [SF₆]₀ and [SF₆]_t are the concentration of SF₆ at time $t = 0$ and time t , respectively, and k_D is the dilution rate. At the time of the experiments, the chamber had a leak rate of ca. 3% h⁻¹.

The pure chemical loss of the substrate was derived by correcting the observed decay for the dilution rate using Eq. V:

$$c_{t_2}^{\text{chem}} = c_{t_1}^{\text{chem}} \times \frac{c_{t_2}^{\text{meas}}}{c_{t_1}^{\text{meas}}} \times e^{k_D(t_2-t_1)} \quad (\text{V})$$

where $c_{t_2}^{\text{chem}}$ and $c_{t_1}^{\text{chem}}$ are the concentration of the substrate at times t_2 and t_1 , respectively, determined from the chemical reaction with OH radicals; $c_{t_2}^{\text{meas}}$ and $c_{t_1}^{\text{meas}}$ are the measured concentration of the substrate t_2 and t_1 , respectively. Wall loss of both 1-butanol and 1-pentanol was negligible.

The measured concentration of the products had also to be corrected for further reaction with OH radicals, photolysis and dilution losses. Corrections have been performed using the mathematical procedure described by Tuazon *et al.* [48] which is based on the reaction sequence:



In this sequence, Y is the formation yield of the primary product from the oxidation of the substrate and k_{OH} , k_{hv} and k_D are the rate coefficients for reaction with OH, photolysis, and wall loss or chamber dilution, respectively.

By making the reasonable assumption that the OH radical concentration was essentially constant over the time intervals between the measurement points, then:

$$[\text{substrate}]_{t_2} = [\text{substrate}]_{t_1} e^{-k_1[\text{OH}](t_2-t_1)} \quad (\text{VI})$$

and

$$[\text{product}]_2 = [\text{product}]_{t_1} e^{-(k_{OH}[\text{OH}] + k_{hv} + k_D)(t_2-t_1)} + \frac{Y_{t_2-t_1} [\text{substrate}]_{t_1} k_1 [\text{OH}]}{(k_{OH} - k_1)[\text{OH}] + k_{hv} + k_D} \left[e^{-k_1[\text{OH}](t_2-t_1)} - e^{-(k_{OH}[\text{OH}] + k_{hv} + k_D)(t_2-t_1)} \right] \quad (\text{VII})$$

where $[\text{substrate}]_{t_1}$, $[\text{product}]_{t_1}$ and $[\text{substrate}]_{t_2}$, $[\text{product}]_{t_2}$ are the substrate and product concentrations measured at times t_1 and t_2 , respectively, and $Y_{t_2-t_1}$ is the formation yield of the individual product over the period time $t_2 - t_1$. The OH radical concentration was calculated from the decay of the substrate using the rate coefficient for the reaction of the substrate with OH radicals, according to the following equation:

$$[\text{OH}] = \frac{\ln([\text{substrate}]_{t_2} / [\text{substrate}]_{t_1})}{k_{OH}^{\text{substrate}} \times (t_2 - t_1)} \quad (\text{VIII})$$

Use of the rate coefficients k_{OH} , k_{hv} and k_D , determined in this study or found in the literature, together with Eq. VI and Eq. VII allowed $Y_{t_2-t_1}$ to be calculated. The product concentrations, corrected for reaction with OH radicals, photolysis and wall loss and/or dilution, are then given by

$$[\text{product}]_{t_2}^{\text{corr}} = [\text{product}]_{t_1}^{\text{corr}} + Y_{t_2-t_1} ([\text{substrate}]_{t_1} - [\text{substrate}]_{t_2}) \quad (\text{IX})$$

where $[\text{product}]_{t_1}^{\text{corr}}$ and $[\text{product}]_{t_2}^{\text{corr}}$ are the corrected product concentrations at times t_1 and t_2 , respectively. The corrected product concentrations were, then, plotted against the consumed amount of the substrate to derive the molar formation yield of the products.

Chapter 3

Kinetic study

All the rate coefficients reported in this work were determined using the relative rate method (see paragraph 2.2.2) at (1000 ± 50) mbar and (296 ± 2) K. Test experiments were performed both for the investigated compounds and the references to check that unwanted adsorptions on the wall of the reactor, dark reaction and photolysis were not occurring under the experimental conditions employed. Normally, these loss processes were found to be negligible on the time scale of the experiments with three exceptions: dimethyl succinate, dimethyl glutarate and dimethyl adipate showed relatively fast wall adsorptions. These losses were taken into account using Eq. II to determine the corrected reaction rate coefficients. Typically two different reference compounds were employed and, at least, two experimental runs were performed in order to verify the reliability of the results and their sensitivity to different references and different concentrations. The reaction rate coefficient of the reference compounds used in the present kinetic study and the experimental conditions employed are reported in Annex B, Table B.1 and Table B.2.

3.1 Hydroxyl radical reaction rate coefficients

3.1.1 Results

Rate coefficients have been measured for the reaction of hydroxyl radicals with 1-butanol and 1-pentanol, methyl propionate (MPR), dimethyl succinate (DBE-4), dimethyl glutarate (DBE-5), and dimethyl adipate (DBE-6). The observed losses of each substrate compound versus those of the reference compounds in the presence of hydroxyl radicals are plotted in Figure 3.1, according either to Eq. I or Eq. II.

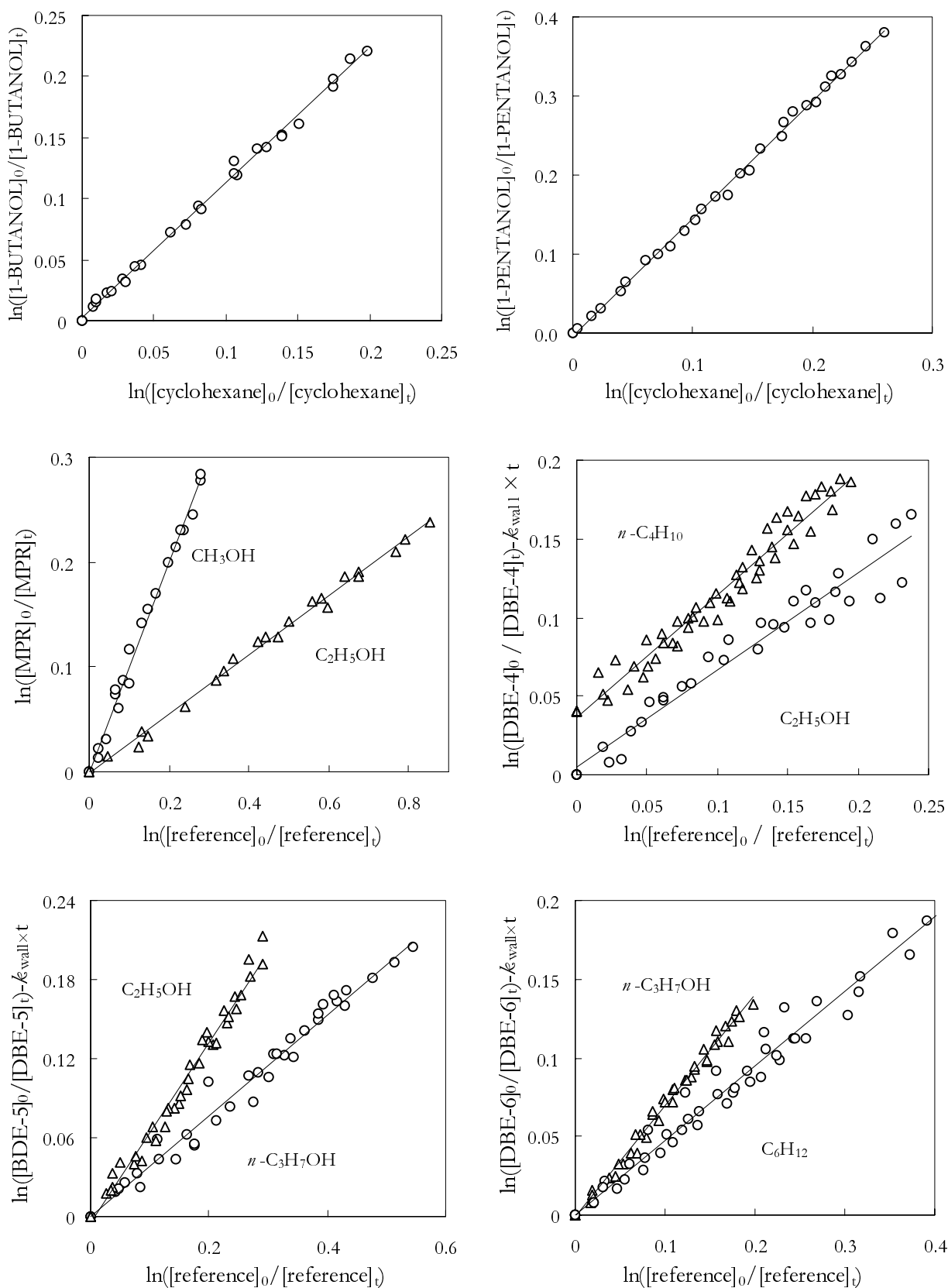
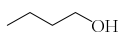
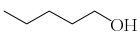
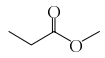
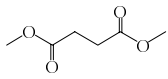
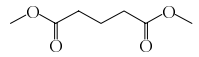
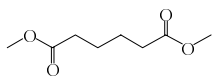


Figure 3.1: Plot of the kinetic data according either to Eq. I or Eq. II for the gas-phase reactions of the OH radical with the investigated oxygenated organic compounds. The data for DBE-4 relative to n -butane have been displaced vertically by 0.04 unit for clarity.

Reasonably good straight line plots were observed and least-square analysis of these data led to the rate coefficient ratios ($\pm 2\sigma$) given in Table 3.1. The rate coefficient ratios were placed on an absolute basis by using the OH reaction rate coefficient of the reference compounds, listed in Annex B, Table B.1. The resulting rate coefficients are also reported in Table 3.1; the quoted errors include 2σ from the statistical analysis plus an estimated additional systematic error of 10% due to uncertainties in the reference rate coefficients.

Table 3.1: Rate coefficient ratios $k_{\text{substrate}}/k_{\text{ref}}$ and rate coefficients k_{OH} for the gas-phase reactions of OH radicals with the oxygenated organic compounds.

Substrate		Reference	$k_{\text{substrate}}/k_{\text{ref}}^a$	$k_{\text{OH}}^{b, c}$
1-butanol		<i>c</i> -hexane	1.10 ± 0.02	8.28 ± 0.85
1-pentanol		<i>c</i> -hexane	1.48 ± 0.03	11.1 ± 1.10
methyl propionate		methanol	1.01 ± 0.04	0.941 ± 0.101
		ethanol	0.28 ± 0.01	0.916 ± 0.097
dimethyl succinate		<i>n</i> -butane	0.78 ± 0.04	1.98 ± 0.22
		ethanol	0.59 ± 0.05	1.93 ± 0.25
dimethyl glutarate		ethanol	0.68 ± 0.03	2.23 ± 0.24
		<i>n</i> -propanol	0.38 ± 0.02	2.12 ± 0.24
dimethyl adipate		<i>n</i> -propanol	0.71 ± 0.02	3.92 ± 0.40
		<i>c</i> -hexane	0.47 ± 0.02	3.54 ± 0.38

^a Indicated errors are two least-squares standard deviations.

^b in $10^{-12} \text{ cm}^3 \text{ molecule}^{-1} \text{ s}^{-1}$ units.

^c Indicated errors include the estimated overall uncertainties in rate coefficients of the reference, k_{ref} .

3.1.2 Discussion

As seen from Table 3.1, the results obtained for each individual compound using different reference compounds showed negligible differences. Therefore, the final values of the hydroxyl reaction rate coefficients, reported in Table 3.2, are averages of the individual determinations together with error limits which encompass the extremes of the individual determinations. The quoted errors reflect the accuracy of the measurements. The results can be compared with the corresponding values found in the literature (Table 3.2).

Table 3.2: Rate coefficients (in $\text{cm}^3 \text{ molecule}^{-1} \text{ s}^{-1}$ units) for the gas-phase reactions of OH radicals with the investigated oxygenated organic compounds. Comparison of the present results with literature data.

Substance	this work	literature
1-butanol	$(8.28 \pm 0.85) \times 10^{-12}$	$(8.31 \pm 0.63) \times 10^{-12}$ [22]
		$(7.80 \pm 0.20) \times 10^{-12}$ [23]
		$(8.56 \pm 0.70) \times 10^{-12}$ [23]
1-pentanol	$(1.11 \pm 0.11) \times 10^{-11}$	$(1.08 \pm 0.11) \times 10^{-11}$ [22]
		$(1.20 \pm 0.16) \times 10^{-11}$ [23]
		$(1.05 \pm 0.13) \times 10^{-11}$ [23]
methyl propionate	$(9.29 \pm 1.13) \times 10^{-13}$	$(10.3 \pm 0.4) \times 10^{-13}$ [25]
		$(8.31 \pm 0.87) \times 10^{-13}$ [26]
dimethyl succinate	$(1.95 \pm 0.27) \times 10^{-12}$	$(1.4 \pm 0.6) \times 10^{-12}$ [27]
dimethyl glutarate	$(2.18 \pm 0.30) \times 10^{-12}$	$(3.3 \pm 1.1) \times 10^{-12}$ [27]
dimethyl adipate	$(3.73 \pm 0.59) \times 10^{-12}$	$(8.4 \pm 2.5) \times 10^{-12}$ [27]

Table 3.2 lists values of the rate coefficients for the reaction of hydroxyl radicals with 1-butanol and 1-pentanol from previous room temperature determinations [22, 23].

An unit-weighted least-squares average of the absolute and relative rate coefficients reported in the literature (see Table 3.2) led to the recommendations of $k_{(\text{OH} + 1\text{-butanol})} = 8.57 \times 10^{-12} \text{ cm}^3 \text{ molecule}^{-1} \text{ s}^{-1}$ and $k_{(\text{OH} + 1\text{-pentanol})} = 1.11 \times 10^{-11} \text{ cm}^3 \text{ molecule}^{-1} \text{ s}^{-1}$, both with an estimated overall uncertainty of $\pm 35\%$ given by Atkinson [21]. There is excellent agreement, within the combined experimental uncertainties, between the results of all the studies reported in the literature and those of the present work for the reaction of OH radicals with 1-butanol and 1-pentanol [49].

As shown in Table 3.2, the rate coefficient measured in this work for the OH + methyl propionate reaction is in good agreement with the absolute rate coefficients $k_{(\text{OH} + \text{methyl propionate})} = (10.3 \pm 0.4) \times 10^{-13}$ and $k_{(\text{OH} + \text{methyl propionate})} = (8.31 \pm 0.87) \times 10^{-13} \text{ cm}^3 \text{ molecule}^{-1} \text{ s}^{-1}$ reported by Wallington *et al.* [25] and Le Calvé *et al.* [26], respectively. In light of the excellent agreement between the three studies, it is recommended that the average of the three determinations, $k_{(\text{OH} + \text{methyl propionate})} = 9.3 \times 10^{-13} \text{ cm}^3 \text{ molecule}^{-1} \text{ s}^{-1}$, is used in models of the atmospheric chemistry of methyl propionate [50].

The values from Aschmann and Atkinson [27] are the only ones reported in the literature for the reaction of the three dibasic esters with OH radicals. While the rate coefficients measured by Aschmann and Atkinson for DBE-4 and DBE-5 are in reasonable agreement with the

present values, there is a significant discrepancy, of approximately a factor 2, in the rate coefficient for DBE-6. The reason for this large difference is, presently, not clear but could lie in the analytical procedure used by Aschmann and Atkinson, in which gas samples, collected from the reaction chamber onto a Tenax-solid adsorbent, were subsequently thermally desorbed and analysed by gas chromatography. This method could, potentially, lead to losses of the sticky substrate compounds, specially of those with higher boiling point, resulting in larger rate coefficients for the investigated hydroxyl radical reactions. However, the present measurements are also affected by uncertainties since the smooth infrared features of the longer DBE esters make a very accurate analysis of the reaction spectra quite difficult. Because of the difficulties in measuring these compounds the agreement between the values measured here and those of Aschmann and Atkinson is acceptable.

Atmospheric implication

The atmospheric degradation of volatile organic compounds is initiated by reaction with OH radicals, Cl atoms, ozone, NO₃ radicals, photolysis and wet/dry deposition.

As discussed by Notario *et al.* [51] and Wallington *et al.* [52], for typical tropospheric concentrations of Cl atoms and OH radicals, the Cl reaction is a negligible loss process for alcohols and esters compared to the OH reaction. Although no kinetic data are available for the gas-phase reactions of O₃ with primary alcohols, the reactions are expected to be of negligible importance; further, since ozone does not react to a significance extent with aldehydes and ketones [53], reaction of O₃ with esters is also not expected to be important. Similarly, the gas-phase reaction of the investigated compounds with NO₃ radicals are expected to be extremely slow. Data of Calvert and Pitts [54] indicate that photolysis of alcohols and esters are only relevant below 200 nm and 240 nm, respectively, and will not be of any significance in the lower troposphere. Further, there were no indication of significant photolysis losses of these compounds in the kinetic experiments performed in this study.

Since the chemical degradation processes mentioned above – reaction with Cl atoms, O₃, NO₃ radicals, and photolysis – are considered to be of no importance as tropospheric loss processes for the investigated compounds, their overall tropospheric lifetimes are expected to be dominated mainly by reactions with OH radicals. The atmospheric concentration levels of hydroxyl radicals exhibit a temporal, geographical and meteorological variability. The diurnally, seasonally and annually averaged global tropospheric hydroxyl radical concentration is ca. 1.0×10^6 molecule cm⁻³ (24 h average) [55]. The OH reaction rate coefficients measured here can be

combined with the above reported hydroxyl radical concentration, to obtain estimates of their tropospheric lifetimes (Table 3.3).

Substance	τ in days
1-butanol	1.4
1-pentanol	1.1
methyl propionate	12.4
dimethyl succinate	6
dimethyl glutarate	5.3
dimethyl adipate	3.1

Table 3.3: Tropospheric lifetimes with respect to reaction with OH radicals.

The tropospheric lifetimes estimated for 1-butanol and 1-pentanol due to reaction with OH are around 1 day. Both alcohols are destroyed relatively rapidly close to the emission source; however, meteorological conditions and local release patterns may also determine their geographical distribution (local-scale transport). 1-Butanol and 1-pentanol have Henry's law coefficients of 128 M atm^{-1} [56] and 80 M atm^{-1} [57], respectively and are readily soluble in water, 77g/L and 27g/L at 20°C for 1-butanol and 1-pentanol, respectively, suggesting that wet deposition may also be an important sink process for these species.

Esters show longer tropospheric chemical lifetimes ranging from a few days for the dibasic esters to 12 days for methyl propionate. These species survive long enough to become well dispersed from the source origin with regional scale transport being likely; urban emissions of these compounds are, therefore, unlikely to contribute to local ozone and photooxidant formation. The low Henry's law coefficients of esters, $K_H = 8 \text{ M atm}^{-1}$, $K_H = 6.1 \text{ M atm}^{-1}$ for methyl acetate and methyl propionate, respectively [58], probably precludes wet deposition from being a significant atmospheric loss mechanism for methyl propionate and the dibasic esters.

While the rate coefficients for the gas-phase reactions of the OH radical with alcohols and esters determine their tropospheric chemical lifetimes, the ozone formation arising from the photooxidation of these compounds in the troposphere also depends on the mechanism and products of the reactions subsequent to the initial OH radical attack. In particular, the amounts of NO converted to NO_2 , organic nitrate formed and OH radicals regenerated during the reactions subsequent to the initial OH attack determine the importance of their ozone formation potentials. These aspects will be discussed in Chapter 7 on the basis of the results of

the product studies on the atmospheric degradation of the two alcohols (1-pentanol and 1-butanol) and two esters (methyl propionate and dimethyl succinate).

SAR method

On the basis of the available kinetic data for gas-phase OH radical reactions, Atkinson and Kwok [28, 29] developed a method to estimate rate coefficients for the reactions of OH radicals with organic compounds at room temperature and atmospheric pressure. This so-called *SAR* (*Structure–Activity Relationship*) method is based on the observation that the gas-phase OH radical reaction with organic compounds proceeds by a number of separate processes which are assumed to be additive and can, therefore, be dealt with individually. For the organic compounds whose OH radical reaction proceeds by a H-atom abstraction from C–H and O–H bonds – the compounds investigated in this work belong to this case – the calculation of overall reaction rate coefficient is based upon the estimation and the addition of group rate coefficients for the H-atom abstraction from the different –CH₃, –CH₂–, >CH– and –OH groups in the molecule. The –CH₃, –CH₂–, >CH– and –OH rate coefficients depend on the identity of the substituents attached to these groups, with:

$$\begin{aligned}k(\text{CH}_3\text{-}X) &= k_{\text{prim}} \cdot F(X) \\k(X\text{-CH}_2\text{-}Y) &= k_{\text{sec}} \cdot F(X) \cdot F(Y) \\k(X\text{-CH-}Y, \text{-}Z) &= k_{\text{tert}} \cdot F(X) \cdot F(Y) \cdot F(Z)\end{aligned}$$

where k_{prim} , k_{sec} and k_{tert} are the rate coefficient per –CH₃, –CH₂– and >CH– group for a “standard” substituent $X = Y = Z = \text{–CH}_3$, and $F(X)$, $F(Y)$ and $F(Z)$ are the substituent factors for the corresponding substituents.

The available kinetic data for gas-phase OH radical reactions enabled group rate coefficients k_{prim} , k_{sec} and k_{tert} to be derived: $k_{\text{prim}} = 0.136 \times 10^{-12} \text{ cm}^3 \text{ molecule}^{-1} \text{ s}^{-1}$; $k_{\text{sec}} = 0.934 \times 10^{-12} \text{ cm}^3 \text{ molecule}^{-1} \text{ s}^{-1}$ and $k_{\text{tert}} = 1.94 \times 10^{-12} \text{ cm}^3 \text{ molecule}^{-1} \text{ s}^{-1}$ [28, 29]. In addition, the rate coefficient for the H-atom abstraction from the –OH group has been derived to be $k_{\text{abst}}(\text{–OH}) = 0.14 \times 10^{-12} \text{ cm}^3 \text{ molecule}^{-1} \text{ s}^{-1}$. The substituent factors used for estimating the OH reaction rate coefficients of the compounds investigated in this work are the following: $F(\text{–CH}_3) = 1$; $F(\text{–CH}_2\text{–}) = 1.23$; $F(\text{–OH}) = 3.5$. In Table 3.4 the experimental rate coefficients from the present work are compared with calculated values using the *SAR* technique.

Table 3.4: Comparison between experimental and calculated rate coefficients (*SAR-1*, -2, and -3) for the reactions of OH radicals with the investigated oxygenated organic compounds.

Substance	this work	<i>SAR-1</i> ^a	<i>SAR-2</i> ^b	<i>SAR-3</i> ^c
1-butanol	$(8.28 \pm 0.85) \times 10^{-12}$	6.92×10^{-12}	<i>d</i>	<i>d</i>
1-pentanol	$(1.11 \pm 0.11) \times 10^{-11}$	8.33×10^{-11}	<i>d</i>	<i>d</i>
methyl propionate	$(9.29 \pm 1.13) \times 10^{-13}$	6.74×10^{-13}	10.37×10^{-13}	8.06×10^{-13}
dimethyl succinate	$(1.95 \pm 0.27) \times 10^{-12}$	1.15×10^{-12}	2.69×10^{-12}	1.71×10^{-12}
dimethyl glutarate	$(2.18 \pm 0.30) \times 10^{-12}$	2.56×10^{-12}	1.53×10^{-11}	5.67×10^{-12}
dimethyl adipate	$(3.73 \pm 0.59) \times 10^{-12}$	3.97×10^{-12}	1.01×10^{-11}	6.02×10^{-12}

^a $F(-\text{CH}_2\text{C}(\text{O})\text{O}) = F(-\text{CH}_2) = 1.23$.

^b $F(-\text{CH}_2\text{C}(\text{O})\text{O}) = F(-\text{CH}_2\text{C}(\text{O})-\text{R}) = 3.9$.

^c $F(-\text{CH}_2\text{C}(\text{O})\text{O}) = 2.2$ [26].

^d no changes.

Fair agreement is found between the OH radical reaction rate coefficients measured for 1-butanol and 1-pentanol and the calculated values. The slight discrepancy – the measured rate coefficients are ca. 15 to 25% higher than the calculated ones – probably indicates that the OH functional group has a more significant effect on the $-\text{CH}_2-$ groups, specially in α and β positions, than that assumed in the *SAR* estimation method.

For the estimation of the OH radical reaction rate coefficients of the esters, additional factors were employed: $F(-\text{OC}(\text{O})\text{R}) = 1.6$ and $F(-\text{C}(\text{O})\text{OR}) = 0.31$ [59]. This latter value was used instead of the value $F(-\text{C}(\text{O})\text{OR}) = 0.74$ derived by Kwok and Atkinson [28, 29] since it is a more definitive derivation of $F(-\text{C}(\text{O})\text{OR})$ from recent measurements of rate coefficients for a series of lactates.

In the calculation (Table 3.4, column *SAR-1*) the substituent factor $F(-\text{CH}_2-\text{C}(\text{O})\text{OR})$ is considered to be equal to $F(-\text{CH}_2-) = 1.23$. It is assumed that the $-\text{C}(\text{O})\text{OR}$ group has no influence on the CH_3 or CH_2 group in β position at the acyl end of the ester. As shown in Table 3.4, the OH reaction rate coefficients calculated for the esters and reported in column *SAR-1* are in reasonable agreement with the measured values.

It can also be assumed that the $-\text{C}(\text{O})\text{OR}$ group has the same influence on the CH_3 or CH_2 group in β position in the acyl end of the ester as the ketone group $-\text{C}(\text{O})\text{R}$; i.e. $F(-\text{CH}_2-\text{C}(\text{O})\text{OR}) = F(-\text{CH}_2-\text{C}(\text{O})\text{R}) = 3.9$ (Table 3.4, column *SAR-2*). In this case, all the calculated values, listed in column *SAR-2*, exceed the experimental ones. On the basis of this observation, Le Calvé *et al.* [26], using a kinetic database for aliphatic acetates and methyl

esters, derived a value $F(-\text{CH}_2-\text{C}(\text{O})\text{OR}) = 2.2$ (Table 3.4, column *SAR-3*), which is intermediate between the values used for the calculation in column *SAR-1* and *SAR-2* of Table 3.4. However, an enhancement of the C–H bonds reactivity at the β position to a carbonyl C=O produces a slightly better fit between calculated and experimental rate coefficients only for the methyl propionate and for dimethyl succinate (Table 3.4); the significant discrepancy shown for dimethyl glutarate and dimethyl adipate suggests the need of a larger database on esters and diesters than that currently available in order to be able to better define the reactivity of the CH_2 group at the β position to the carbonyl group in ester molecules.

In conclusion, the *Structure–Activity Relationship* method appears to be relatively effective in predicting rate coefficients for the reaction of OH radicals with alcohols and esters and can be used to approximately estimate the relative importance of the attack of the OH radical at the individual sites of the molecule.

3.2 Chlorine atom reaction rate coefficients

3.2.1 Results

Rate coefficients have been measured for the reaction of chlorine atoms with methyl propionate (MPR) and its major degradation products – propionic formic anhydride (PRFA), propionic acid (PRA) and methyl pyruvate (MPYR) – and with the three dibasic esters dimethyl succinate (DBE-4), dimethyl glutarate (DBE-5), dimethyl adipate (DBE-6). The observed losses of each substrate compound versus those of reference compounds in the presence of chlorine atoms are plotted in Figure 3.2, according to either Eq. I or Eq. II, depending on whether or not correction for wall loss was necessary.

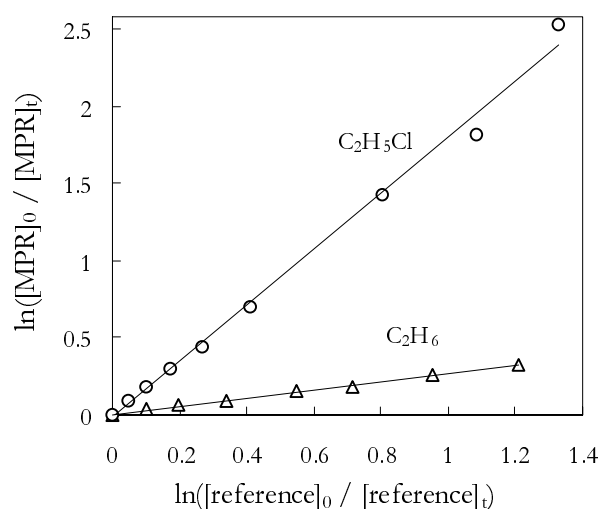
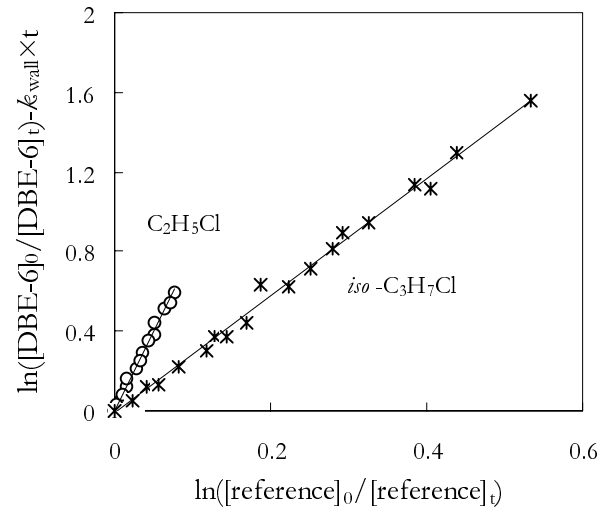
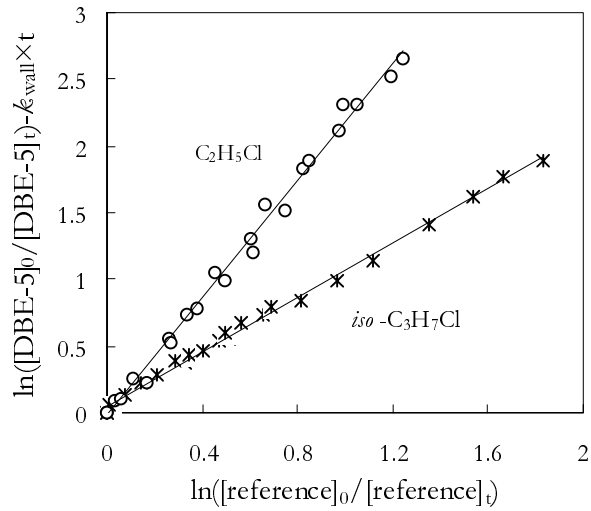
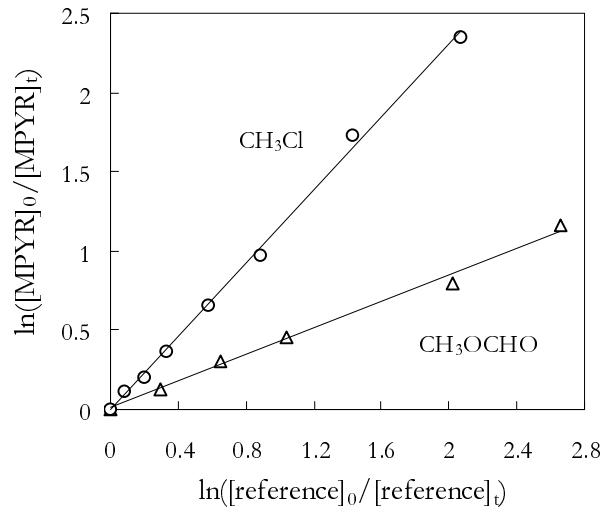
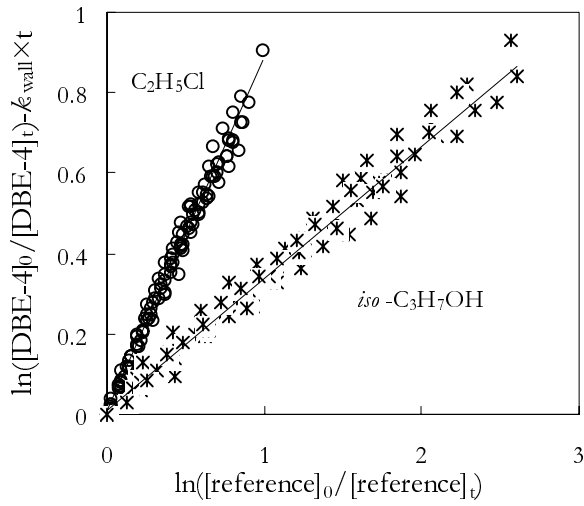
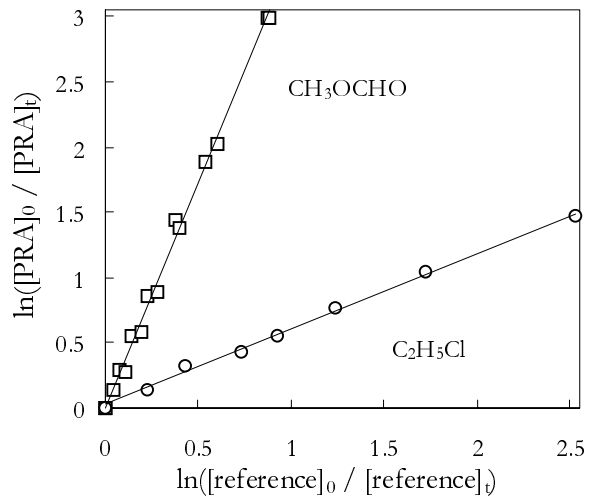
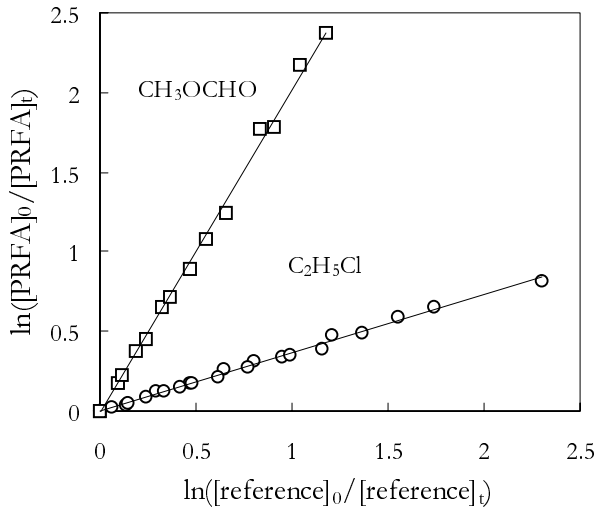
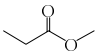
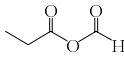
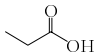
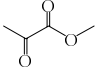
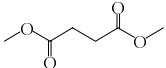
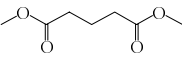
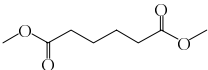


Figure 3.2: Plot of the kinetic data according to either Eq. I or Eq. II for the gas-phase reactions of Cl atoms with the investigated oxygenated organic compounds.



Reasonably good straight line plots were observed and least-square analysis of these data led to the rate coefficient ratios ($\pm 2\sigma$) given in Table 3.5.

Table 3.5: Rate coefficient ratios $k_{\text{substrate}}/k_{\text{ref.}}$ and rate coefficients k_{Cl} (in $10^{-12} \text{ cm}^3 \text{ molecule}^{-1} \text{ s}^{-1}$ units) for the gas-phase reactions of Cl atoms with the investigated oxygenated organic compounds.

Substrate	Reference	$k_{\text{substrate}}/k_{\text{ref.}}^a$	k_{Cl}^b
methyl propionate 	Cl-ethane	1.77 ± 0.02	14.9 ± 1.5
	ethane	0.27 ± 0.02	15.4 ± 1.9
propionic formic anhydride 	Cl-ethane	0.36 ± 0.01	2.94 ± 0.31
	methyl formiate	2.04 ± 0.07	2.58 ± 0.31
propionic acid 	Cl-ethane	0.58 ± 0.03	4.66 ± 0.53
	methyl formiate	3.42 ± 0.20	4.79 ± 0.55
methyl pyruvate 	methyl formiate	0.42 ± 0.04	0.58 ± 0.08
	Cl-methane	1.16 ± 0.12	0.55 ± 0.08
dimethyl succinate 	Cl-ethane	0.87 ± 0.02	7.00 ± 0.72
	<i>iso</i> -Cl-propane	0.33 ± 0.01	6.58 ± 0.68
dimethyl glutarate 	Cl-ethane	2.19 ± 0.08	17.7 ± 1.9
	<i>iso</i> -Cl-propane	1.02 ± 0.02	20.3 ± 2.0
dimethyl adipate 	Cl-ethane	7.80 ± 0.30	62.7 ± 6.7
	<i>iso</i> -Cl-propane	2.94 ± 0.10	58.8 ± 6.2

^a Indicated errors are two least-squares standard deviations.

^b Indicated errors include the estimated overall uncertainties in rate coefficients of the reference, $k_{\text{ref.}}$.

The rate coefficient ratios were placed on an absolute basis using the Cl reaction rate coefficient of the reference compounds, listed in Annex B, Table B.1. The resulting rate coefficients are also reported in Table 3.5; the quoted errors include 2σ from the statistical analysis plus an additional estimated systematic error 10% due to uncertainties in the reference rate coefficients.

3.2.2 Discussion

For all the investigated compounds, the results obtained from experiments using different reference compounds showed negligible differences. Therefore, the final values of the Cl reaction rate coefficients, reported in Table 3.6, are averages of the individual determinations together with error limits which encompass the extremes of the individual determinations.

With the exception of methyl propionate, the present work represents the first report of the rate coefficients for the reaction of chlorine atoms with all the investigated compounds [50].

Using an absolute technique, Notario *et al.* [51] reported $k_{(\text{Cl} + \text{methyl propionate})} = 1.98 \times 10^{-11} \text{ cm}^3 \text{ molecule}^{-1} \text{ s}^{-1}$ which is 24% higher than that obtained in this study. Interestingly, Christensen *et al.* [35] measured a value of $k_{(\text{Cl} + \text{methyl acetate})}$ which was 23% lower than that reported by Notario *et al.* Langer *et al.* [60] measured a value of $k_{(\text{Cl} + t\text{-butyl acetate})}$ which was 34% lower than that reported by Notario *et al.* [51], and Wallington *et al.* [61] measured a value of $k_{(\text{Cl} + \text{methyl formate})}$ which was 23% lower than that reported by Notario *et al.* [51]. It would appear that Notario *et al.* [51] have systematically overestimated the reactivity of Cl atoms towards esters.

Table 3.6: Rate coefficients (in $\text{cm}^3 \text{ molecule}^{-1} \text{ s}^{-1}$ units) for the gas-phase reactions of Cl atoms with the investigated oxygenated organic compounds.

Substance	this work
methyl propionate	$(1.51 \pm 0.22) \times 10^{-11}$
propionic formic anhydride	$(2.89 \pm 0.35) \times 10^{-12}$
propionic acid	$(4.72 \pm 0.62) \times 10^{-12}$
methyl pyruvate	$(4.99 \pm 0.96) \times 10^{-13}$
dimethyl succinate	$(6.79 \pm 0.93) \times 10^{-12}$
dimethyl glutarate	$(1.90 \pm 0.33) \times 10^{-11}$
dimethyl adipate	$(6.08 \pm 0.86) \times 10^{-11}$

Notario *et al.* [51] have tentatively applied the *Structure–Activity Relationship (SAR)* method to the reaction of chlorine atoms with a series of esters. The parameters $k_{\text{prim}} = 3.32 \times 10^{-11} \text{ cm}^3 \text{ molecule}^{-1} \text{ s}^{-1}$; $k_{\text{sec}} = 8.34 \times 10^{-11} \text{ cm}^3 \text{ molecule}^{-1} \text{ s}^{-1}$; $k_{\text{tert}} = 6.09 \times 10^{-11} \text{ cm}^3 \text{ molecule}^{-1} \text{ s}^{-1}$ and $F(-\text{CH}_3) = 1$ and $F(-\text{CH}_2-) = 0.79$ were deduced from the existing kinetic database for the gas-phase reactions of Cl atoms with alkanes [62]. The substituent factors specific to the esters were derived from the kinetic data for the Cl atom reaction rate coefficients of a series of esters [51]: $F(-\text{CH}_2-\text{C}(\text{O})\text{OCH}_3) = 0.46$; $F(-\text{OC}(\text{O})\text{R}) = 0.05$ and $F(-\text{C}(\text{O})) = 0.04$.

The estimation method provides the following rate coefficients (in $\text{cm}^3 \text{ molecule}^{-1} \text{ s}^{-1}$ units): $k_{(\text{Cl} + \text{methyl propionate})} = 2.03 \times 10^{-11}$; $k_{(\text{Cl} + \text{DBE-4})} = 6.39 \times 10^{-12}$; $k_{(\text{Cl} + \text{DBE-5})} = 2.62 \times 10^{-11}$; $k_{(\text{Cl} + \text{DBE-6})} = 6.90 \times 10^{-11}$ for the reaction of chlorine atoms with methyl propionate, dimethyl succinate, dimethyl glutarate and dimethyl adipate, respectively. The calculated rate coefficients are in reasonable agreement with the measured values.

Chapter 4

Atmospheric oxidation of alcohols

In this work, mechanistic studies were carried out on the atmospheric degradation of two primary alcohols: 1-butanol and 1-pentanol.

The dominant chemical loss process for aliphatic alcohols in the troposphere is by reaction with the OH radical [21, 63]. The OH radical initiated oxidation of both alcohols was performed, under atmospheric conditions and in the presence of NO_x , in the *EUPHORE* outdoor photoreactor [March 1999: 1-pentanol oxidation; March 2000: 1-butanol oxidation].

A few laboratory experiments were also performed in the 480 ℓ reactor in Wuppertal.

In the following section, a general degradation mechanism for both alcohols will be developed, and afterwards, the experimental results will be presented and discussed for the individual alcohols.

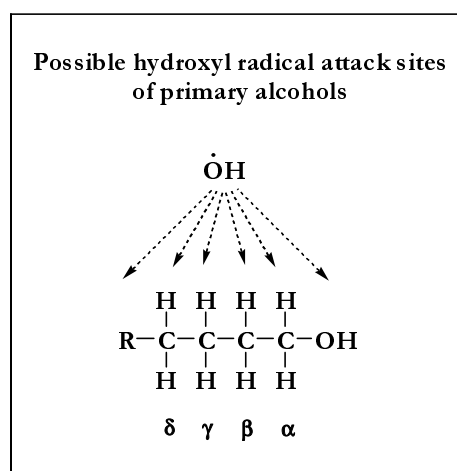
4.1 General mechanistic considerations on the degradation of primary alcohols

The OH radical reaction with alcohols proceeds by H-atom abstraction from the various $-\text{CH}_3$, $-\text{CH}_2-$ and $-\text{OH}$ groups present in the molecule.

The estimation technique (*SAR* method) of Atkinson and Kwok [28, 29] allows the percentage of OH attack at the individual sites to be approximately estimated. The method clearly indicates that, in the case of 1-butanol and 1-pentanol, the H-atom abstraction from the $-\text{CH}_3$, and $-\text{OH}$ groups are expected to be of negligible importance, accounting

for only 2.4% and 2.5%, respectively, of the overall reaction of 1-butanol with OH radical and for 2% and 1%, respectively, of the overall reaction of 1-pentanol with OH radical.

Thus, the only processes which require consideration in the degradation of the two investigated primary alcohols are the H-atom abstractions from the various $-\text{CH}_2-$ groups. In



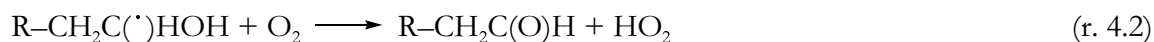
particular, the present product studies strongly suggest that the main degradation pathway of primary alcohol is hydrogen abstraction from the $-\text{CH}_2-$ group at the α position to the $-\text{OH}$ functional entity due to the activating effect of this group. Furthermore, the reaction pathways involving the H-atom abstraction from $-\text{CH}_2-$ groups at the β , γ etc. positions gradually lose in importance since the activating effect lessens with increasing distance from the functional group.

In the following discussion, the general formula $\text{R}-\text{CH}_2\text{CH}_2\text{OH}$ is used to indicate both investigated primary alcohols, with $\text{R} = \text{CH}_3\text{CH}_2$ in the case of 1-butanol and with $\text{R} = \text{CH}_3\text{CH}_2\text{CH}_2$ in the case of 1-pentanol.

- H-atom abstraction from $-\text{CH}_2-$ entity in α position to the $-\text{OH}$ functional group produces an α hydroxy alkyl radical:

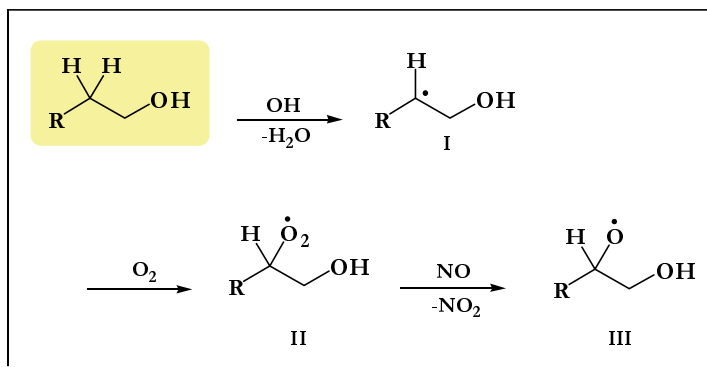


The α hydroxy alkyl radical then reacts rapidly with oxygen to form the corresponding aldehyde in unit yield [21]:



To determine the role of atmospheric oxygen in the reaction with α hydroxy alkyl radicals, Baxley and Wells [31] performed studies on the reaction of ^{18}O labelled 2-butanol with OH. The product analysis showed the formation, among the reaction products, of methyl ethyl ketone which could only be formed by the OH abstraction of the α hydrogen and the subsequent reaction of the α hydroxy alkyl radical with O_2 . Methyl ethyl ketone, $\text{CH}_3\text{CH}_2\text{C}(^{18}\text{O})\text{CH}_3$, analysed for the presence of ^{18}O contained only ^{18}O and no ^{16}O . Similar observations were made for 2-pentanol [31]. Hence, atmospheric oxygen merely abstracts a hydrogen atom from the α hydroxy alkyl radical and does not attach to form a peroxy radical. Furthermore, the mechanisms proposed by Stemmler *et al.* in their studies of the reaction of 2-ethoxyethanol [64] and 2-butoxyethanol [65] with OH also support that the reaction of the α hydroxy alkyl radical with O_2 proceeds via hydrogen abstraction rather than O_2 addition, since no other products such as carboxylic acids were found in the product analysis. Consequently, the α hydroxy alkyl radicals formed in the reaction of 1-butanol and 1-pentanol with OH are also expected to react with oxygen in a similar manner.

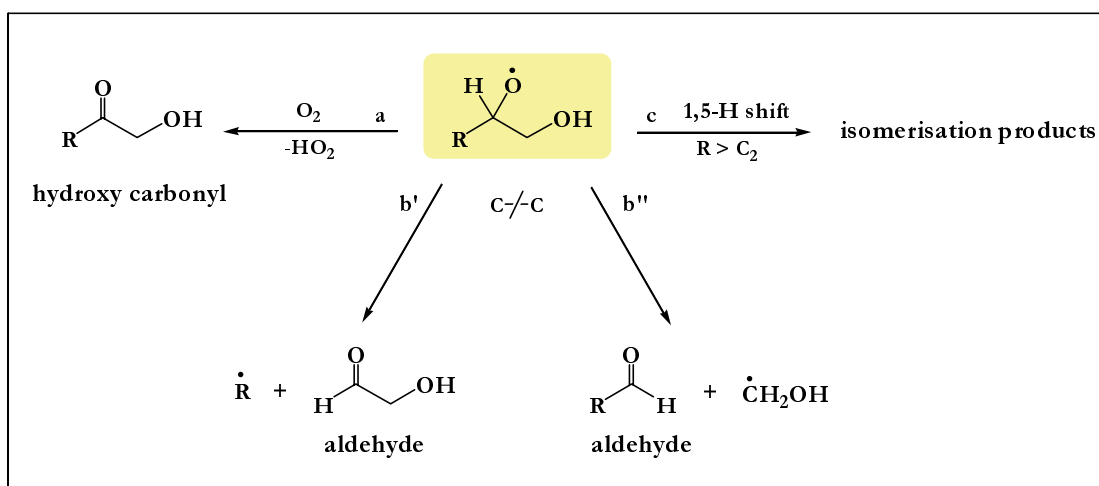
- H-atom abstraction from $-\text{CH}_2-$ groups at the β , γ etc. positions to the $-\text{OH}$ functional entity produces the corresponding (β , γ etc.) hydroxy alkyl radicals (**I**, in Scheme 4.1) which react rapidly under atmospheric conditions solely with O_2 to form (β , γ etc.) hydroxy alkyl peroxy radicals, $\text{RO}_2\cdot$ (**II**, in Scheme 4.1). The further reaction of the hydroxy alkyl peroxy radicals with NO leads to the formation of the corresponding (β , γ etc.) hydroxy alkoxy radical, $\text{RO}\cdot$, (**III**, in Scheme 4.1). The reaction pathways described above are outlined in Scheme 4.1 for H-atom abstraction from $-\text{CH}_2-$ groups at the β , γ etc. positions in the alcohol molecule.



Scheme 4.1: Reaction scheme for the OH radical initiated oxidation of alcohols, $\text{R}-\text{CH}_2\text{CH}_2\text{OH}$: H-atom abstraction from $-\text{CH}_2-$ groups at the β , γ etc. positions.

Analogous to the alkoxy radicals formed from the alkanes, the (β , γ etc.) hydroxy alkoxy radicals can then react with O_2 , unimolecularly decompose into two shorter-chain species, or, if possible, isomerise. These three reactions are shown in Scheme 4.2 for a general hydroxy alkoxy radical.

Bimolecular reaction with O_2 (channel a, in Scheme 4.2) leads to the formation of a (β , γ etc.) hydroxy carbonyl and the HO_2 radical. The decomposition pathway has two possible channels (channels b' and b''), both yielding an aldehyde and an alkyl radical. The unimolecular isomerisation of alkoxy radicals (channel c) proceeds via a cyclic transition state in which an H-atom is abstracted by the alkoxy oxygen. Because of the ring strain involved, 1,4-H shift isomerisations are calculated to be much less important (by a factor of $\sim 5 \times 10^3$ at 298 K [66]) than 1,5-H shift isomerisations proceeding through a six-membered, essentially strain-free, transition state.



Scheme 4.2: Tropospheric reactions of β , γ etc. hydroxy alkoxy radicals derived from alcohols.

The relative importance of the reaction pathways for the individual β , γ etc. hydroxy alkoxy radicals described above – reaction with O_2 , decomposition and isomerisation – will be discussed separately, for 1-pentanol and 1-butanol, on the basis of the results from the present and previous [67, 68, 69] product studies. The empirical estimation method proposed by Atkinson [70, 71, 72] to calculate the rate constants for the alkoxy radical reaction pathways is also applicable to the hydroxy alkoxy radicals formed from the reaction of 1-pentanol and 1-butanol with OH, therefore, these estimation predictions will be compared, in the following discussion, with the experimental data concerning the dominant reaction pathways.

4.2 Atmospheric degradation of 1-pentanol

The products studies on the gas-phase oxidation of 1-pentanol were carried out in the *EUPHORE* outdoor photoreactor in Valencia/Spain in March 1999. The oxidation of 1-pentanol was initiated by reaction with OH radicals generated by the photolysis of HONO, prepared as described in Annex D. To compensate for the consumption of HONO during the 3-5 hours duration of the experiments, addition of HONO was normally repeated at least twice to maintain the level of OH radicals and also the conversion of $\text{RO}_2\cdot$ to $\text{RO}\cdot$ via $\text{RO}_2\cdot + \text{NO}$ reactions. Test experiments on a 1-pentanol-air mixture showed that losses of the compound to the wall of the reactor or via photolysis were negligible compared to the measured decay of 1-pentanol during the experiments.

The experimental conditions employed are listed in Annex B, Table B.3.

4.2.1 Results

GC-PID and HPLC analysis of the products formed on irradiation of HONO-1-pentanol-air mixtures showed the formation of pentanal, butanal, propanal, ethanal and formaldehyde among the products. Typical GC-PID chromatograms for the reaction of 1-pentanol + OH radicals are shown in Figure 4.1.

In addition, a product has been tentatively identified as 5-hydroxy-2-pentanone on the basis of a comparison of its HPLC retention time and its infrared spectrum with that of the authentic compound. Vapour samples of 5-hydroxy-2-pentanone were introduced into the evacuated chamber by injecting known amounts of liquid samples of the commercially available compound into a stream of N_2 entering the chamber. The infrared spectra thus acquired showed a relatively rapid ($k = 2.19 \times 10^{-1} \text{ s}^{-1}$) conversion of the δ hydroxy carbonyl to 4,5-dihydro-2-methyl furan. A calibrated IR spectrum of 4,5-dihydro-2-methyl furan obtained from the authentic sample was used to subtract its IR features from the mixed 5-hydroxy-2-pentanone/4,5-dihydro-2-methyl furan spectrum to derive a semi-quantitative spectrum of 5-hydroxy-2-pentanone.

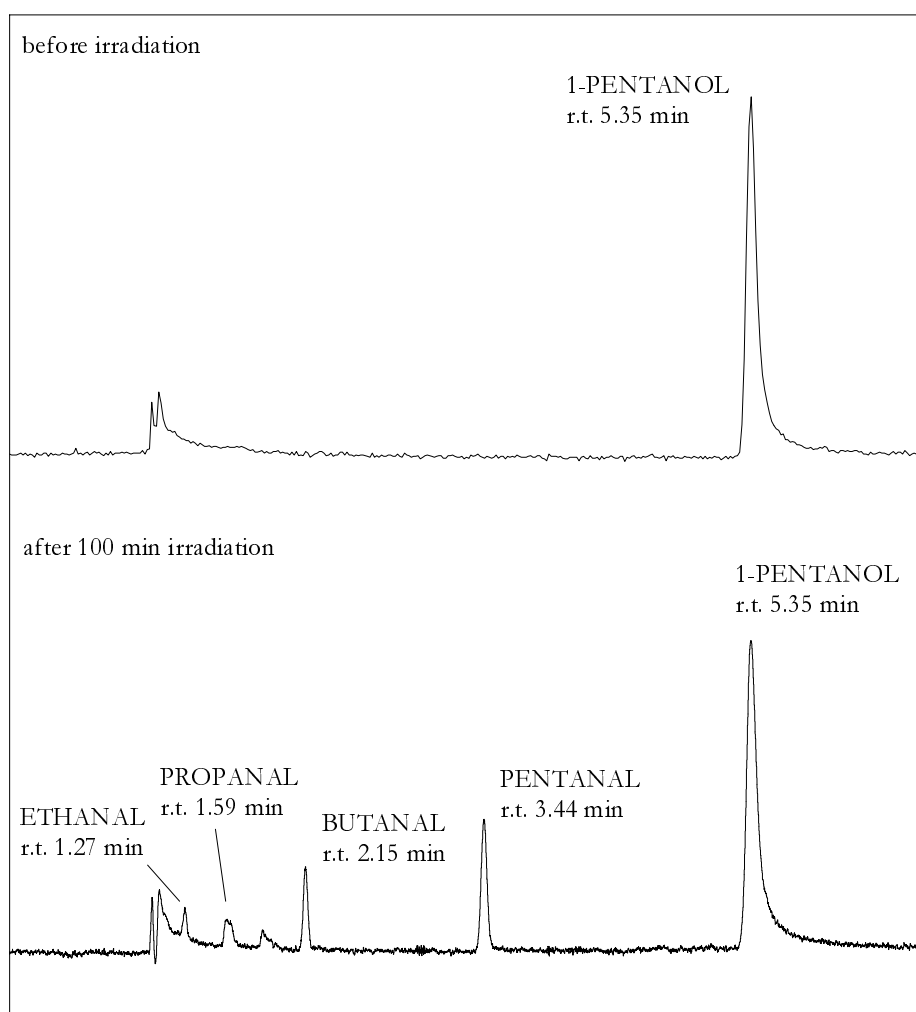
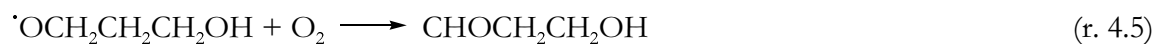
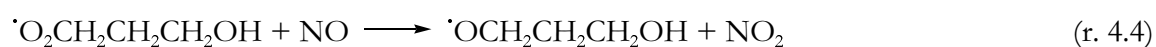
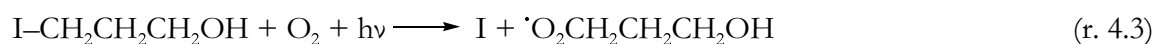


Figure 4.1: GC-PID chromatograms obtained from a HONO-1-pentanol-air mixture before irradiation (above) and after 100 min irradiation.

Other residual absorptions in the infrared product spectra indicated the possible presence of hydroxy and aldehydic groups such as would be expected from 3-hydroxy propanal. 3-Hydroxy propanal is not commercially available. An infrared spectrum of 3-hydroxy propanal, $\text{CHOCH}_2\text{CH}_2\text{OH}$, was generated by the 254 nm photolysis of 3-iodo-propanol in the presence of NO at 1000 mbar of air.



Photolysis of I-CH₂CH₂CH₂OH gives the ·CH₂CH₂CH₂OH radical which after addition of O₂ and reaction with NO leads to the ·OCH₂CH₂CH₂OH alkoxy radical. Since the ·OCH₂CH₂CH₂OH radical cannot undergo isomerisation, there are only two possible fates for it; reaction with O₂ to give 3-hydroxy propanal and elimination of HCHO to give the ·OCH₂CH₂OH radical. The major fate of the ·OCH₂CH₂CH₂OH radical was observed to be the oxygen reaction to form 3-hydroxy propanal which was identified by the virtue of its IR features at 3618, 2825, 2724, 1743 and 1070 cm⁻¹. Decomposition via elimination of HCHO accounted for about 9% of the loss of the ·OCH₂CH₂CH₂OH alkoxy radical.

Butanal, propanal, ethanal and HCHO could also be formed in secondary reactions of some of the primary aldehydic products. However, under the conditions employed in the experiments, the contribution from secondary reactions is probably very minor. With the high NO_x concentrations employed in the experiments, the main fate of the alkyl peroxy radicals, formed in the degradation reactions of the higher aldehydes, will be formation of the corresponding stable peroxy acyl nitrate and not a lower aldehyde.

To derive the formation yields of the aldehydic products, their measured concentrations had to be corrected for further reaction with OH radicals, photolysis and dilution losses. Corrections were performed using the procedure [48] described in section 2.3. Rate coefficients for reaction of OH radicals with the aldehydic products were taken from the literature [72, 73]. The following values of k_{OH} (in units of 10⁻¹¹ cm³ molecule⁻¹s⁻¹) were used: pentanal, 2.96 ± 0.39; butanal, 2.06 ± 0.30; propanal, 1.71 ± 0.24; and ethanal, 1.22 ± 0.27. Photolysis frequencies for the aldehydes, k_{hv} , were taken from the literature [74]. The mean of $J(\text{NO}_2)$, measured during the experiments, was used as an indicator of the light intensity, in order to select the frequencies. The following values of k_{hv} (in units of 10⁻⁵ s⁻¹) were employed: pentanal, 2.20 ± 0.09; butanal, 0.55 ± 0.03; propanal, 1.04 ± 0.05; and ethanal, 0.29 ± 0.01.

The correction factors, $[\text{RHO}]_i^{\text{corr}} / [\text{RHO}]_i^{\text{meas}}$, were ≤3.5 for pentanal, ≤1.9 for butanal, ≤1.7 for propanal and ≤1.8 for ethanal. The estimated overall uncertainties in the OH reaction rate coefficient of 1-pentanol and in the rate coefficients for the reaction with OH and photolysis of the products led to maximum uncertainties in the correction factors of <± 15% for the formation of pentanal, butanal and ethanal and ± 6% for the formation of propanal.

The corrected aldehyde concentrations are plotted against the amount of 1-pentanol consumed in Figure 4.2. The measurement errors were principally caused by the low concentration of 1-pentanol employed in the experiments and consequently low concentrations of the products.

The random scatter of the data plotted in Figure 4.2 reflects the extent of these measurement errors in both, $\Delta[1\text{-pentanol}]$ and $[\text{RHO}]_i^{\text{corr}}$.

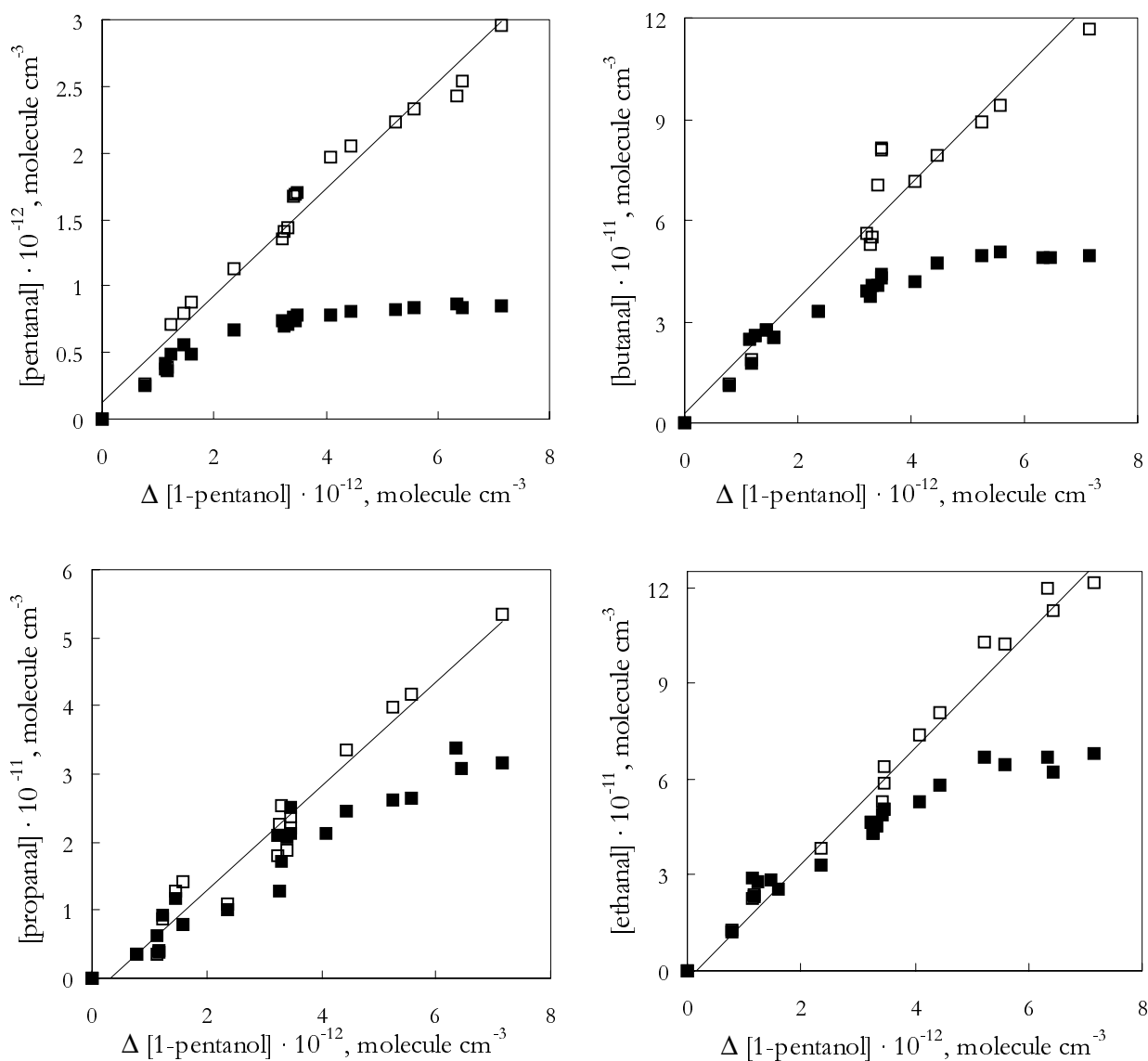


Figure 4.2: Plots of pentanal, butanal, propanal and ethanal uncorrected (■) and corrected (□) for reaction with OH radicals and photolysis (see text) against the amount of 1-pentanol consumed.

The corrected values for the formation yields are given in Table 4.1.

Table 4.1: Product formation yields from the gas-phase reaction of the OH radical with 1-pentanol in the presence of NO_x .

Product	Formation yield
Pentanal	0.405 ± 0.082
Butanal	0.161 ± 0.037
Propanal	0.081 ± 0.019
Ethanal	0.181 ± 0.042
Formaldehyde	0.251 ± 0.013
C-yield	0.70 ± 0.14

The molar formation yield of 0.251 ± 0.013 given for HCHO was derived from the uncorrected concentrations plotted against the consumption of 1-pentanol in the early stage of the reaction, when secondary processes can largely be neglected. The indicated errors in Table 4.1 are 2 least-squares standard deviations of the data shown in Figure 4.2 combined with a contribution for the overall uncertainties in the alcohol and carbonyl GC-PID calibration factors and in the correction factors (see above).

The carbonyl products observed and quantified in this work account for 70 ± 14 %C of the OH radical reaction with 1-pentanol.

4.2.2 Discussion: mechanistic considerations based on SAR and the product yield data

Using the *Structure–Activity Relationship* (SAR) technique [28, 29] it can be estimated that the relative importance of OH attack at the various $-\text{CH}_3$, $-\text{CH}_2-$ and $-\text{OH}$ groups of 1-pentanol is: from the $-\text{OH}$ group, 1%; from the $-\text{CH}_2-$ group at the α position 49%; from the $-\text{CH}_2-$ group at the β position and γ position 17%; from the $-\text{CH}_2-$ group at the δ position 14%; and from the $-\text{CH}_3$ group 2%.

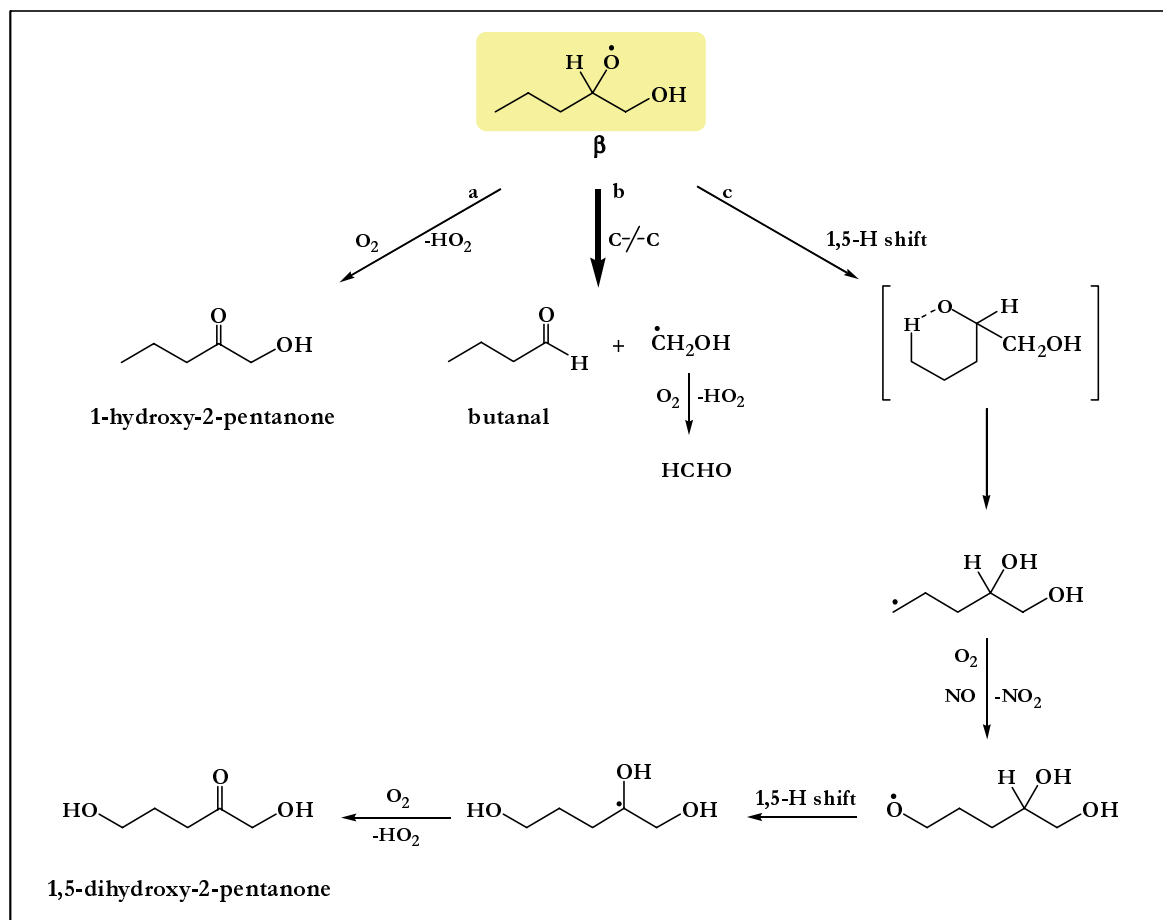
As discussed in section 4.1, the α hydroxy alkyl radical, formed by H-atom abstraction from the $-\text{CH}_2-$ group at the α position, reacts with O_2 to form pentanal in unit yield [21]:



The hydroxy alkyl radicals (**I**, in Scheme 4.1) formed after H-atom abstraction from the $-\text{CH}_2-$ group at the β , γ and δ positions will add O_2 to form hydroxy alkyl peroxy radicals (**II**, in Scheme 4.1) which can react with NO or NO_2 . Addition of NO_2 will form thermally unstable hydroxy alkyl peroxy nitrates. In the presence of NO , the hydroxy alkyl peroxy radicals form hydroxy alkyl nitrates or hydroxy alkoxy radicals (**III**, in Scheme 4.1) plus NO_2 . The contribution of the channel forming organic nitrates in these $\text{RO}_2^\cdot + \text{NO}$ reactions is considered to be small ($\leq 6\%$). In other studies [67, 72], it has been found that, at room temperature and atmospheric pressure, hydroxy alkyl nitrate formation from the reaction of C_n -hydroxy alkyl peroxy radicals with NO is approximately half of the alkyl nitrate formation yields from the reactions of C_n -alkyl peroxy radical with NO . The yield of pentyl nitrate [75], relative to the n -pentane consumed in $\text{CH}_3\text{ONO-NO-}n$ -pentane air irradiations, is 0.117 ± 0.013 .

The further expected reactions of the alkoxy radicals are outlined in Scheme 4.3, Scheme 4.4 and Scheme 4.5. In these reaction schemes, the alkyl and alkyl peroxy radicals have been omitted for clarity and only the reactions of the alkoxy and acyl radicals involved are shown.

The β hydroxy alkoxy radical (β , in Scheme 4.3) formed after the H-atom abstraction from the $-\text{CH}_2-$ group at the β position (Scheme 4.3) can react with O_2 (channel a), decompose (channel b) or isomerise via a 1,5-H shift through a six-membered transition state (channel c). The alkoxy radical $^\cdot\text{OCH}_2\text{CH}_2\text{CH}_2\text{CH}(\text{OH})\text{CH}_2\text{OH}$, formed after the isomerisation reaction, is predicted to undergo a further isomerisation, significantly more rapid than the first isomerisation, to give 1,5-dihydroxy-2-pentanone, $\text{HOCH}_2\text{CH}_2\text{CH}_2\text{C}(\text{O})\text{CH}_2\text{OH}$ [21]. However, the isomerisation reaction, which involves an H-atom abstraction from a $-\text{CH}_3$ group, is expected to be minor [68, 69]. Of the remaining pathways, the experimental data of the present study strongly support that decomposition of the β hydroxy alkoxy radical to butanal and HCHO will dominate over reaction with oxygen. Considering that the β hydroxy alkoxy radical is calculated to account for 17% of the overall reaction of 1-pentanol with OH and that butanal is identified with a molar formation yield of $16.1 \pm 3.7\%$, this implies that decomposition is the dominant reaction pathway of the β hydroxy alkoxy (β , in Scheme 4.3). The present results are in good agreement with the experimental data of previous studies [68, 69].

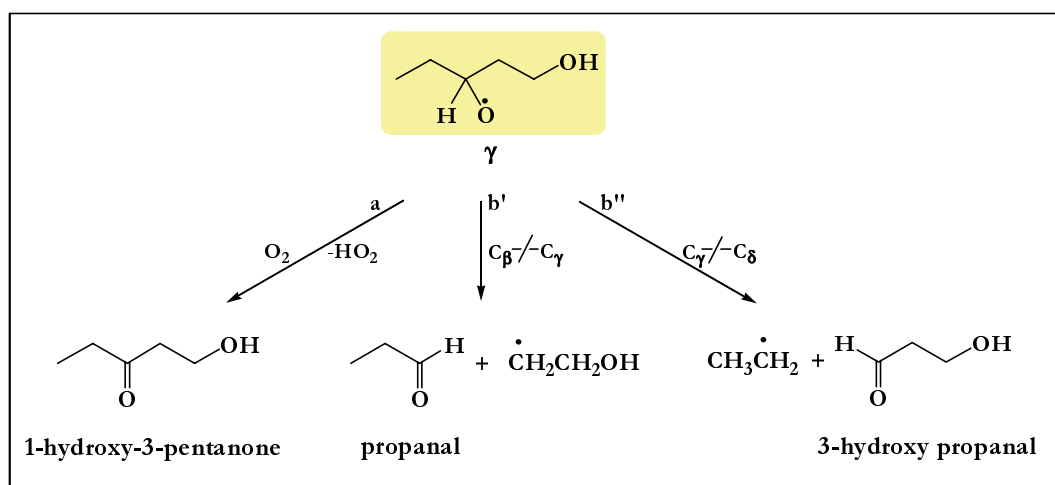


Scheme 4.3: Reactions of the β hydroxy alkoxy radical: this radical accounts for an estimated 17% of the overall reaction of 1-pentanol with OH.

On the basis of the enthalpy for the O_2 reaction and decomposition of the $\text{CH}_3\text{CH}_2\text{CH}_2\text{CH}(\text{O}^\cdot)\text{CH}_2\text{OH}$ alkoxy radical, and using the estimation method of Atkinson [70, 71], decomposition of the β hydroxy alkoxy radical is predicted to dominate over the reaction with oxygen with a estimated decomposition rate k_d of $1.0 \times 10^5 \text{ s}^{-1}$ [76] compared to a O_2 reaction rate $k_{\text{O}_2}[\text{O}_2]$ of $4.1 \times 10^4 \text{ s}^{-1}$, at 298 K [76]. The isomerisation rate constant, k_{isom} , is calculated to be $2.0 \times 10^5 \text{ s}^{-1}$. This would indicate that decomposition and isomerisation of the β hydroxy alkoxy radical (β , in Scheme 4.3) may well be of comparable importance at room temperature. There are, therefore, quantitative differences between the calculated ratio $k_{\text{isom}}/k_d = 2$ [76] and the experimental ratio $k_{\text{isom}}/k_d \approx 0.2$ as derived from previous studies [68, 69] and supported by the present experimental observations.

The γ hydroxy alkoxy radical (γ , in Scheme 4.4) formed after the H-atom abstraction from the $-\text{CH}_2-$ group at the γ position (Scheme 4.4) cannot undergo isomerisation via a six-membered transition state, and hence reaction with O_2 and decomposition (for which there are two

channels) are the only possible pathways. The two decomposition channels can lead to the formation of either propanal and the $\dot{\text{C}}\text{H}_2\text{CH}_2\text{OH}$ radical (channel b') or 3-hydroxy propanal and the $\text{CH}_3\dot{\text{C}}\text{H}_2$ radical (channel b''). A previous study [77] has indicated that the fate of the $\dot{\text{O}}\text{CH}_2\text{CH}_2\text{OH}$ alkoxy radical is 82% decomposition to form HCHO, as a result of the "hot alkoxy radical effect". The other possible pathway of the $\dot{\text{O}}\text{CH}_2\text{CH}_2\text{OH}$ radical is reaction with O_2 (18%) forming glycolaldehyde, CHOCH_2OH . Glycolaldehyde formation was not observed using any of the analytical techniques (GC-PID, HPLC and FTIR absorption spectroscopy) indicating that its yield must be very low. Under atmospheric conditions, reaction with O_2 to form ethanal is the sole loss process of the ethyl radical [21, 78].



Scheme 4.4: Reactions of the γ hydroxy alkoxy radical: this radical accounts for an estimated 17% of the overall reaction of 1-pentanol with OH.

Residual absorptions in the infrared product spectra indicate the possible presence of hydroxy and aldehydic groups such as would be expected from 3-hydroxy propanal. Unfortunately, the multitude of all possible hydroxy carbonyl products formed in the system made a reliable identification of 3-hydroxy propanal difficult and speculative.

For unimolecular decompositions of hydroxy alkoxy radicals, the decomposition rate constants, k_d , are given by the Arrhenius expression:

$$k_d = A_d e^{-E_d/RT} \text{ s}^{-1} \quad (\text{X})$$

$$\text{with } A_d = 2 \times 10^{14} \times d \text{ s}^{-1} \quad (\text{XI})$$

A_d is the pre-exponential factor, d is the reaction path degeneracy, R is the ideal gas constant, T the temperature in Kelvin and E_d is the Arrhenius activation energy for the alkoxy radical decomposition reaction in kcal mol^{-1} . The observations of Choo and Benson [79] support that the energetics of alkoxy radical decompositions depend on the specific alkyl leaving group and are governed by the following expression:

$$E_d = a + b \Delta H_d, \text{ kcal mol}^{-1} \quad (\text{XII})$$

where ΔH_d is the decomposition enthalpy in kcal mol^{-1} . The activation energy is dependent on the specific alkyl leaving group, represented in Eq. XII by parameter a . Based on the literature data for the decomposition reactions of alkoxy radicals [72, 76], Atkinson extended the previous approach of Choo and Benson [79] and derived values for a and b :

$$E_d = [2.4 \times (\text{I.P.}) - 8.1] + 0.36 \Delta H_d, \text{ kcal mol}^{-1} \quad (\text{XIII})$$

where the value of a is correlated with the ionisation potential, I.P., in eV of the alkyl radical leaving-group and $b = 0.36$.

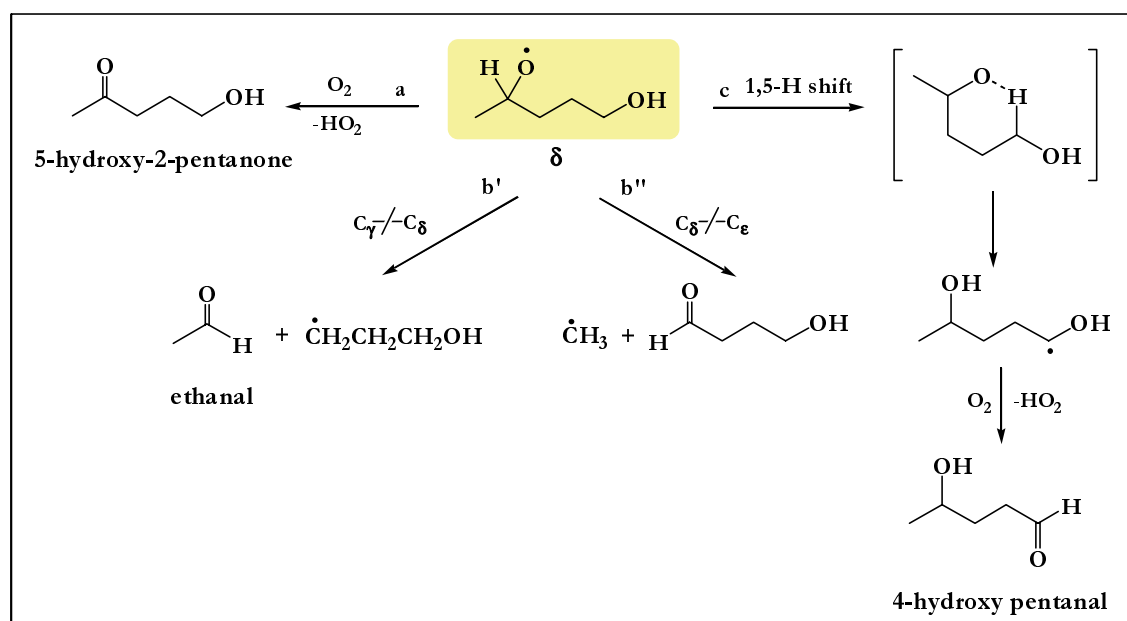
For the two leaving radicals, $\text{CH}_3\text{CH}_2\cdot$ and $\cdot\text{CH}_2\text{CH}_2\text{OH}$, involved in the γ hydroxy alkoxy radical decompositions the following values of a (in kcal mol^{-1}) are reported [80]: ethyl radical, $\text{CH}_3\text{CH}_2\cdot$, 11.4; and general primary alkyl radicals, $\text{RCH}_2\cdot$, 11.1. Therefore, the application of this estimation method indicates that both decomposition channels, b' and b'' , (Scheme 4.4) of the γ hydroxy alkoxy radical (γ , in Scheme 4.4) will occur with similar decomposition rates, k_d (Eq. X), and hence will be of comparable importance.

Since a 8% molar yield has been measured for propanal, the arguments above support by default an $\sim 8\%$ molar yield for 3-hydroxy propanal from 1-pentanol. Considering that the γ hydroxy alkoxy radical is calculated to account for 17% of the overall reaction of 1-pentanol, this implies that its reaction with O_2 will be very minor and the decomposition pathways will dominate. It is not presently possible to ascertain whether or not 1-hydroxy-3-pentanone is being formed.

The δ hydroxy alkoxy radical (δ , in Scheme 4.5) formed after the H-atom abstraction from the $-\text{CH}_2-$ group at the δ position can undergo, as shown in Scheme 4.5, reaction with O_2 (channel a) to form 5-hydroxy-2-pentanone, decomposition (channels b' and b'') yielding either ethanal and $\cdot\text{CH}_2\text{CH}_2\text{CH}_2\text{OH}$ or 4-hydroxy butanal and the methyl radical and/or

isomerisation (channel c) by an H-atom abstraction from a $-\text{CH}_2-$ group through a six-membered transition state.

Isomerisation of this δ hydroxy alkoxy radical to ultimately form 4-hydroxy pentanal after subsequent H-abstraction by O_2 , is predicted to be its dominant pathway with an isomerisation rate $k_{\text{isom}} = 3.2 \times 10^5 \text{ s}^{-1}$ [81, 82]. Hence O_2 reaction of this δ hydroxy alkoxy radical with a recommended rate constant $k_{\text{O}_2} = 8 \times 10^{-15} \text{ cm}^3 \text{ molecule}^{-1} \text{ s}^{-1}$ and decomposition with an estimated rate constant $k_{\text{d}} = 4.7 \times 10^3 \text{ s}^{-1}$ are, therefore, expected to be of minor importance [83].



Scheme 4.5: Reactions of the δ hydroxy alkoxy radical: this radical accounts for an estimated 14% of the overall reaction of 1-pentanol with OH.

To date, there are no direct experimental data concerning the relative importance of the above described reaction pathways of this δ hydroxy alkoxy radical. It is of interest to note that the $\text{CH}_3\text{CH}(\text{O}^\bullet)\text{CH}_2\text{CH}_2\text{CH}_2\text{OH}$ alkoxy radical (δ , in Scheme 4.5) is identical to that formed after a 1,5-H shift isomerisation of the 1-pentoxy radical; however, very few data exist on the isomerisation of alkoxy radicals formed from alkanes. Atkinson *et al.* [21, 84] and Kwok *et al.* [85], in studies on the OH initiated reaction of *n*-pentane observed the formation of generic δ hydroxy carbonyl compounds using a direct air sampling atmospheric pressure ionisation mass spectrometry technique. Though these results prove the isomerisation of possibly both alkoxy radicals 1-pentoxy and 2-pentoxy, they cannot provide any clear evidence for the occurrence of a further isomerisation pathway of the $\text{CH}_3\text{CH}(\text{O}^\bullet)\text{CH}_2\text{CH}_2\text{CH}_2\text{OH}$ alkoxy radical intermediate since: i) the fraction of 1-pentoxy radical formed from OH radical reaction of *n*-pentane is very

minor compared to that of 2-pentoxy radical; ii) 4-hydroxy pentanal and 5-hydroxy-2-pentanone can also result from the O_2 reaction and isomerisation, respectively, of the δ hydroxy alkoxy radical formed from isomerisation of 2-pentoxy radical; iii) in these studies [84, 85] it was not possible to distinguish between the two different δ hydroxy carbonyls since they both produce identical CAD spectra (MS/MS with collision-activated dissociation spectra) and, hence, it was not possible to establish the relative importance of the O_2 reaction and isomerisation for both δ hydroxy alkoxy radicals.

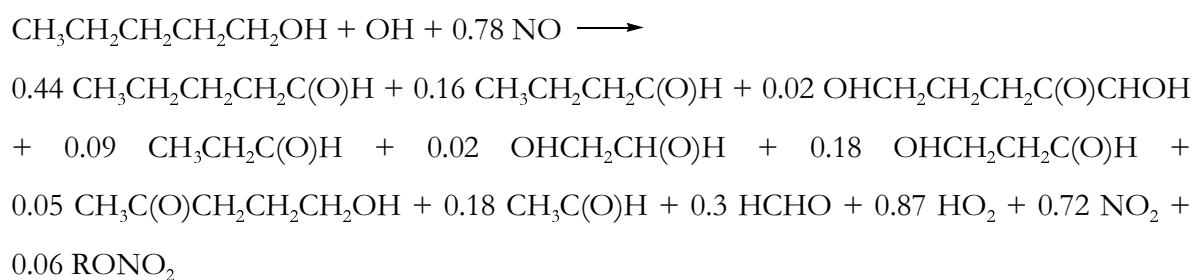
The experimental product data of this work suggest the occurrence of a decomposition pathway for the δ hydroxy alkoxy radical (δ , in Scheme 4.5) forming ethanal. As noted in Scheme 4.4, ethanal can also be formed from the decomposition of the $CH_3CH_2CH(O\cdot)CH_3CH_2OH$ radical. Based on the measured yield of 8% for propanal, the molar yield of ethanal from the channel b'' in Scheme 4.4 cannot exceed $\sim 8\%$ [see above the discussion on the γ hydroxy alkoxy radical]. Since the observed total yield of ethanal is 18% this points to the existence of (at least) two sources for this compound. Decomposition of the δ hydroxy alkoxy radical (δ , in Scheme 4.5) could also lead to the formation of ethanal. If there are no additional sources of ethanal in the experimental system, then this channel (channel b' in Scheme 4.5) would account for the remaining 10% ethanal and would also constitute the main reaction channel for the δ hydroxy alkoxy radical.

The possibility of the existence of another decomposition channel (channel b'', in Scheme 4.5) leading to a methyl radical and 4-hydroxy butanal cannot be excluded because of the lack of an authentic sample of the compound; this decomposition pathway is, however, expected to be of minor relevance, because of the lower stability of the methyl radical compared to $\cdot CH_2CH_2CH_2OH$ [86]. On the basis of the similarity of its HPLC retention time and its infrared spectrum with that of an authentic sample, a product has been tentatively identified as 5-hydroxy-2-pentanone. This product can be formed from the reaction of O_2 with the δ hydroxy alkoxy radical (δ , in Scheme 4.5). However, due to a lack of any analytical characterisation data for 4-hydroxy pentanal and because of the probable similarity of these data with those available for 5-hydroxy-2-pentanone, both being δ hydroxy carbonyl compounds, it cannot completely be excluded that the observed product is 4-hydroxy pentanal. It is evident from the above discussion, that the analyses carried out in this work cannot give definitive information on the relative importance of the decomposition, isomerisation and O_2 reaction channels of the δ hydroxy alkoxy radical. There is, however, evidence that the decomposition channel might dominate. The possible disagreement between the present product study and the estimation predictions concerning the fate of the δ hydroxy alkoxy

radical (δ , in Scheme 4.5) highlights the need to perform more experiments on systems where reactions of the δ hydroxy alkoxy radical will dominate the product distribution.

In summary, the carbonyl products identified and quantified in this work account for 70 ± 14 %C of the overall OH radical reaction with 1-pentanol. When the organic nitrate yield is included, the observed products account for 76 ± 15 %C.

From the results and the considerations presented above it is proposed, for the purposes of modelling oxidant formation in urban air masses, that the atmospheric chemistry of 1-pentanol can be represented by:



In the derivation of the above equation, in order to obtain a 100% mass balance, slightly more significance has been attributed to the attack of the OH radical at the α position of the alcohol than that found from the experimental results and the possible occurrence of the isomerisation pathway of the β hydroxy alkoxy radical to form 1,5-dihydroxy-2-pentanone has been included. Further, a molar formation yield of 0.05 has been assumed for 5-hydroxy-2-pentanone as estimated from the concentration of the reference FTIR spectrum and it has also been assumed that the fate of the $\cdot\text{CH}_2\text{CH}_2\text{CH}_2\text{OH}$ radical is the reaction with O_2 to give 3-hydroxy propanal.

4.3 Atmospheric degradation of 1-butanol

The product studies on the gas-phase oxidation of 1-butanol were carried out in the *EUPHORE* outdoor photoreactor in Valencia/Spain in March 2000. The oxidation of 1-butanol was initiated by reaction with OH radicals generated by the photolysis of HONO, prepared as described in Annex D. Test experiments on a 1-butanol-air mixture showed that losses of the compound to the wall of the photoreactor or via photolysis were negligible compared to the measured decay of 1-butanol during the experiments. A few preparatory experiments were also performed in the 480 *l* reactor in Wuppertal.

The experiments conditions employed are listed in Annex B, Table B.4.

4.3.1 Results

GC-PID and HPLC analysis of the products formed on irradiation of HONO-1-butanol-air mixtures showed the formation of butanal, propanal, ethanal and formaldehyde among the degradation products. Typical GC-PID chromatograms for the reaction of 1-butanol + OH radicals are shown in Figure 4.3.

In addition, a product eluted at or very close to the retention time of 4-hydroxy-2-butanone. While the HPLC retention time of this product closely matched that of an authentic standard of 4-hydroxy-2-butanone, the residual absorptions in the FTIR product spectra of irradiated HONO-1-butanol-air mixtures could not easily be compared with those of the authentic standard, because of the weak residual signals and the high amounts of water in the spectra. Based on the HPLC analysis and the possible reaction channels, it is believed that this product observed by HPLC is 4-hydroxy-2-butanone. The HPLC response factor – HPLC peak area/concentration – used to quantify this product was obtained with an authentic standard.

Propanal, ethanal and HCHO could also be formed in secondary reactions of some of the primary aldehydic products. However, under the conditions employed in the experiments, the contribution from secondary reactions is probably very minor. With the high NO_x concentrations employed in the experiments, the main fate of the alkyl peroxy radicals, formed in the degradation reactions of the higher aldehydes, will be formation of the corresponding stable peroxy acyl nitrate and not a lower aldehyde.

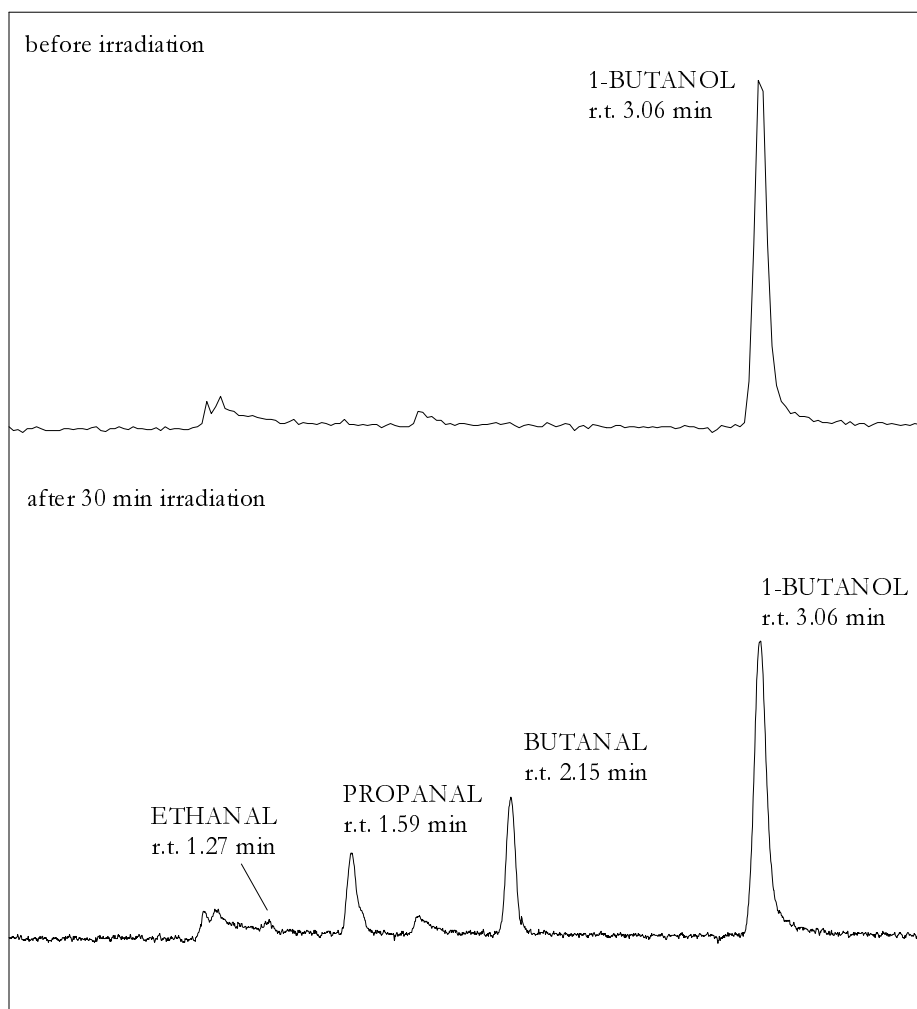


Figure 4.3: GC-PID chromatograms obtained from a HONO-1-butanol-air mixture before irradiation (above) and after 30 min irradiation.

To determine the product formation yields, the secondary reactions of the aldehydic products – reaction with OH radicals, photolysis and dilution losses – were taken into account as described by Tuazon *et al.* [48] (see section 2.3). Rate coefficients for reaction of OH radicals with the aldehydic products were taken from the literature [73, 87]. The following values of k_{OH} (in units of $10^{-11} \text{ cm}^3 \text{ molecule}^{-1} \text{ s}^{-1}$) were used: butanal, 2.47 ± 0.15 [87]; propanal, 2.02 ± 0.14 [87]; and ethanal, 1.22 ± 0.27 [73]. Photolysis frequencies for the aldehydes, k_{hp} , were taken from the literature [74]. The mean of $J(\text{NO}_2)$, measured during the experiments, was used as an indicator of the light intensity in order to select the frequencies. The following values of k_{hp} (in

units of 10^{-5} s^{-1}) were employed: butanal, 1.26 ± 0.06 ; propanal, 1.12 ± 0.05 ; and ethanal, 0.23 ± 0.01 .

The correction factors, $[\text{RHO}]_y^{\text{corr}} / [\text{RHO}]_y^{\text{meas}}$, were ≤ 1.5 for butanal, ≤ 1.3 for propanal and ≤ 1.1 for ethanal. The estimated overall uncertainties in the OH reaction rate coefficient of 1-butanol and in the rate coefficients for the reaction with OH and photolysis of the products led to maximum uncertainties in the correction factors of $\pm 8\%$ for the formation of butanal, $\pm 10\%$ for the formation of propanal and $\pm 13\%$ for the formation of ethanal.

The corrected aldehydes concentrations are plotted against the amount of 1-butanol consumed in Figure 4.4.

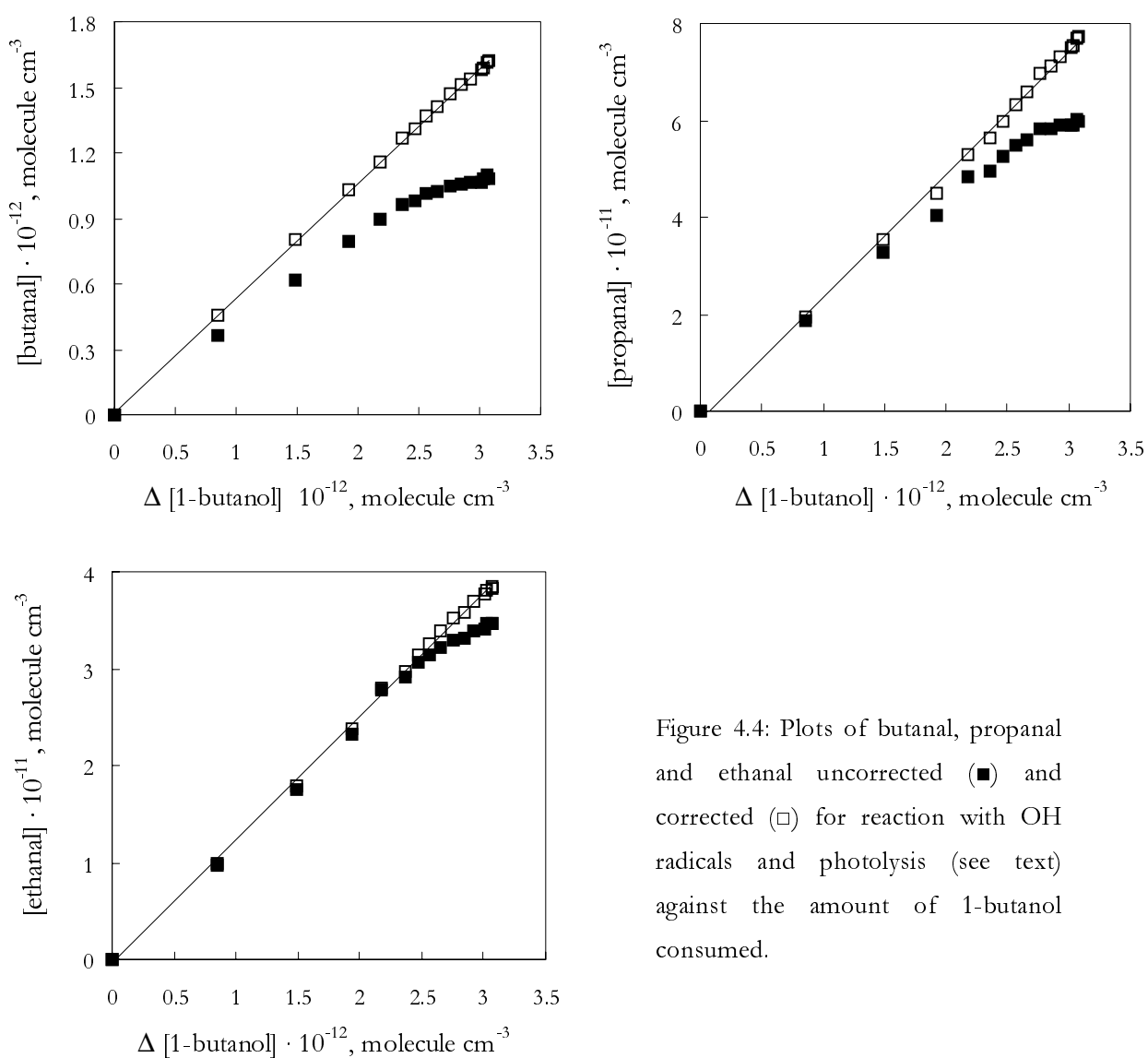


Figure 4.4: Plots of butanal, propanal and ethanal uncorrected (■) and corrected (□) for reaction with OH radicals and photolysis (see text) against the amount of 1-butanol consumed.

The corrected values for the formation yields are given in Table 4.2.

Table 4.2: Product formation yields from the gas-phase reaction of the OH radical with 1-butanol in the presence of NO_x.

Product	Formation yield
Butanal	0.518 ± 0.071
Propanal	0.234 ± 0.035
Ethanal	0.127 ± 0.022
Formaldehyde	0.434 ± 0.024
4-Hydroxy-2-butanone	0.05 ± 0.01
C-yield	0.92 ± 0.16

Indicated errors are 2 least-squares standard deviations of the data shown in Figure 4.4 combined with a contribution for the overall uncertainties in the alcohol and carbonyl GC-PID calibration factors and in the correction factors (see above). The molar formation yield of 0.434 ± 0.024 given for HCHO was derived from the uncorrected concentrations plotted against the consumption of 1-butanol in the early stage of the reaction, when secondary processes can largely be neglected. Similarly, the value of 0.05 ± 0.01 indicated for 4-hydroxy-2-butanone represents its semi-quantitative molar formation yield obtained by plotting the uncorrected HPLC concentrations of 4-hydroxy-2-butanone against the amounts consumed of 1-butanol in the early stage of the reaction.

In summary, the carbonyl and the hydroxy carbonyl products observed and quantified in this work account for 92 ± 16 %C of the reaction of OH radicals with 1-butanol.

4.3.2 Discussion: mechanistic considerations based on SAR and the product yield data

Using the *Structure–Activity Relationship* (SAR) technique [28, 29] it can be estimated that the relative importance of OH attack at the various –CH₃, –CH₂– and –OH groups of 1-butanol is: from the –OH group, 2.4%; from the –CH₂– group at the α position 58.3%; from the –CH₂– group at the β position 20.4%; from the –CH₂– group at the γ position 16.5%; and from the –CH₃ group 2.4%.

As described in section 4.1, the α hydroxy alkyl radical, formed by H-atom abstraction from the $-\text{CH}_2-$ group at the α position, yields butanal and HO_2 in a direct reaction with oxygen [21]:



and consequently does not produce an α hydroxy alkoxy radical that could form butyric acid ($\text{CH}_3\text{CH}_2\text{CH}_2\text{COOH}$) which was not found in the product analysis.

The hydroxy alkyl radicals (**I**, in Scheme 4.1) formed after H-atom abstraction from the $-\text{CH}_2-$ group at the β , and γ positions will add O_2 to form hydroxy alkyl peroxy radicals (**II**, in Scheme 4.1) which can react with NO or NO_2 . Addition of NO_2 will form thermally labile hydroxy alkyl peroxy nitrates. In the presence of NO , the hydroxy alkyl peroxy radicals form hydroxy alkyl nitrate or hydroxy alkoxy radicals (**III**, in Scheme 4.1) plus NO_2 .

The contribution of the channel forming organic nitrates in these $\text{RO}_2' + \text{NO}$ reactions is considered to be small ($\leq 4\%$). This value was derived from the yield of butyl nitrates, 0.077 ± 0.009 [88], obtained in $\text{CH}_3\text{ONO-NO-}n\text{-butane}$ air irradiations. The results of previous studies [67, 68, 72] suggest that hydroxy butyl nitrate formation yields from the reaction of hydroxy butyl peroxy radicals with NO is a factor of ~ 2 lower than the butyl nitrate formation yields from the OH reaction with n -butane in the presence of NO .

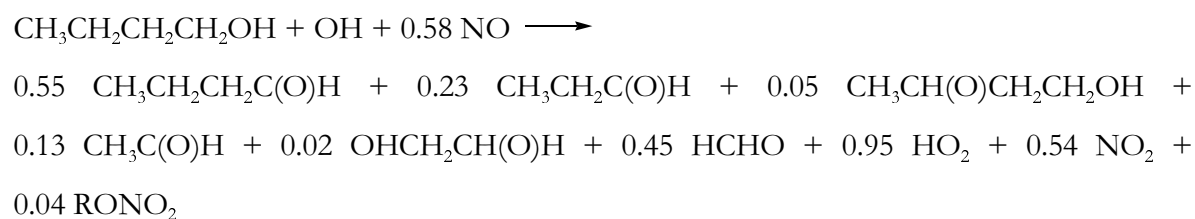
The further expected reactions of the alkoxy radicals are outlined in Scheme 4.6 and Scheme 4.7. In these reaction schemes, the alkyl and alkyl peroxy radicals have been omitted for clarity and only the reactions of the alkoxy and acyl radicals involved are shown.

The β hydroxy alkoxy radical (**β** , in Scheme 4.6) formed after the H-atom abstraction from the $-\text{CH}_2-$ group at the β position can react with O_2 to form 4-hydroxy-3-butanone (channel a) or decompose to propanal and HCHO (channel b). Isomerisation by a 1,5-H shift via a six-membered transition state cannot occur for this β hydroxy alkoxy radical. Furthermore, isomerisations by a 1,4-H shift via a five-membered transition state are expected to be 3-4 orders of magnitude slower at 296 K than the 1,5 H shift isomerisations [66] because of the higher ring strain involved and are, therefore, of negligible importance.

The δ hydroxy alkoxy radical, $\cdot\text{OCH}_2\text{CH}_2\text{CH}_2\text{CH}_2\text{OH}$, formed after the H-atom abstraction from the CH_3 - group has a very marginal importance in the atmospheric OH initiated degradation mechanism of 1-butanol, accounting for only an estimated 2.4% of the overall reaction. The possible products of the alkoxy radical reactions could not be identified in the present study because of their presumably very low concentrations. However, this δ hydroxy alkoxy radical [note that the $\cdot\text{OCH}_2\text{CH}_2\text{CH}_2\text{CH}_2\text{OH}$ radical is identical to that formed after the isomerisation via a 1,5-H shift of a 1-butoxy radical] is believed to undergo a 1,5-H shift isomerisation to ultimately yield 4-hydroxy butanal. The isomerisation channel is expected to dominate over the O_2 reaction and decomposition with a calculated rate constant of $k_{\text{isom}} = 3.2 \times 10^6 \text{ s}^{-1}$ [81, 82]. The expected δ hydroxy carbonyl has been tentatively observed from the OH radical initiated reaction of *n*-butane by Kwok *et al.* [85], using a direct air sampling atmospheric pressure ionisation tandem mass spectrometry technique.

In summary, the carbonyl and the hydroxy carbonyl products identified and quantified in this work account for $92 \pm 16 \%$ of the overall OH radical reaction with 1-butanol. When the estimated organic nitrate yield is included, the observed products account for $96 \pm 17 \%$.

From the experimental data and mechanistic considerations discussed above it is proposed, for the purposes of modelling oxidant formation in urban air masses, that the atmospheric chemistry of 1-butanol can be represented by:



In the derivation of the above equation, in order to achieve 100% mass balance, slightly more significance has been attributed to the attack of the OH radical at the α position of the alcohol than that found in the experimental results.

Chapter 5

Atmospheric oxidation of esters

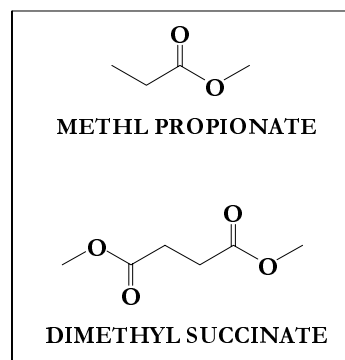
In this work, mechanistic studies were carried out on the atmospheric degradation of two esters: methyl propionate and dimethyl succinate.

The major atmospheric sink for the investigated esters is expected to be reaction with OH radicals which is, however, relatively slow, with $k_{(\text{OH} + \text{methyl propionate})} = (9.35 \pm 1.15) \times 10^{-13}$ and $k_{(\text{OH} + \text{dimethyl succinate})} = (1.95 \pm 0.27) \times 10^{-12} \text{ cm}^3 \text{ molecule}^{-1} \text{ s}^{-1}$ [this work]. This makes photoreactor chamber studies of the products difficult because of the long time coefficients of the experiments required to convert sufficient reactant amounts necessary for an accurate product analysis. Thus, the faster reaction with chlorine atoms was employed as a surrogate to mimic the OH radical induced atmospheric oxidation of methyl propionate and dimethyl succinate. Although reaction of VOC with Cl atoms is somewhat less selective than with OH radicals, the subsequent chemistry is the same and thus it is a convenient method to emulate OH radical initiated chemistry. The chlorine atom initiated oxidation of methyl propionate and dimethyl succinate was performed under atmospheric conditions in the presence of NO_x in the 405 ℓ reactor in Wuppertal.

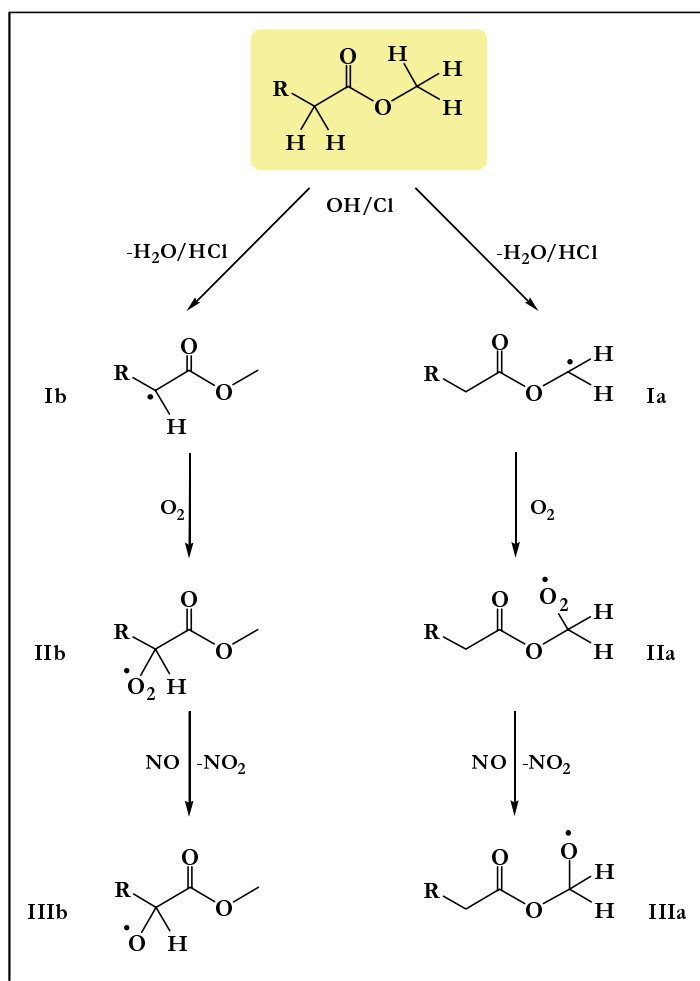
In the following section, a general degradation mechanism for both esters will be illustrated, and, afterward, the experimental results will be presented and discussed for the individual esters.

5.1 General mechanistic considerations on the degradation of esters

As seen from the molecular structure, methyl propionate contains the $-\text{CH}_2\text{C}(\text{O})\text{OCH}_3$ entity which is also present in the dibasic ester, dimethyl succinate, therefore, it is possible to represent both esters with the general formula $\text{R}-\text{CH}_2\text{C}(\text{O})\text{OCH}_3$, where $\text{R} = \text{CH}_3$ in the case of methyl propionate and $\text{R} = \text{CH}_3\text{OC}(\text{O})\text{CH}_2$ in the case of dimethyl succinate.



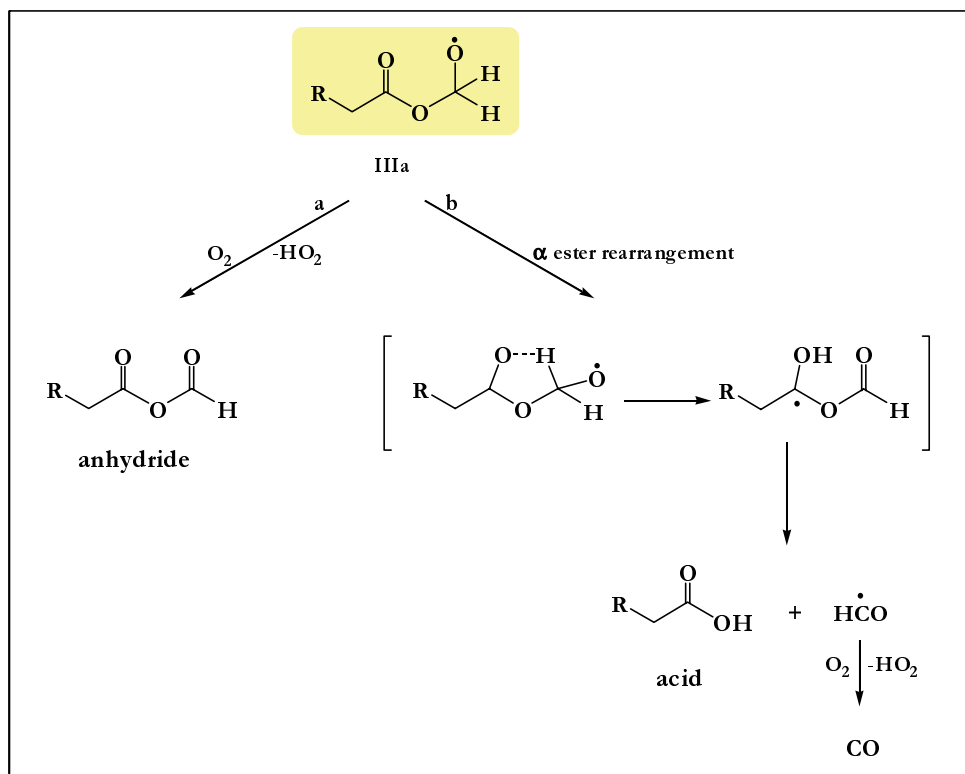
The atmospheric oxidation of esters is initiated by the reaction with OH radicals which proceeds via H-atom abstraction from the various $-\text{CH}_3$ and $-\text{CH}_2-$ groups. Under atmospheric conditions the alkyl radicals (**Ia**, **Ib**, in Scheme 5.1) react with oxygen to give peroxy radicals (**IIa**, **IIb**). Peroxy radicals react with NO, NO₂, HO₂, and other peroxy radicals in the atmosphere [90, 91]. Reaction with NO dominates in polluted air and proceeds via two channels giving alkoxy radicals (**IIIa**, **IIIb**) as major and organic nitrates as minor products.



Scheme 5.1: Reaction scheme for the OH radical/Cl atom initiated oxidation of R-CH₂C(O)OCH₃ esters: H-atom abstraction from the $-\text{CH}_2-$ and $-\text{CH}_3$ groups.

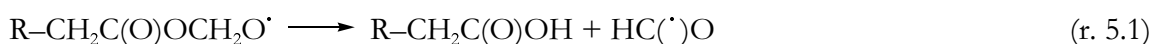
- H-atom abstraction from the terminal methyl group at the ether end ultimately yields the R-CH₂C(O)OCH₂O[•] alkoxy radical (**IIIa**, in Scheme 5.1). This alkoxy radical undergoes (Scheme 5.2) an α ester rearrangement reaction (first observed by Tuazon *et al.* [35] for ethyl acetate) in which an hydrogen atom on the alkoxy carbon migrates to the carbonyl oxygen

associated with the ester functionality through a five-membered transition state. This results in the formation of the acid $R-CH_2C(O)OH$ and the formyl radical $HC(\dot{C})O$.



Scheme 5.2: Atmospheric fate of $R-CH_2C(O)OCH_2O\cdot$ alkoxy radical formed after H-atom abstraction from the $-C(O)OCH_3$ entity of $R-CH_2C(O)OCH_3$ esters.

The overall reaction



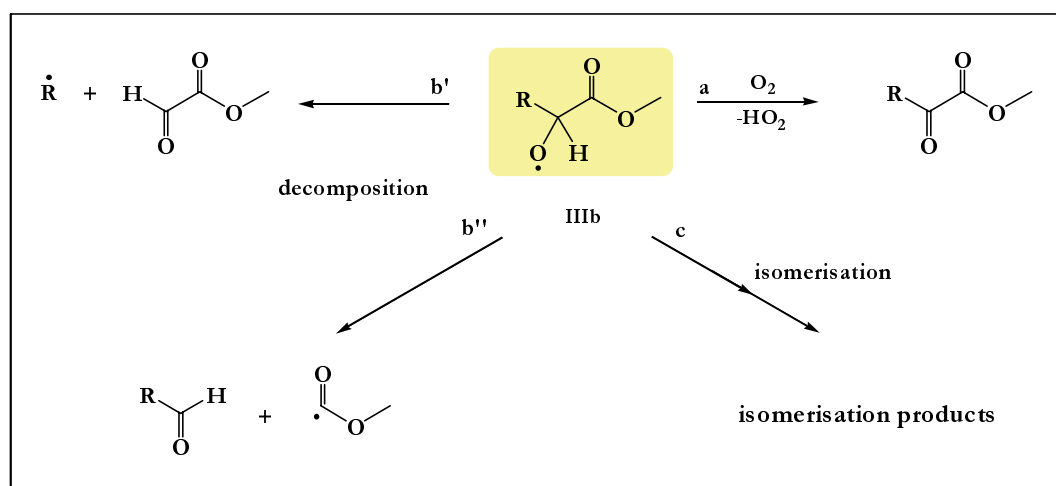
is calculated [71] to be exothermic by $\sim 21 \text{ kJ mol}^{-1}$, and the potential intermediate radical, $R-CH_2C(\dot{C})OHOC(O)H$, is calculated to be more stable than the $R-CH_2C(O)OCH_2O\cdot$ alkoxy radical by the difference in the O–H and C–H bond dissociation energies of $\sim 42\text{--}63 \text{ kJ mol}^{-1}$ [111]. However, the presumed five-membered transition state is expected to have a significant ring strain of $\sim 25 \text{ kJ mol}^{-1}$ [92], and it is not clear whether the reaction proceeds via the intermediary of the $R-CH_2C(\dot{C})OHOC(O)H$ radical or as a concerted process.

The $R-CH_2C(O)OCH_2O\cdot$ (**IIIa**, in Scheme 5.2) radical can react with O_2 yielding the anhydride, $R-CH_2C(O)OC(O)H$. In Scheme 5.2, the possible decomposition pathway proceeding by C–O bond cleavage to the $R-CH_2C(O)O\cdot$ radical and HCHO has been omitted. Previous studies of the atmospheric fates of structurally analogous alkoxy radicals derived from

methyl acetate $\text{CH}_3\text{C}(\text{O})\text{OCH}_3$ [36] and dimethyl glutarate $\text{CH}_3\text{OC}(\text{O})\text{CH}_2\text{CH}_2\text{CH}_2\text{C}(\text{O})\text{OCH}_3$ [37] support that decomposition of $\text{R}-\text{CH}_2\text{C}(\text{O})\text{OCH}_2\text{O}^\bullet$ is of negligible importance.

- H-atom abstraction from the $-\text{CH}_2\text{C}(\text{O})\text{O}-$ entity produces via the reaction sequence outlined in Scheme 5.1, the $\text{R}-\text{CH}(\text{O}^\bullet)\text{C}(\text{O})\text{OCH}_3$ alkoxy radical (**IIIb**, in Scheme 5.1).

This alkoxy radical shows three possible different reaction pathways (Scheme 5.3).



Scheme 5.3: Atmospheric fate of $\text{R}-\text{CH}(\text{O}^\bullet)\text{C}(\text{O})\text{OCH}_3$ alkoxy radicals formed after H-atom abstraction from the $-\text{CH}_2\text{C}(\text{O})\text{O}-$ entity of $\text{R}-\text{CH}_2\text{C}(\text{O})\text{OCH}_3$ esters.

- Reaction with oxygen (channel a) forming the carbonyl compound $\text{R}-\text{C}(\text{O})\text{C}(\text{O})\text{OCH}_3$.
- Decomposition via C–C bond cleavage, which can proceed by two channels (channels b' and b''), both producing an aldehydic product and a radical.
- A 1,5-H shift isomerisation, if possible, via a six-membered transition state yielding different multifunctional products. The relative importance of these reaction pathways for $\text{R}-\text{CH}(\text{O}^\bullet)\text{C}(\text{O})\text{OCH}_3$ alkoxy radicals will be discussed separately for methyl propionate and dimethyl succinate on the basis of the results from the present product studies.

For completeness, it has to be noted that in the case of methyl propionate, $\text{CH}_3\text{CH}_2\text{OC}(\text{O})\text{OCH}_3$, a H-atom abstraction from the methyl group of terminal CH_3CH_2- entity is also possible. The alkoxy radical $\text{H}-\text{CH}(\text{O}^\bullet)\text{CH}_2\text{C}(\text{O})\text{OCH}_3$ then formed has an atmospheric fate similar to that of the $\text{R}-\text{CH}(\text{O}^\bullet)\text{C}(\text{O})\text{OCH}_3$ alkoxy radical described above (i.e. reaction with O_2 and decomposition).

5.2 Atmospheric degradation of methyl propionate

All the experiments on the gas-phase oxidation of methyl propionate, $\text{CH}_3\text{CH}_2\text{C}(\text{O})\text{OCH}_3$, were performed in the 405 ℓ reactor in Wuppertal. The oxidation of methyl propionate was initiated by the reaction with Cl atoms generated by photolysis of molecular chlorine in the presence of NO. To test for heterogeneous and/or photolytic losses of methyl propionate and its oxidation products, two control experiments were performed. First, methyl propionate-air mixtures were left to stand in the dark and were then subjected to UV irradiation for up to 20 min: there was no observable loss (<3%) of methyl propionate. Second, product mixtures obtained by the UV irradiation of methyl propionate- Cl_2 - NO_x -air mixtures were left to stand in the dark chamber for 20 min. There was no observable loss (<3%) of any products.

The experimental conditions employed are listed in Annex B, Table B.5.

5.2.1 Results

By virtue of their characteristic IR spectra, propionic formic anhydride, propionic acid, CO, methyl pyruvate, ethanal, methoxy formylperoxynitrate, formaldehyde and methyl glyoxylate were identified among the degradation products of methyl propionate.

Methyl glyoxylate is not available commercially. An infrared spectrum of methyl glyoxylate, $\text{H}(\text{O})\text{CC}(\text{O})\text{OCH}_3$, was therefore generated by the 254 nm photolysis of methyl bromoacetate in the presence of NO in 1000 mbar of air.



Photolysis of $\text{BrCH}_2\text{C}(\text{O})\text{OCH}_3$ gives the $\cdot\text{CH}_2\text{C}(\text{O})\text{OCH}_3$ radical which after addition of O_2 and reaction with NO leads to the $\cdot\text{OCH}_2\text{C}(\text{O})\text{OCH}_3$ alkoxy radical. There are three possible pathways for the $\cdot\text{OCH}_2\text{C}(\text{O})\text{OCH}_3$ radical; reaction with O_2 to give methyl glyoxylate, elimination of HCHO to give a $\cdot\text{C}(\text{O})\text{OCH}_3$ radical or isomerisation to give $\text{HOCH}_2\text{C}(\text{O})\text{OCHO}$ and/or $\text{HC}(\text{O})\text{C}(\text{O})\text{OCH}_2\text{OH}$. The major fate of $\cdot\text{OCH}_2\text{C}(\text{O})\text{OCH}_3$ was found to be reaction with O_2 to yield methyl glyoxylate which was identified by virtue of its IR features at 2966, 2850, 1754, 1741, 1289, 1225 and 1024 cm^{-1} . Decomposition via elimination of HCHO accounted for 4% of the loss of the $\cdot\text{OCH}_2\text{C}(\text{O})\text{OCH}_3$ alkoxy radical. The lack of any distinctive OH stretching vibrational features in the residual spectra at $\sim 3670 \text{ cm}^{-1}$ showed

that isomerisation to $\text{HOCH}_2\text{C}(\text{O})\text{OCHO}$ and/or $\text{HC}(\text{O})\text{C}(\text{O})\text{OCH}_2\text{OH}$ is of little or no importance. The methyl glyoxylate spectrum was, therefore, calibrated by assuming a 96% photolytic conversion of methyl bromoacetate to methyl glyoxylate. For completeness, experiments were performed in which ozone was added to methyl crotonate, $\text{CH}_3\text{-CH=CHC}(\text{O})\text{O-CH}_3$ -air mixtures. The ozonolysis of methyl crotonate is expected to produce methyl glyoxylate and ethanal in unit yields [93]. The methyl glyoxylate spectrum was calibrated in this case assuming its yield equal to the measured concentration of ethanal. The infrared absorption cross sections obtained for methyl glyoxylate from these experiments were within $\pm 10\%$ of those obtained from the photolysis of methyl bromoacetate, thus giving additional confidence in the calibration of the methyl glyoxylate reference spectrum.

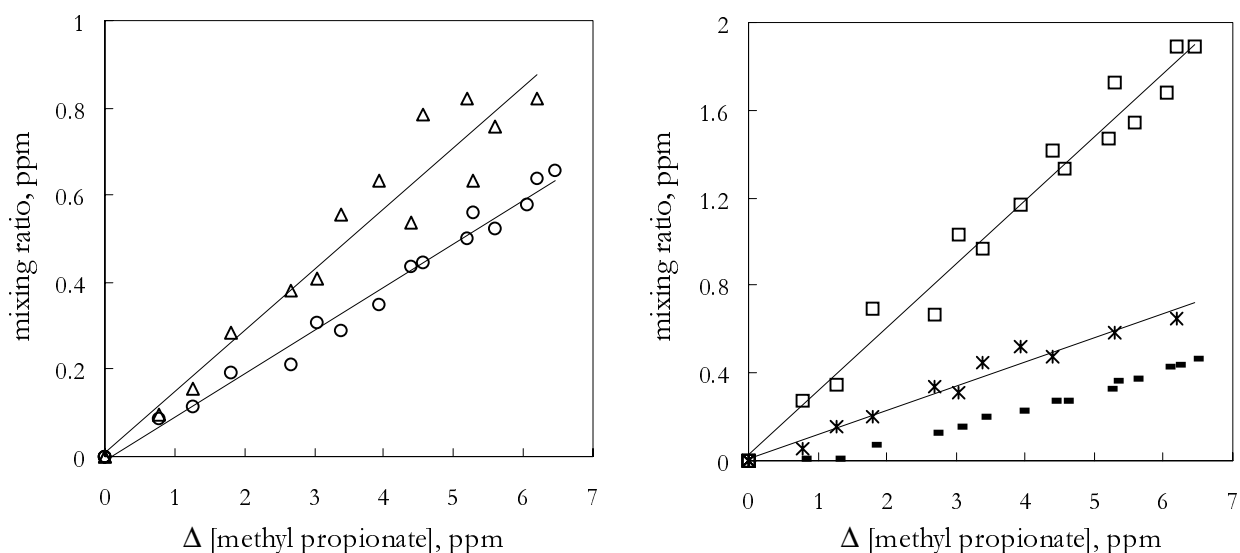
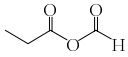
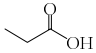
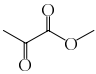
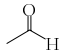
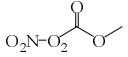
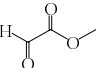


Figure 5.1: Formation of propionic formic anhydride (circles), propionic acid (triangles), methyl glyoxylate (stars) and methyl pyruvate (squares) versus loss of methyl propionate observed following the Cl atom initiated oxidation of methyl propionate in air in the presence of NO_x . The methoxy formyl peroxy nitrate (dashes) data plot shows curvature. This is caused by changes in the NO/NO_2 ratio during the experiment (see text).

Figure 5.1 shows the observed formation of propionic formic anhydride, propionic acid, methyl pyruvate and methyl glyoxylate versus loss of methyl propionate. The linearity of the propionic formic anhydride, propionic acid, methyl pyruvate and methyl glyoxylate product plots in Figure 5.1 suggests that these species are formed as primary products during the oxidation of methyl propionate and are not lost to any significant extent by secondary reactions. Least-squares analysis of these data gave the product yields listed in Table 5.1.

Table 5.1: Molar yields of the products observed in the Cl atom initiated oxidation of methyl propionate in the presence of NO_x .

Product		Formation yield
Propionic formic anhydride		0.099 ± 0.019
Propionic acid		0.139 ± 0.027
Carbon monoxide		0.132 ± 0.026
Methyl pyruvate		0.289 ± 0.057
Ethanal		0.077 ± 0.015
Methoxy formyl peroxy nitrate		0.083 ± 0.016
Methyl glyoxylate		0.111 ± 0.022
C-yield		0.716 ± 0.143

Molar product yields of 0.132 ± 0.026 and 0.077 ± 0.015 given, in Table 5.1, for CO and ethanal, respectively, refer to the early stage of the reaction, when secondary processes can largely be neglected. In the case of formaldehyde, secondary formation and removal processes occurring in the system under the experimental conditions employed made a reliable determination of its molar formation yield difficult.

In the product analysis distinctive spectral features at 1835, 1748, 1308, 1237 and 799 cm^{-1} remain in the residual spectra after subtraction of all identified products. By comparison with literature spectra, these characteristic absorptions can be assigned to methoxy formyl peroxy nitrate, $\text{CH}_3\text{OC}(\text{O})\text{OONO}_2$ [94, 95]. The formation of this compound is dependent on the NO/NO_2 ratio in the experimental system and, therefore, its yield is low at the beginning of the experiment when the NO/NO_2 ratio is high and increases gradually during the course of the experiment as the NO/NO_2 ratio becomes smaller (see Figure 5.1). An estimation of the concentration of the peroxy nitrate has been made using the value of $4.43 \times 10^{-19} \text{ cm}^2 \text{ molecule}^{-1}$ (base 10) for the absorption cross section of peroxy acetyl nitrate at 1835 cm^{-1} available in the literature [96]; its molar formation yield was found to be 0.083 ± 0.016 at the end of the experiments.

The residual product spectra also show the presence of RONO_2 -type bands at approximately 1670, 1300 and 845 cm^{-1} . The specific RONO_2 product(s) formed could not be identified.

However, an estimate of the molar RONO_2 concentration was made from the integrated intensity of the 1670 cm^{-1} absorption band and the average integrated absorption coefficient of $(2.5 \pm 0.2) \times 10^{-17}\text{ cm molecule}^{-1}$ (base10) reported in the literature for the corresponding band of other organic nitrates [37]. Using this value, the average RONO_2 molar formation yield obtained from five experiments was $7 \pm 2\%$, the estimated total error includes uncertainties associated with the absorption coefficient. There are two possible sources of organic nitrates in the present experiments; the nitrate channel of the reaction of peroxy radicals with NO (r. 5.6), or the addition of NO_2 to alkoxy radicals (r. 5.7).



Within the experimental uncertainties, the organic nitrate(s) product features at 1670 , 1300 and 845 cm^{-1} were observed to increase linearly with methyl propionate consumption. During the experiment the NO_2 concentration substantially increased from essentially zero prior to the start of the irradiation to $4\text{-}6 \times 10^{14}\text{ molecule cm}^{-3}$ at the end of the experiment. The linearity of the RONO_2 formation suggests that reaction (r. 5.6) rather than reaction (r. 5.7) is the source of the observed RONO_2 . Accordingly, an effective branching ratio of $k_{5,6}/(k_{5,5}+k_{5,6}) = 0.07 \pm 0.02$ has been estimated for the mixture of the three different peroxy radicals formed following Cl attack on methyl propionate in the presence of O_2 .

The reaction of peroxy radicals with NO is believed to involve the formation of a short-lived ROONO complex which can either decompose to give RO and NO_2 or rearrange to give the nitrate RONO_2 [97]. With increasing size of the R moiety, the importance of the RONO_2 producing channel increases (R = CH_3 , $k_{5,6}/(k_{5,5}+k_{5,6}) < 0.01$ [98, 99], R = C_3H_7 , $k_{5,6}/(k_{5,5}+k_{5,6}) = 0.036$ [47]; R = *t*-butyl, $k_{5,6}/(k_{5,5}+k_{5,6}) = 0.18$ [100], R = C_6H_{11} , $k_{5,6}/(k_{5,5}+k_{5,6}) = 0.22$ [47]). Methyl propionate has six "heavy" atoms and has a molecular weight which is comparable to that of hexane. It is interesting to note that the nitrate forming channel of the $\text{RO}_2 + \text{NO}$ reactions occurring during the oxidation of methyl propionate is substantially (approximately a factor of 3) less important than that in the corresponding reactions of alkyl peroxy radicals of the same size. This observation is similar to recent findings for halogenated peroxy radicals which, when compared to unsubstituted alkyl peroxy radicals, produce a much lower nitrate yield in their reactions with NO [101]. It appears that the electron withdrawing influence of the oxygen or halogen substituents reduces the branching ratio $k_{5,6}/(k_{5,5}+k_{5,6})$. The different

factors governing the nitrate yields in reaction (r. 5.6) are poorly understood and need further study.

The reaction products identified and quantified in this work account for 71.6 ± 14.3 %C. When the organic nitrate yield is included, the observed products account for 79 ± 16 %C.

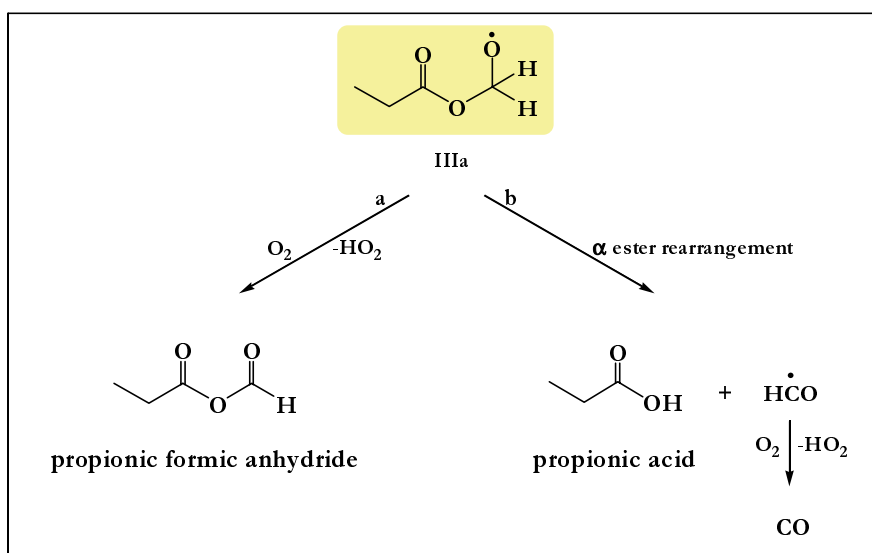
5.2.2 Discussion

As discussed above, the reaction of Cl atoms with methyl propionate, $\text{CH}_3\text{CH}_2\text{C}(\text{O})\text{OCH}_3$, can proceed by H-atom abstraction from all three of the hydrogenated carbons in the molecule. Under atmospheric pressure the alkyl radicals formed after the H-atom abstraction, react solely with O_2 to form the corresponding alkyl peroxy radicals [21, 72]. Reaction with NO then leads to formation of the corresponding alkoxy radicals (Scheme 5.1). The products observed following UV irradiation of methyl propionate- Cl_2 - NO_x -air mixtures allow the elucidation of the fate of the alkoxy radicals formed during the atmospheric oxidation of methyl propionate in the presence of NO_x . The possible reaction channels for each of the 3 alkoxy radicals, $\text{CH}_3\text{CH}_2\text{C}(\text{O})\text{OCH}_2\text{O}^\bullet$, $\text{CH}_3\text{CH}(\text{O}^\bullet)\text{C}(\text{O})\text{OCH}_3$ and $\text{CH}_2(\text{O}^\bullet)\text{CH}_2\text{C}(\text{O})\text{OCH}_3$, are outlined in Scheme 5.4, Scheme 5.5 and Scheme 5.6. These schemes form the basis for the following discussion.

Atmospheric fate of $\text{CH}_3\text{CH}_2\text{C}(\text{O})\text{OCH}_2\text{O}^\bullet$ radicals

Scheme 5.4 shows possible fates of the $\text{CH}_3\text{CH}_2\text{C}(\text{O})\text{OCH}_2\text{O}^\bullet$ alkoxy radical (**IIIa**).

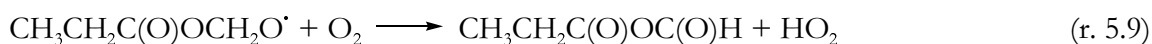
The observation in the present work of the formation of equivalent amounts of propionic acid and CO suggest that the $\text{CH}_3\text{CH}_2\text{C}(\text{O})\text{OCH}_2\text{O}^\bullet$ radical undergoes an α ester rearrangement (channel b) (see section 5.1). Furthermore, the identification of propionic formic anhydride shows that the bimolecular reaction with O_2 (channel a) competes with α ester rearrangement for the available $\text{CH}_3\text{CH}_2\text{C}(\text{O})\text{OCH}_2\text{O}^\bullet$ radicals. A similar competition was reported by Christensen *et al.* [36] for the analogous alkoxy radicals formed during the atmospheric oxidation of methyl acetate, $\text{CH}_3\text{C}(\text{O})\text{OCH}_2\text{O}^\bullet$. It is interesting to note that the relative importance of α ester rearrangement versus bimolecular reaction with O_2 reported by Christensen *et al.* [36] for the $\text{CH}_3\text{C}(\text{O})\text{OCH}_2\text{O}^\bullet$ radical, $(65 \pm 14)/(35 \pm 5) = 1.9 \pm 0.7$, is very similar to that observed here for $\text{CH}_3\text{CH}_2\text{C}(\text{O})\text{OCH}_2\text{O}^\bullet$ radical, $(0.139 \pm 0.027)/(0.099 \pm 0.019) = 1.4 \pm 0.4$.



Scheme 5.4: Proposed reaction mechanism for the Cl atom initiated oxidation of methyl propionate: abstraction from the $-C(O)O-CH_3$ entity.

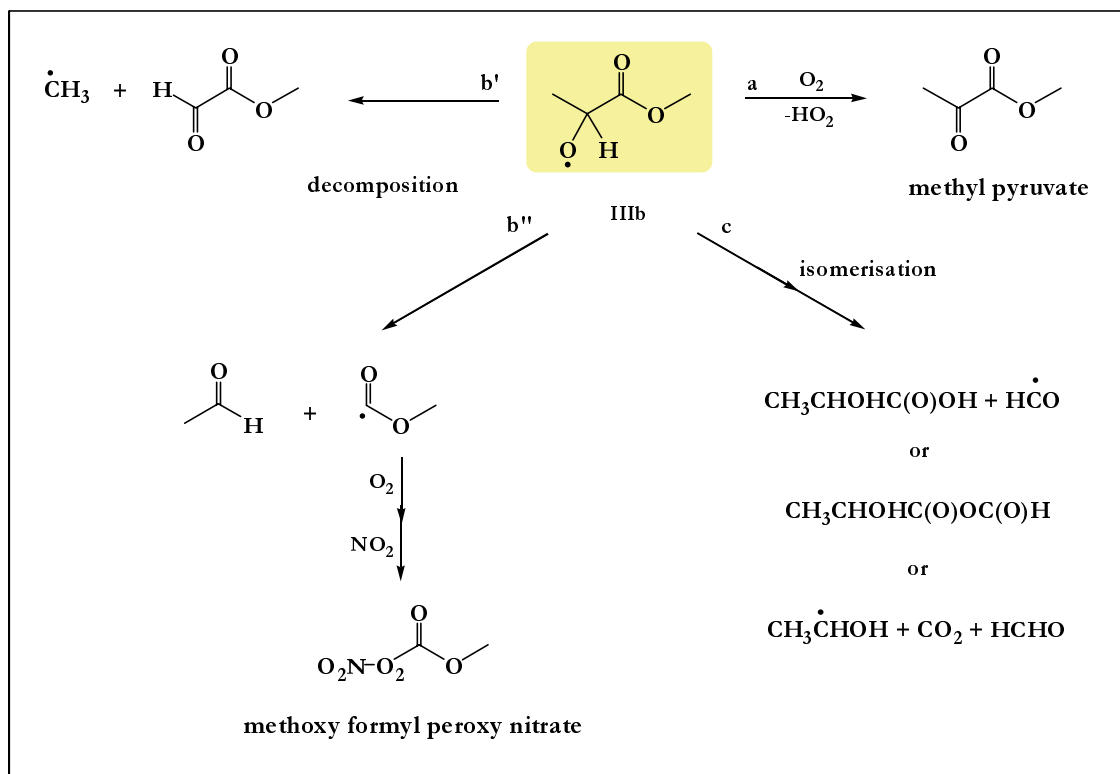
In Scheme 5.4, the possible decomposition of the alkoxy radical via C–O bond scission to the $CH_3CH_2C(O)^\bullet$ radical and HCHO has not been included for two reasons. First, the observed products can be explained without invoking this reaction channel. Second, in studies of the atmospheric fates of structurally analogous alkoxy radicals derived from methyl acetate, $CH_3C(O)OCH_2O^\bullet$ [36], dimethyl glutarate, $CH_3OC(O)CH_2CH_2CH_2C(O)OCH_2O^\bullet$ [37], and dimethyl succinate, $CH_3OC(O)CH_2CH_2C(O)OCH_2O^\bullet$ [this work], no evidence of HCHO elimination has been observed. By analogy with the reported behaviour of structurally similar radicals it seems unlikely that decomposition via C–O bond scission is significant for the $CH_3CH_2C(O)OCH_2O^\bullet$ radical.

In conclusion, the fate of $CH_3CH_2C(O)OCH_2O^\bullet$ radicals formed in the atmospheric oxidation of methyl propionate in the presence of NO_x is α ester rearrangement and reaction with O_2 with $k_{5.8}/(k_{5.9}[O_2]) = 1.4 \pm 0.4$.



Atmospheric fate of $\text{CH}_3\text{CH}(\text{O}^\bullet)\text{C}(\text{O})\text{OCH}_3$ radicals

The alkoxy radical $\text{CH}_3\text{CH}(\text{O}^\bullet)\text{C}(\text{O})\text{OCH}_3$ (**IIIb**, in Scheme 5.5), formed after the H-atom abstraction from the $-\text{CH}_2\text{C}(\text{O})\text{O}-$ entity, can react with O_2 to form methyl pyruvate (channel a), decompose via C–C bond cleavage (channels b' and b'') or undergo isomerisation (channel c) (Scheme 5.5).



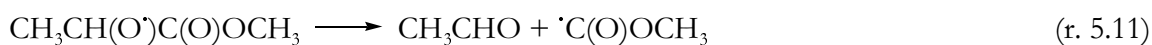
Scheme 5.5: Proposed reaction mechanism for the Cl atom initiated oxidation of methyl propionate: abstraction from the $-\text{CH}_2\text{C}(\text{O})\text{O}-$ entity.

The bond cleavage can proceed by two pathways, producing either methyl glyoxylate and the CH_3^\bullet radical (channel b') or ethanal and the methoxy formyl radical, $\text{C}(\text{O})\text{OCH}_3^\bullet$ (channel b''). As already noted, because of the greater stability of the $\text{C}(\text{O})\text{OCH}_3^\bullet$ radical compared to the methyl radical [86, 89], the channel producing ethanal and the $\text{C}(\text{O})\text{OCH}_3^\bullet$ radical is predicted to dominate.

The observation of a substantial yield of methyl pyruvate shows that reaction with O_2 is an important channel for $\text{CH}_3\text{CH}(\text{O}^\bullet)\text{C}(\text{O})\text{OCH}_3$ radicals (**IIIb**, in Scheme 5.5). In addition, the observation of comparable yields of ethanal and methoxy formylperoxynitrate suggests that decomposition of the $\text{CH}_3\text{CH}(\text{O}^\bullet)\text{C}(\text{O})\text{OCH}_3$ radical to give a $\text{C}(\text{O})\text{OCH}_3^\bullet$ radical and CH_3CHO is also significant. The yield of ethanal was observed to decrease for methyl

propionate consumptions greater than 15-20%. This observation can be attributed to secondary loss of ethanal via reaction with Cl atoms which occurs with a rate coefficient of $7.8 \times 10^{-11} \text{ cm}^3 \text{ molecule}^{-1} \text{ s}^{-1}$ [102] by H-atom abstraction from the $-\text{CHO}$ group forming the $\text{CH}_3\text{C}(\text{O})\cdot$ acyl radical, which then adds O_2 to form the acyl peroxy radical. In the presence of NO_x , the acyl peroxy radical can add NO_2 to form peroxy acetyl nitrate (PAN) [21]. Under the experimental conditions employed, the major pathway of the methoxy formyl radical is expected to be the addition of O_2 and the further reaction with NO_2 to form methoxy formyl peroxy nitrate, rather than decomposition to CO_2 and $\cdot\text{CH}_3$ [103]. The alkoxy radical $\text{CH}_3\text{CH}(\text{O})\text{C}(\text{O})\text{OCH}_3$ (**IIIb**, in Scheme 5.5) can also undergo a 1,5-H shift isomerisation via a six-membered transition state. Unfortunately, due to a lack of an infrared spectrum of the expected isomerisation product it was not possible to ascertain whether this process is occurring.

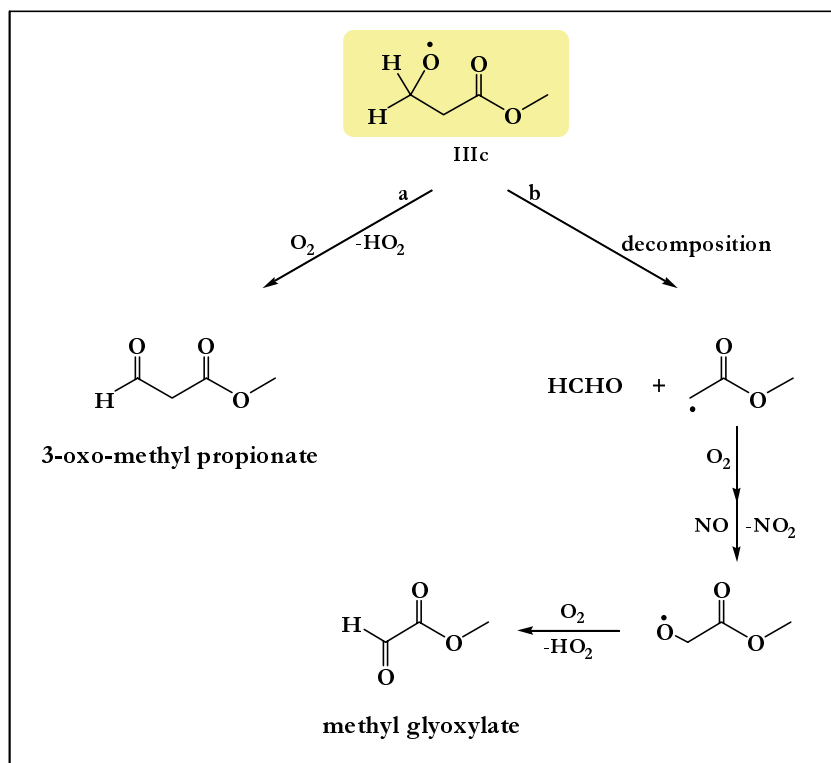
In conclusion, the atmospheric fate of the $\text{CH}_3\text{CH}(\text{O})\text{C}(\text{O})\text{OCH}_3$ radical is reaction with O_2 to give methyl pyruvate and decomposition via C–C bond cleavage to give a $\cdot\text{C}(\text{O})\text{OCH}_3$ radical and CH_3CHO with $k_{5,11}/(k_{5,10}[\text{O}_2]) = 8/29 = 0.28 \pm 0.08$.



Atmospheric fate of $\cdot\text{OCH}_2\text{CH}_2\text{C}(\text{O})\text{OCH}_3$ radicals

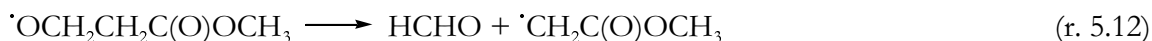
The alkoxy radical $\cdot\text{OCH}_2\text{CH}_2\text{C}(\text{O})\text{OCH}_3$ (**IIIc**) shown in Scheme 5.6 cannot form a six-membered transition state, hence isomerisation via internal H-atom abstraction does not occur, and reaction with O_2 and decomposition via C–C bond scission are the only possible fates for the alkoxy radical.

Reaction of the $\cdot\text{OCH}_2\text{CH}_2\text{C}(\text{O})\text{OCH}_3$ alkoxy radical (**IIIc**, in Scheme 5.6) with O_2 will lead to the formation of 3-oxo-methyl propionate (channel a). Since a reference spectrum for 3-oxo-methyl propionate was not available, it was not possible to search for IR product features from this compound. However, after subtraction of IR features attributable to all the identified products (propionic formic anhydride, propionic acid, methyl pyruvate, methyl glyoxylate, ethanal and methoxy formyl peroxy nitrate), residual features remain which suggest the possible presence of 3-oxo-methyl propionate.



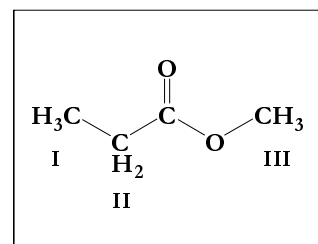
Scheme 5.6: Proposed reaction mechanism for the Cl atom initiated oxidation of methyl propionate: abstraction from the methyl group of the CH_3CH_2 - entity.

Decomposition of $\dot{\text{O}}\text{CH}_2\text{CH}_2\text{C}(\text{O})\text{OCH}_3$ leads to the formation of formaldehyde and the $\dot{\text{C}}\text{H}_2\text{C}(\text{O})\text{OCH}_3$ radical (channel b). The $\dot{\text{C}}\text{H}_2\text{C}(\text{O})\text{OCH}_3$ radical will add O_2 and react with NO to give the $\dot{\text{O}}\text{CH}_2\text{C}(\text{O})\text{OCH}_3$ alkoxy radical. As discussed in paragraph 5.2.1, control experiments employing the photolysis of methyl bromoacetate in mixtures of air in the presence of NO showed that in air under atmospheric pressure the fate of $\dot{\text{O}}\text{CH}_2\text{C}(\text{O})\text{OCH}_3$ radicals is mainly reaction with O_2 to give methyl glyoxylate. Methyl glyoxylate was an observed product with a molar yield of 0.11. As shown in Scheme 5.5 and Scheme 5.6, methyl glyoxylate can be formed following the decomposition of both $\text{CH}_3\text{CH}(\text{O}^\cdot)\text{C}(\text{O})\text{OCH}_3$ and $\dot{\text{O}}\text{CH}_2\text{CH}_2\text{C}(\text{O})\text{OCH}_3$ radicals. As described above, it is believed that the fate of $\text{CH}_3\text{CH}(\text{O}^\cdot)\text{C}(\text{O})\text{OCH}_3$ radicals is dominated by reactions (r. 5.10) and (r. 5.11), and hence the observed methyl glyoxylate product is assigned to decomposition of $\dot{\text{O}}\text{CH}_2\text{CH}_2\text{C}(\text{O})\text{OCH}_3$ radicals via elimination of HCHO (see Scheme 5.6). Because of the lack of positive evidence for the formation of 3-oxo methyl propionate, it is proposed that the sole fate of $\dot{\text{O}}\text{CH}_2\text{CH}_2\text{C}(\text{O})\text{OCH}_3$ is decomposition:



In summary, the reaction products identified and quantified in this work account for 71.6 ± 14.3 %C. When the organic nitrate yield is included, the observed products account for 79 ± 16 %C.

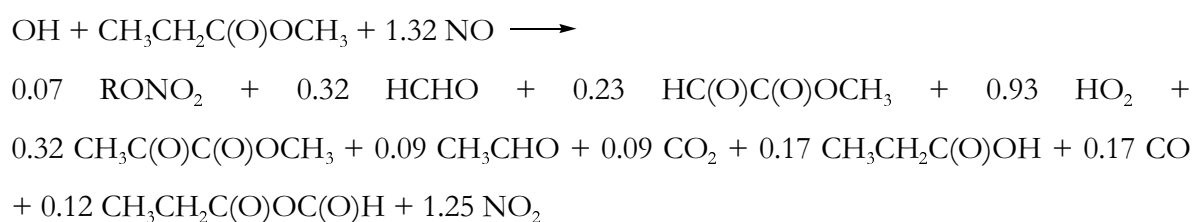
The atmospheric oxidation of methyl propionate is initiated by reaction with OH radicals. Using structure-activity relationships it can be estimated that the relative importance of OH attack at the three possible sites is: 25% (I), 43% (II) and 32% (III) [28, 29, 59].



The OH radical reaction will produce three alkyl radicals which will add O_2 to give peroxy radicals.



For conditions prevailing in polluted urban air masses the dominant fate of the peroxy radicals will be reaction with NO leading to alkoxy radicals as the major products with small amounts of organic nitrates (7%). From the results presented in sections 5.2.1 and 5.2.2 it is recommended, for the purposes of modelling oxidant formation in urban air masses, that the atmospheric chemistry of methyl propionate be represented as:



In the derivation of the above equation it has been assumed that the 7% organic nitrate yield is composed of 3% $\text{CH}_3\text{CH}_2\text{C}(\text{O})\text{OCH}_2\text{ONO}_2$, 2% $\text{CH}_3\text{CH}(\text{ONO}_2)\text{C}(\text{O})\text{OCH}_3$ and 2% $\text{O}_2\text{NOCH}_2\text{CH}_2\text{C}(\text{O})\text{OCH}_3$, and that the fate of $\cdot\text{C}(\text{O})\text{OCH}_3$ radicals is addition of O_2 , followed by reaction with NO and decomposition to give CO_2 and CH_3O radicals.

5.3 Atmospheric degradation of dimethyl succinate

All the experiments on the gas-phase oxidation of dimethyl succinate, $\text{CH}_3\text{OC}(\text{O})\text{CH}_2\text{CH}_2\text{C}(\text{O})\text{OCH}_3$, were performed in the 405 ℓ reactor in Wuppertal. The oxidation of dimethyl succinate was initiated by reaction with Cl atoms, generated by photolysis of molecular chlorine in the presence of NO. Control experiments on dimethyl succinate-air mixtures were performed i) in the dark and ii) at the maximum light intensity for up to 40 min to check for losses of dimethyl succinate by wall adsorption and photolysis, respectively. Dimethyl succinate showed a wall loss rate of $5.05 \times 10^{-5} \text{ s}^{-1}$.

The experiment conditions employed are listed in Annex B, Table B.6.

5.3.1 Results

Based on FTIR reference spectra, succinic formic anhydride, $\text{CH}_3\text{OC}(\text{O})\text{CH}_2\text{CH}_2\text{C}(\text{O})\text{OC}(\text{O})\text{H}$, *mono*-methyl succinate, $\text{CH}_3\text{OC}(\text{O})\text{CH}_2\text{CH}_2\text{C}(\text{O})\text{OH}$, dimethyl oxaloacetate, $\text{CH}_3\text{OC}(\text{O})\text{C}(\text{O})\text{CH}_2\text{C}(\text{O})\text{OCH}_3$, methoxy formyl peroxy nitrate and CO were identified among the degradation products. The measured concentrations of these products are plotted as a function of the amounts of dimethyl succinate reacted in Figure 5.2.

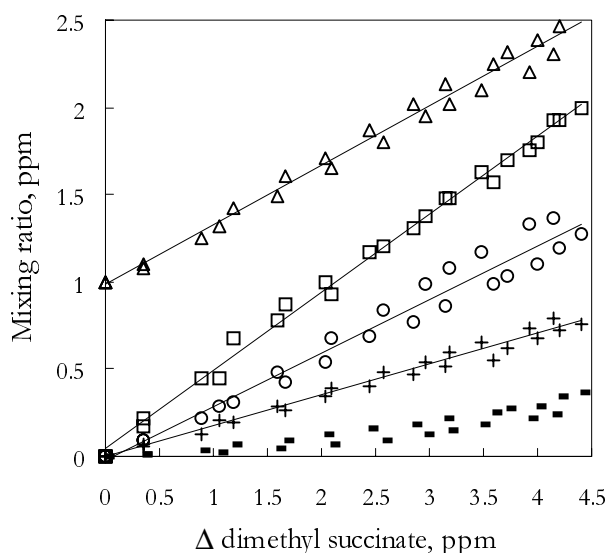
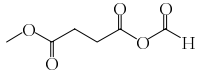
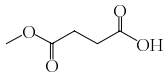
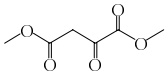
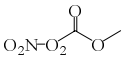


Figure 5.2: Formation of succinic formic anhydride (triangles), *mono*-methyl succinate (squares), CO (circles), dimethyl oxaloacetate (plus) and methoxy formyl peroxy nitrate (dashes) versus loss of dimethyl succinate observed following the Cl atom initiated oxidation of dimethyl succinate in air in the presence of NO_x . The data for succinic formic anhydride (triangles) have been displaced vertically by 1 ppm for clarity.

Good straight line plots were obtained; the lack of curvature in the plots strongly supports that all the products are primary and that no secondary reactions generated or removed these reaction products during the time period of the experiments. Least-squares analysis of these data lead to the product formation yields given in Table 5.2.

Table 5.2: Molar yields of the products observed in the Cl atom initiated oxidation of dimethyl succinate in the presence of NO_x .

Product		Formation yield
Succinic formic anhydride		0.341 ± 0.068
<i>Mono</i> -methyl succinate		0.447 ± 0.111
Carbon monoxide		0.307 ± 0.061
Dimethyl oxaloacetate		0.176 ± 0.044
Methoxy formyl peroxy nitrate		0.032-0.084
C-yield		0.824 ± 0.164

The calibrations of *mono*-methyl succinate and dimethyl oxaloacetate were not straightforward because the IR spectra suggested that more than one form of each compound exists in equilibrium in the liquid state and that this equilibrium persists in the gas-phase.

It was attempted to obtain an IR spectrum of *mono*-methyl succinate by heating and flushing a solid sample into the evacuated chamber and then filling to atmospheric pressure with synthetic air. No change in the IR features was observed over a time period of 1 h. It was also attempted to calibrate the solid sample by dissolving it in a solvent, CH_2Cl_2 , followed by injection into the chamber. The spectra, in this case, showed with time a slight decrease in the absorption bands of what is most likely the dimer and an increase in the intensities of bands attributed to the monomer. Neither the use of solvents with higher polarity, the heating of the injected solution nor the increase of the temperature of the reaction chamber resulted in further conversion of the compound to the monomeric form. Therefore, it is presently not possible to ascertain if the calibrated IR spectrum of *mono*-methyl succinate really represents the pure monomeric form or a mixture of the dimer and monomer. An analysis of the product spectra from the product experiments afforded an average yield of 0.447 ± 0.111 for methyl succinate. The estimated overall error ($\pm 25\%$) includes uncertainties associated with the analysis of the features of *mono*-methyl succinate.

Dimethyl oxaloacetate exhibits, as reported in the literature [104], complete enolisation in the crystal phase. Being a 1,3-dicarbonyl compound, in solution it exists as an equilibrium mixture of keto and enol forms, the proportionation depending on the polarity of the solvent.

Vapour samples of dimethyl oxaloacetate, introduced into the chamber by heating and flushing samples of the solid with N_2 , showed IR features of both keto and enol forms, with an extremely slow conversion rate between the forms compared to the overall dark decay loss to the chamber walls. Therefore, in order to derive a calibrated spectrum for each form, NMR and FTIR spectra of dimethyl oxaloacetate dissolved in $CDCl_3$ and $CHCl_3$ were recorded over a time period of seven days. Both spectra showed complete enolisation for the initial freshly prepared solution and, with time, a progressive increase in the fraction of the keto form. Thus, infrared spectra of the pure enol form and, then of the equilibrium mixture of the keto and enol forms were obtained. Furthermore, the NMR solution spectra indicated that the position of the keto-enol equilibrium in $CDCl_3$ was 83.5% for the keto form and 16.5% for the enol form. Expansions into the reaction chamber of known amounts of the solution at equilibrium allowed keto and enol infrared absorption bands to be calibrated. On the basis of the band positions and the well-behaved subtraction of the reference spectrum from the product spectra, dimethyl oxaloacetate was identified as a product of dimethyl succinate mainly (possibly solely) in the keto form. An evaluation of the total errors involved in the calibration of the IR spectrum of dimethyl oxaloacetate and in the analysis of its features resulted in a yield of 0.176 ± 0.044 .

As evident from the above discussion, the FTIR quantification of *mono*-methyl succinate and dimethyl oxaloacetate concentrations are subject to significant uncertainties.

In the product spectra, spectral features are observed at 1835, 1748, 1308, 1237 and 799 cm^{-1} . These characteristic absorptions are assigned to methoxy formyl peroxy nitrate. The formation of this compound is very dependent on the NO/NO₂ ratio in the experimental system and, consequently, its yield is low at the beginning of the experiment when the NO/NO₂ ratio is high and increases gradually during the course of the experiment as the NO/NO₂ ratio becomes smaller (Figure 5.2). An estimation of the concentration of the peroxy nitrate has been made using the value of $1.09 \times 10^{-3} \text{ ppm}^{-1} \text{ m}^{-1}$ for the absorption cross section of peroxy acetyl nitrate at 1835 cm^{-1} available in the literature [96]. Its yield was found to increase from approximately 3 to 8 mol % during the progression of an experiment. The residual product spectra also show the presence of RONO₂-type bands at ~ 843 , ~ 1298 and $\sim 1679 \text{ cm}^{-1}$. The specific RONO₂ product(s) formed could not be identified. However, an estimate of the molar RONO₂ concentration was made from the integrated intensity of the 1679 cm^{-1} absorption band and the average integrated absorption coefficient (base10) of $(2.5 \pm 0.2) \times 10^{-17} \text{ cm molecule}^{-1}$ of the corresponding band of other organic nitrates [37]. Using this value, the average RONO₂ molar formation yield obtained from four experiments was $3.4 \pm 0.6\%$. The

estimated total error includes uncertainties associated with the absorption coefficient used and the generally weak signals observed.

There are no direct quantitative measurements of nitrate yields from any of the peroxy radicals expected to be formed in photooxidations of compounds such as esters, but indirect estimates of overall nitrate yields can be obtained from model simulation of environmental chamber incremental reactivity experiments which are sensitive to this parameter. Such experiments [105] involving the reaction of dimethyl succinate with OH radicals in the presence of NO predicted overall nitrate yields of $\sim 10\text{-}14\%$ depending on the other mechanistic assumptions which were made.

The reaction products identified and quantified in this work account for $82.4 \pm 16.4 \%$. When the organic nitrate yield is included, the observed products account for $86 \pm 17 \%$.

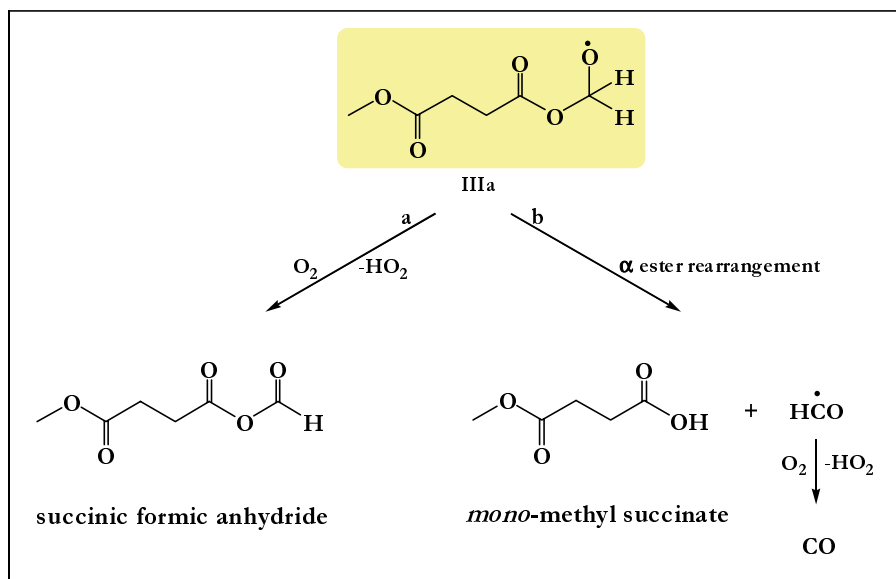
5.3.2 Discussion

The chlorine atom initiated oxidation of dimethyl succinate can proceed by only two pathways, H-atom abstraction from the terminal methyl groups and from the central $-\text{CH}_2\text{CH}_2-$ entity, since dimethyl succinate is a symmetrical molecule. In the troposphere, the alkyl radicals formed after the H-atom abstractions react solely with O_2 to form the corresponding alkyl peroxy radicals [21, 72]. Further reaction with NO then leads to formation of the analogous alkoxy radicals (Scheme 5.1). The products observed following UV irradiation of dimethyl succinate- Cl_2 - NO_x -air mixtures give an insight into the atmospheric fate of the alkoxy radicals formed during the atmospheric oxidation of dimethyl succinate in the presence of NO_x .

The possible reaction pathways of both alkoxy radicals are outlined in Scheme 5.7 and Scheme 5.8.

In the Scheme 5.7, the alkoxy radical $\text{CH}_3\text{OC}(\text{O})\text{CH}_2\text{CH}_2\text{C}(\text{O})\text{OCH}_2\text{O}^\bullet$ (**IIIa**), formed after the H-atom abstraction at the terminal $-\text{CH}_3$ groups of the dibasic ester, undergoes reaction with O_2 to form succinic formic anhydride and an α ester rearrangement to form *mono*-methyl succinate and the formyl radical which reacts with O_2 to give CO. If there are no additional sources of CO and *mono*-methyl succinate in the system, as supported by the absence of curvature in plots of their measured concentrations against reacted dimethyl succinate (Figure 5.2), then the molar formation yield of the two products should be identical. The observed discrepancy of 14% between the molar formation yield measured for CO and that for *mono*-methyl succinate is likely attributable to the significant uncertainties in the calibration of the

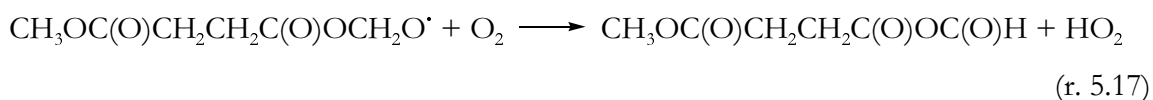
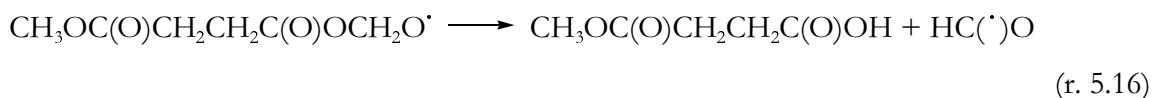
acid. It is reasonable to assume that the molar formation yield of CO reflects the upper limit for the molar formation yield for *mono*-methyl succinate.

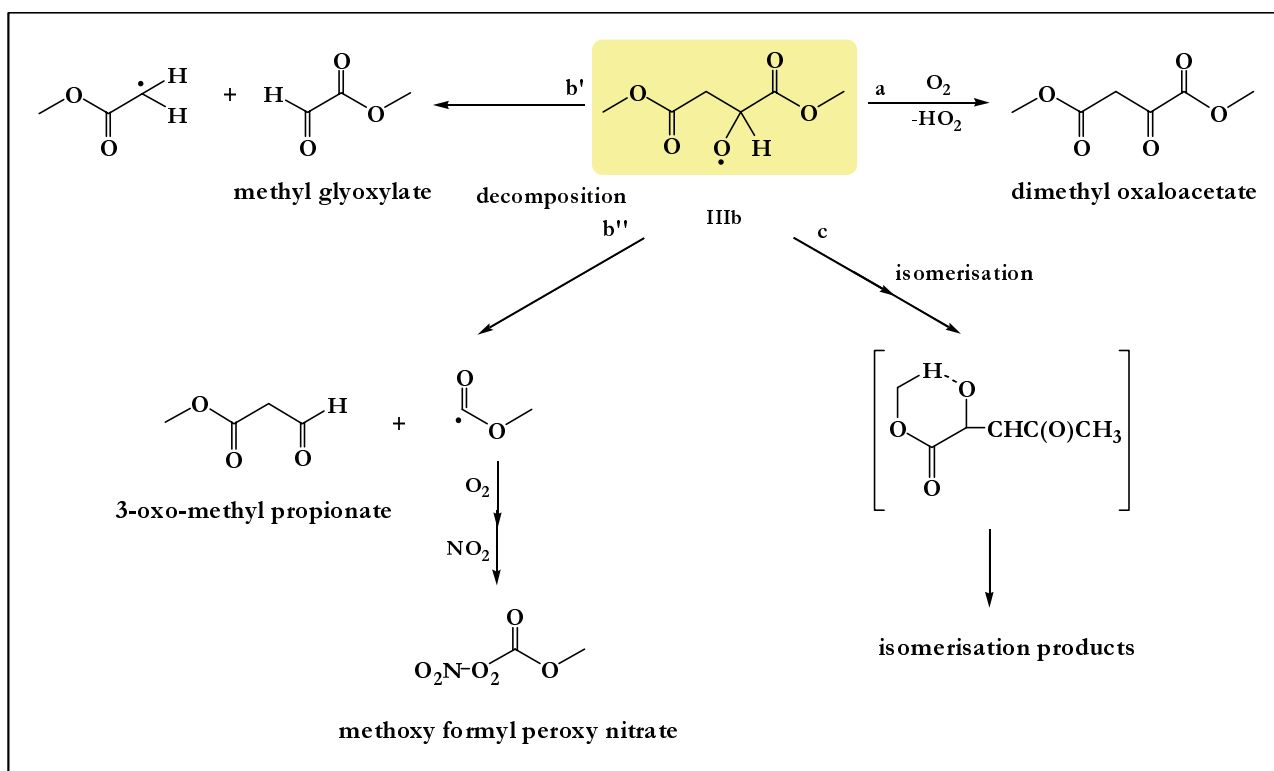


Scheme 5.7: Proposed reaction mechanism for the Cl atom initiated oxidation of dimethyl succinate: abstraction from the terminal CH₃ entity.

In the FTIR spectra of the reaction mixture, formation of HCHO was not observed allowing the decomposition channel of the alkoxy radical CH₃OC(O)CH₂CH₂C(O)OCH₂O• to be excluded. This conclusion conforms with similar observations in previous studies on the degradation mechanism of dimethyl glutarate with OH radicals [37] and of methyl propionate with chlorine atoms [this work].

It is concluded from the present data that the atmospheric fate of the CH₃OC(O)CH₂CH₂C(O)OCH₂O• radicals is an α ester rearrangement and reaction with O₂ with $k_{5.16}/(k_{5.17}[O_2]) = 0.90 \pm 0.25$.





Scheme 5.8: Proposed reaction mechanism for the Cl atom initiated oxidation of dimethyl succinate: abstraction from the $-\text{CH}_2\text{CH}_2-$ entity.

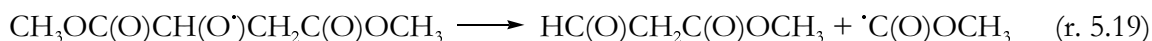
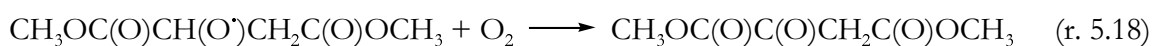
In Scheme 5.8, the alkoxy radical $\text{CH}_3\text{OC}(\text{O})\text{CH}(\text{O}^\cdot)\text{CH}_2\text{C}(\text{O})\text{OCH}_3$ (**IIIb**) formed after H-atom abstraction at the $-\text{CH}_2-$ groups of dimethyl succinate can react by four different pathways:

- i) Reaction with O_2 will form dimethyl oxaloacetate.
- ii) Decomposition of this alkoxy radical via C–C cleavage will lead to 3-oxo-methyl propionate and the methoxy formyl radical, $^\cdot\text{C}(\text{O})\text{OCH}_3$. As previously discussed in the case of methyl propionate, the major pathway of the $^\cdot\text{C}(\text{O})\text{OCH}_3$ radical, under the experimental conditions of this study, is expected to be addition of O_2 and further reaction with NO_2 to form mainly methoxy formyl peroxy nitrate, rather than decomposition to CO_2 and $^\cdot\text{CH}_3$ [103]. Because of the lack of a calibrated spectrum for 3-oxo-methyl propionate identification and quantification was not possible, however, the identification of methoxy formyl peroxy nitrate provided evidence for the occurrence of this pathway.
- iii) Decomposition of the alkoxy radical $\text{CH}_3\text{OC}(\text{O})\text{CH}(\text{O}^\cdot)\text{CH}_2\text{C}(\text{O})\text{OCH}_3$ (**IIIb**, in Scheme 5.8) via C–C cleavage of the central carbon atoms would produce 2 molecules of methyl glyoxylate. However, this channel obviously is of negligible importance since the compound

was not observed among the products. This result confirms the observations of a previous study [105], which deduced that the reaction channel was unimportant because of its relatively high estimated endothermicity.

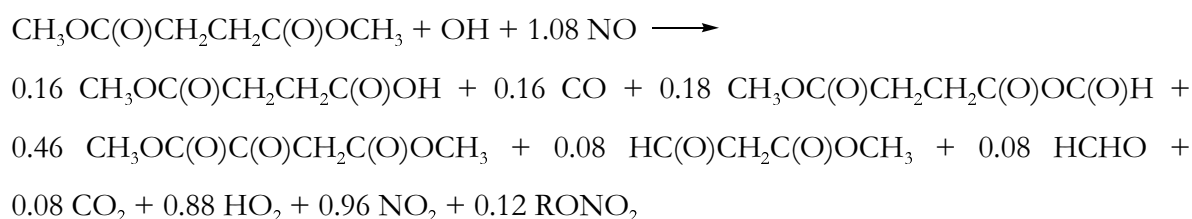
iv) The alkoxy radical $\text{CH}_3\text{OC}(\text{O})\text{CH}(\text{O}^\bullet)\text{CH}_2\text{C}(\text{O})\text{OCH}_3$ (**IIIb**, in Scheme 5.8) can also undergo a 1-5 H shift isomerisation through a six-membered transition state: because of a lack of the spectra of the several possible polyfunctional products, it is not possible to gauge the relative importance of this pathway in the degradation mechanism of dimethyl succinate.

In conclusion the atmospheric fate of $\text{CH}_3\text{OC}(\text{O})\text{CH}(\text{O}^\bullet)\text{CH}_2\text{C}(\text{O})\text{OCH}_3$ radicals is reaction with O_2 to give dimethyl oxaloacetate and decomposition via C–C cleavage to give 3-oxo-methyl propionate and $^\bullet\text{C}(\text{O})\text{OCH}_3$ radical with $k_{5,19}/(k_{5,18}[\text{O}_2]) = 0.18 \pm 0.10$.



The results of the present investigation have helped to elucidate several aspects of the atmospheric photooxidation mechanism of dimethyl succinate. However, the uncertainties encountered in the characterisation and quantification of several of the product species demonstrate the need for the use of complementary analytical methods to study the complex atmospheric chemistry of much large organic compounds.

The atmospheric oxidation of dimethyl succinate is initiated by reaction with OH radicals. Using structure-activity relationships it can be estimated that the relative importance of OH attack on the terminal $-\text{CH}_3$ sites and central $-\text{CH}_2-$ sites is 38% and 62%, respectively [28, 29, 59]. Therefore, combining the estimated relative importance of the two alkoxy radicals formed in the atmospheric degradation of dimethyl succinate with the results presented in sections 5.3.1 and 5.3.2 concerning their atmospheric fates, it is recommended for the purposes of modelling oxidant formation in urban air masses that the atmospheric chemistry of dimethyl succinate be represented as:



In the derivation of the above equation, in order to achieve 100% mass balance more significance (12%) has been attributed to the formation of organic nitrate according to the predicted overall nitrate yields of ~ 10-14% obtained from model simulation of environmental chamber incremental reactivity experiments involving the reaction of dimethyl succinate with OH radicals in the presence of NO [105]. Further it has been assumed that the 12% organic nitrate yield is composed of 4% $\text{CH}_3\text{OC}(\text{O})\text{CH}_2\text{CH}_2\text{C}(\text{O})\text{OCH}_2\text{ONO}_2$ and 8% $\text{CH}_3\text{OC}(\text{O})\text{CH}_2\text{CH}(\text{ONO}_2)\text{C}(\text{O})\text{OCH}_3$ and that the fate of $\cdot\text{C}(\text{O})\text{OCH}_3$ radicals is addition of O_2 followed by reaction with NO and decomposition to give CO_2 and CH_3O radicals.

Chapter 6

Functional group reactivity

6.1 Alcohol

In an attempt to better define the OH functional group reactivity in VOCs, the rate coefficients for the reaction of OH radicals with 1-butanol and 1-pentanol are considered, in the following discussion, together with the OH reaction kinetic data for a series of aliphatic alcohols and analogous *n*-alkanes (see Table 6.1).

Table 6.1: Rate coefficients (in units of 10^{-12} cm³ molecule⁻¹ s⁻¹) for the reaction of OH radicals and Cl atoms with a series of aliphatic alcohols and the corresponding *n*-alkanes.

<i>n</i> -alkane	k_{OH} [21]	k_{Cl} [72]	aliphatic alcohol	k_{OH} [21]	k_{Cl} [23]
CH ₄	0.00686	0.01	CH ₃ OH	0.944	47.9
C ₂ H ₆	0.257	59	C ₂ H ₅ OH	3.27	101
C ₃ H ₈	1.15	137	C ₃ H ₇ OH	5.57	149
C ₄ H ₁₀	2.54	218	C ₄ H ₉ OH	8.57	204
C ₅ H ₁₂	3.94	280	C ₅ H ₁₁ OH	11.1	251
C ₆ H ₁₄	5.61	340	C ₆ H ₁₃ OH	12.5	295
C ₇ H ₁₆	7.15	390	C ₇ H ₁₅ OH	13.7	349
C ₈ H ₁₈	8.68	460	C ₈ H ₁₇ OH	14.4	394

The reaction of OH radicals with alcohols may involve hydrogen atom abstraction from both the C–H and O–H bonds, the former process being more favoured on thermochemical grounds; e.g., $D(\text{H}-\text{CH}_2\text{OH}) = 393.3 \pm 8.4$ kJ mol⁻¹ and $D(\text{CH}_3\text{O}-\text{H}) = 435.1 \pm 4.2$ kJ mol⁻¹ [86]. The available evidence suggests that H-atom abstraction from the alcohol group in CH₃OH accounts for a maximum of 15% of the reaction at room temperature [106, 107]. The contribution to the overall rate coefficient from this channel for the reaction of OH radicals with higher members of the aliphatic alcohol series is likely to be less significant.

The increase in reactivity observed for H-atom abstraction by OH radicals for CH₃OH and C₂H₅OH compared to the corresponding alkanes can be rationalised in terms of the lowering of the C–H bond dissociation energy for the carbon bound to an alcoholic oxygen. Thus, the observed increase in reactivity of the CH₃ group in CH₃OH, $k(\text{OH} + \text{CH}_3\text{OH}) = 9.44 \times 10^{-13} \text{ cm}^3 \text{ molecule}^{-1} \text{ s}^{-1}$, compared to C₂H₆, $k(\text{OH} + \text{C}_2\text{H}_6) = 2.57 \times 10^{-13} \text{ cm}^3 \text{ molecule}^{-1} \text{ s}^{-1}$ [21, 72] is entirely consistent with a lowering of the C–H bond dissociation energy of about 17–21 kJ mol⁻¹, $D(\text{H}-\text{CH}_2\text{OH}) = 393.3 \pm 8.4 \text{ kJ mol}^{-1}$ and $D(\text{CH}_3\text{CH}_2-\text{H}) = 410 \pm 4 \text{ kJ mol}^{-1}$ [86]. The increase in reactivity for secondary H atoms of the alcohols over those of the analogous alkane is less pronounced, presumably as a result of the smaller decrease in bond dissociation energies. The data reported in Table 6.1 indicate that the rate coefficients for the reaction of OH radicals with straight chain alcohols increase almost linearly with the alkyl chain length up to about 5 carbons atoms. Furthermore, the addition of further CH₂ groups to the alkyl chain of the alcohol produces an increase in the reactivity of the molecule toward OH larger than that found for CH₂ group addition in the corresponding unsubstituted alkanes. In an attempt to quantify this increase in terms of the alkyl chain length over which this effect is operative, rate coefficient contributions for H-atom abstraction from the *n*-alkyl groups attached to a –CH₃ and to the –OH in the alcohols have been calculated. The difference between the estimated rate coefficient contributions for H-atom abstraction from the alkyl group (R) in the two compounds is Δk in Table 6.2.

Table 6.2: Calculated rate coefficient differences Δk (in units of 10⁻¹³ cm³ molecule⁻¹ s⁻¹) between *n*-alkanes and alcohols for OH radical attack at the linear aliphatic chain (R).

R	k_{OH} in R–CH ₃ ^a	k_{OH} in R–OH ^b	Δk ^c
CH ₃	1.3	9.44	+8.14
C ₂ H ₅	10.2	32.7	+22.5
C ₃ H ₇	24.1	55.7	+31.6
C ₄ H ₉	38.1	85.7	+47.6
C ₅ H ₁₁	54.8	111	+56.2
C ₆ H ₁₃	70.2	125	+54.8
C ₇ H ₁₅	85.5	137	+51.5

^a Calculated from OH rate coefficient data for alkanes [21] minus contribution from a terminal CH₃ group [$k(\text{CH}_3) = 0.5 k(\text{OH} + \text{C}_2\text{H}_6)$].

^b Rate coefficient data for alcohols [21]. Abstraction from –OH is assumed to be negligible.

^c $\Delta k = k(\text{R}-\text{OH}) - k(\text{R}-\text{CH}_3)$.

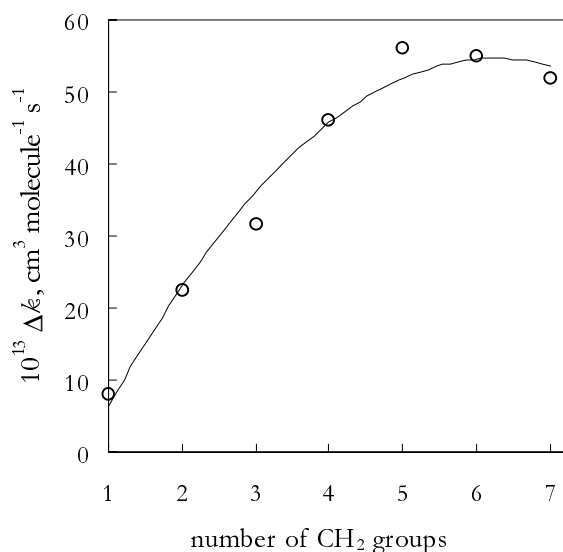


Figure 6.1: Δk values from Table 6.2 vs. the number of CH_2 groups in the aliphatic chain.

Figure 6.1 shows a plot of the Δk values determined in Table 6.2 as a function of the number of CH_2 groups. When the addition of a CH_2 group to the chain has the same effect as that in the n -alkanes, the plot should reach a plateau. The graph shows that the activating effect of the OH functional group extends up to 5 carbon atoms in the alcohol chain. The slight curvature exhibited by the plot up to C_5 indicates that the activating effect gradually lessens on increasing the number of CH_2 groups in the alkyl chain: as the chain length increases, the increase of the reactivity of the alcohol should eventually reach that found in the unsubstituted alkanes.

Based on the kinetic data reported in Table 6.1, Wallington *et al.* [22] and Nelson *et al.* [23] proposed a “long range activating effect” theory as interpretation of this enhanced reactivity of the alcohols. The OH functional group was suggested to have an activating effect for the reaction with OH radicals which extends over about 4 carbon atoms: the CH_2 groups in the C_2 to C_4 position would then have similar reactivities which appear to be about a factor of 2 higher in the alcohols than in the corresponding alkanes. The “long range activating effect” of the OH group is, however, unexpected in terms of thermochemical data since the available bond dissociation energies indicate any decrease in the C–H bond strength should be limited to the α carbon atoms [86]. Similarly, it is unlikely that inductive effects can operate over such a large number of carbon atoms. Hence, the increased reactivity must result from some other mechanistic effect, indicating possibly an alternative reaction pathway to the direct concerted H-atom abstraction process observed for n -alkanes. A correlation between the reactivities of OH radicals and Cl atoms for their reaction with alcohols might be expected since they are electrophilic species and both reactions involve H-atom abstraction. As discussed for the OH reactions, the abstraction of H-atoms bound to an α carbon atom is enhanced relative to the

corresponding *n*-alkane, this is also true for the Cl reactions. However, for the reaction of Cl atoms with alcohols, the observed increases in reactivity due to addition of further CH₂ groups to the alkyl chain are those expected on the basis of the CH₂ group rate coefficients derived from reactions of Cl atom with unsubstituted alkanes, $k_{\text{Cl}} = 5.6 \times 10^{-11} \text{ cm}^3 \text{ molecule}^{-1} \text{ s}^{-1}$ [62] (Table 6.1). Hence, in contrast to the OH radical reaction, for Cl atom reactions, the OH group does not appear to activate C–H bonds other than that at the C atom directly bonded to the functional group. It is possible that Cl atom reactions are sufficiently facile that any long range effect on the reactivity may be small and not easily identified. However, the kinetic data indicate that H-atom abstraction from alcohols by OH radicals and Cl atoms may be a mechanistically different process. It has been proposed [108, 109] that the enhanced reactivity observed in reactions of OH with alcohols may be due to the stabilisation of the transition states for the reactions resulting from the interaction of the attacking OH radical with the alcohol functional group through hydrogen bonding. Thus, reaction of OH radicals with an H-atom at the α carbon atom of an alcohol would involve a five-membered ring while hydrogen abstraction from β and γ carbon atoms would give rise to six- and seven-membered ring transition states, respectively. In terms of ring strain and entropy, it is likely that the five- and six-membered ring structure for reaction at the α and β carbon atom will provide a higher degree of stabilisation than the seven-membered ring formed by abstraction at the γ carbon. Product studies [30, 31, 32, 49, this work] on the degradation mechanism of alcohols strongly support that the main reaction pathway involves a H-atom abstraction from the carbon at the α position and the reaction pathways involving the H-atom abstraction from CH₂ groups at the β , γ etc. positions decrease in importance with increasing distance from the functional group. The final product distribution and the OH reaction rate coefficients allow the derivation of group rate coefficients for the different CH₂ groups present in the molecule. The results suggest that the OH functional group mainly enhances the activity almost exclusively of the carbon in α and β positions to the –OH group and that the other carbons show a reactivity similar to that observed for the alkanes. Thus, the addition of further CH₂ groups – up to five carbons – to the alcohol chain appears to favour, by inductive (electron donating) effect, the reactivity of the carbon in the α and β positions to the –OH group.

6.2 Ester

In an attempt to draw some general conclusions about the structure-reactivity relationship for esters, rate coefficients for the reaction of OH radicals with a series esters has been compared, in the following discussion, with those of the corresponding *n*-alkyl ethers and ketones which are the component functional groups of esters.

Table 6.3: Calculated contribution (in units of $10^{-13} \text{ cm}^3 \text{ molecule}^{-1} \text{ s}^{-1}$) of the alkyl groups (R) in alkanes, ethers and esters to the overall reaction rate coefficient with OH radicals.

R	CH ₃ -R ^a	RO-R ^b	CH ₃ C(O)O-R ^c
CH ₃	1.3	14	2.8
C ₂ H ₅	10.2	68	16.3
C ₃ H ₇	24.1	108	33.8
C ₄ H ₉	38.1	135	54.8
C ₃ H ₁₁	54.8	170	73

^a Calculated from OH rate coefficient data for alkanes minus the contribution from a terminal CH₃ group: $k(\text{CH}_3) = 0.5k_{\text{OH}}(\text{C}_2\text{H}_6)$ [21].

^b Calculated as $0.5k_{\text{OH}}(\text{RO-R})$ [110].

^c Calculated from OH rate coefficient data for CH₃C(O)O-R minus the contribution from CH₃C(O)O-group, $k(\text{CH}_3\text{C(O)O-}) = 4.21 \times 10^{-14} \text{ cm}^3 \text{ molecule}^{-1} \text{ s}^{-1}$ [28, 29].

The contribution of *n*-alkyl groups (R) to the overall rate coefficients with OH radicals has been calculated for alkanes, ethers and esters. The group rate coefficients, derived from the literature, are listed in Table 6.3. The significant changes in reactivity of -CH₃ and -CH₂CH₃ groups bonded directly to the oxygenated functional groups, compared to their reactivity in ethane and propane, respectively, can be rationalised, at least in part, in terms of changes in the C-H bond energies at carbon atoms positioned α to an ether oxygen; thus, the increase in reactivity of the -CH₃ in CH₃-O-CH₃ relative to that in ethane is in line with a lowering of the C-H bond dissociation energy of approximately 34 kJ mol⁻¹, $D(\text{CH}_3\text{CH}_2\text{-H}) = 423 \pm 1 \text{ kJ mol}^{-1}$ and $D(\text{CH}_3\text{OCH}_2\text{-H}) = 389 \text{ kJ mol}^{-1}$ [111]. Moving to longer *n*-alkyl chains, the rate coefficients per -CH₂- group are found to be significantly higher in the ethers than in the corresponding alkanes (Table 6.3). The activating effect of the ether group operative over about four carbon atoms, cannot, however, be explained in terms of bond energies or inductive effects and suggests an alternative reaction pathway to the direct concerted hydrogen abstraction process observed for alkanes. It has been proposed [108, 109] that this enhancement of the group reactivity toward OH may be due to the stabilisation of transition

states resulting from the co-ordination of the attacking OH radical with the ether group. It appears, from the data set presented in Table 6.3, that ester (CH₃C(O)O-) substituent also activates aliphatic chains bound to the ether oxygen with respect to OH radicals in a manner similar to the ether (RO-); however, the significant reduction in the reactivity of the alkoxy group in the esters compared to that in ethers is presumably a result of the deactivating inductive effect of the ester carbonyl adjacent to the alkoxy group.

The contribution of *n*-alkyl groups (R) to the overall rate coefficients with OH radicals has been calculated for alkanes, ketones and methyl esters. The group rate coefficients, derived from the literature, are listed in Table 6.4.

Table 6.4: Calculated contribution (in units of 10⁻¹³ cm³ molecule⁻¹ s⁻¹) of the *n*-alkyl groups (R) in alkanes, ketones and methyl esters to the overall reaction rate coefficient with OH radicals.

R	CH ₃ -R ^b	CH ₃ C(O)-R	CH ₃ OC(O)-R
CH ₃	1.3	1.1 ^b	0.67 ^d
C ₂ H ₅	10.2	10.4 ^c	6.8 ^e

^a Calculated from OH rate coefficient data for alkanes minus the contribution from a terminal CH₃ group: $k(\text{CH}_3) = 0.5 \cdot k(\text{OH} + \text{C}_2\text{H}_6)$ [21].

^b Calculated as $0.5 \cdot k(\text{OH} + \text{CH}_3\text{C}(\text{O})\text{CH}_3)$ [113].

^c Calculated as $0.5 \cdot k(\text{OH} + \text{CH}_3\text{CH}_2\text{C}(\text{O})\text{CH}_2\text{CH}_3)$ [113].

^d $k(-\text{OC}(\text{O})\text{CH}_3) = 0.67$ as derived from the results of a product study on OH reaction with ethyl acetate [35].

^e Calculated as $k(\text{OH} + \text{CH}_3\text{OC}(\text{O})\text{CH}_2\text{CH}_3) - k(\text{CH}_3\text{OC}(\text{O})-)$; where $k(\text{CH}_3\text{OC}(\text{O})-) = 2.5$ as derived from $k(\text{OH} + \text{CH}_3\text{OC}(\text{O})\text{CH}_3) - k(-\text{OC}(\text{O})\text{CH}_3)$.

Rather surprisingly, in ketones the carbonyl functional group (CH₃C(O)-) appears to have little effect on the reactivity of the -CH₃ and -CH₂CH₃ groups: the rate coefficients for reaction of OH with ethane and acetone and with propane and 2-propanone are very similar [21] [$k_{(\text{OH} + \text{ethane})} = 0.257$; $k_{(\text{OH} + \text{acetone})} = 0.219$; $k_{(\text{OH} + \text{propane})} = 1.15$; $k_{(\text{OH} + 2\text{-propanone})} = 1.15$, in units of 10⁻¹² cm³ molecule⁻¹ s⁻¹]. This result may be expected in terms of bond dissociation energies since the C-H bond strengths in acetone and ethane and 2-propanone and propane are approximately equal [111]. However, the carbonyl group is strongly electron withdrawing and hence reaction of the electrophilic OH radical with ketones might be expected to be considerably less facile than with alkanes. It is instructive to compare the reactivity of ketones towards Cl atoms with that of alkanes, in particular, the rate coefficient for reaction of Cl atoms with acetone is around four times smaller than that with ethane [112]. Presumably this decrease in reactivity is due to the decrease in electron density on the methyl hydrogen atoms

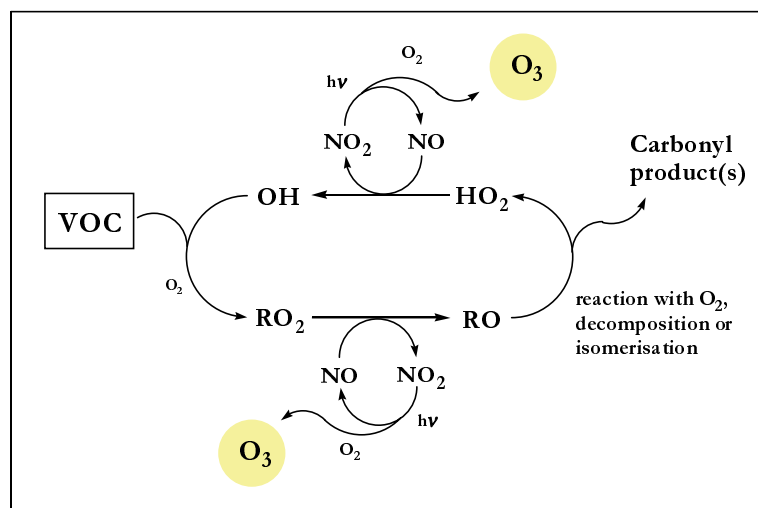
in acetone due to the negative inductive effect of the electron withdrawing carbonyl group. On this basis, it would be expected that the reaction of OH radicals with $\text{CH}_3\text{C}(\text{O})\text{CH}_3$ would also be less facile than with C_2H_6 . Carr *et al.* [112] and Wallington *et al.* [113] have suggested that the deactivating effect of the carbonyl group in acetone and in larger ketones is compensated, in their reaction with OH radicals, by the stabilisation of the transition state involving a coordination of the electrophilic hydroxyl radical with the carbonyl ketone group. Such stabilisation of the transition state via hydrogen bonding is not possible in Cl atom reactions and this accounts for the observation that the reaction of Cl with acetone is significantly slower than that with ethane [112]. The comparison between the reactivities of $-\text{CH}_3$ and $-\text{CH}_2\text{CH}_3$ groups bonded to the carbonyl group in esters and those in ketones reveals that the carbonyl functional group in the esters, contrary to what is observed for ketones, has a strong deactivating influence on the adjacent aliphatic chains, R ($\text{R}-\text{C}(\text{O})\text{OCH}_3$) (Table 6.4). Presumably, replacement of an electron donating methyl group in ketones ($\text{R}-\text{C}(\text{O})\text{CH}_3$) by a withdrawing $-\text{O}-$ leads to a considerable increase in the deactivating inductive effect of the carbonyl group on adjacent *n*-alkyl groups in methyl esters ($\text{R}-\text{C}(\text{O})\text{OCH}_3$).

Chapter 7

Atmospheric implications

It has been recognised for the last fifty years that each individual organic compound may have a different quantitative impact on photochemical ozone formation [114], and hence that the application of oxidant control strategies requires stringent emission reductions for highly reactive VOCs and replacement programmes by low-reactivity organics [115]. This in turn leads to a requirement for a rational assessment of VOC reactivity – role and contribution of individual VOC to ozone and secondary photooxidant formation – as a basis for control decisions.

The atmospheric fate of primary aliphatic alcohols and methyl esters appears to be largely controlled by their reaction with the OH radical, since photolysis and reaction with O_3 and NO_3 radicals are very slow [21]. As shown in Scheme 7.1, in the presence of NO_x the hydroxyl radicals initiate a rapid sequence of reactions involving organic peroxy, RO_2 , and alkoxy, RO , radicals, and the hydroperoxy radical, HO_2 , ultimately leading to the regeneration of OH.



Scheme 7.1: Schematic representation of the free radical initiated oxidation of a VOC into its first generation carbonyl product(s) in the presence of NO_x and the associated formation ozone.

Whereas the rates of reaction with OH govern the lifetimes and oxidation rates of VOCs, the reactions of the peroxy radicals, RO_2^\cdot and HO_2^\cdot , provide the coupling with NO_x chemistry by oxidising NO to NO_2 , and, thus, cause an increase in ozone formed from the photolysis of NO_2 and the subsequent reaction with oxygen.

Although the OH radical rate coefficients for 1-butanol, 1-pentanol, methyl propionate and dimethyl succinate [this work, Table 3.2] are much higher than the rate coefficient of $2.7 \times 10^{-13} \text{ cm}^3 \text{ molecule}^{-1} \text{ s}^{-1}$ for ethane [21] – the compound used by the U. S. Environmental Protection Agency, EPA, as the informal standard for determining “negligible” reactivity –, on a per mass basis the rate coefficients relative to ethane are 12.4 and 13.9 for 1-butanol, 1-pentanol, respectively and 1.17 and 1.47, for methyl propionate and dimethyl succinate, respectively. This means that if the amount reacted is quantified by mass, then the alcohols react relatively more rapidly in the atmosphere than ethane does but the esters are only slightly more reactive than ethane in this respect. However, it may be inappropriate to attempt to derive a single reactivity scale for organic compounds that depends only on how rapidly they react, since their atmospheric reactivity in terms of ozone formation potential depends significantly on the nature of reaction mechanisms, oxidation products and the type of environment in which the organics are emitted (VOC/ NO_x ratio).

- **Alcohols.** The experimental results in sections 4.2 and 4.3 indicate that the OH radical reaction with alcohols proceeds largely by the H-atom abstraction from the site adjacent to the hydroxy functional group; the further reaction with O_2 of the α hydroxy alkyl radicals formed yields HO_2 directly and the corresponding aldehyde, such that RO_2^\cdot and RO^\cdot radicals do not participate in this initial oxidation step. In contrast, OH radical attack at the position β , γ and δ of the two primary alcohols leads to formation of peroxy radicals and then alkoxy radicals which show the tendency to undergo mainly thermal decomposition and/or isomerisation; in these cases, a sequence of reactions involves additional peroxy radicals and additional NO oxidations (see Scheme 7.1).

The first generation oxidation products resulting from all the reaction pathways of primary alcohols are mainly aldehydes and, to a minor extent, hydroxy aldehydes, hydroxy ketones and hydroxy alkyl nitrates. It is clearly of interest to consider the propensity of the oxidation products to generate ozone, noting however, that VOCs also affect ozone formation indirectly. If the reactions of a VOC enhance or inhibit overall radical levels, it would, consequently, affect how rapidly all other VOCs present react and form ozone. While the photolysis of the aldehydes, especially of formaldehyde, has a positive effect on the ozone formation by secondary radical formation, the reaction of OH radicals with the aldehydes ($\geq \text{C}_2$) slows up

ozone formation, since it leads to the generation of peroxy acyl nitrates [$\text{R-C(O)O}_2\cdot + \text{NO}_2 \rightarrow \text{R-C(O)OONO}_2$] which act as temporary reservoirs for free radicals and NO_x . Peroxy acyl nitrates typically have thermal decomposition lifetimes of less than 1 h [116] under the conditions in the planetary boundary layer, before regeneration of NO_x and free radicals by the reverse reaction. The hydroxy ketone products, formed to a minor extent in the degradation of 1-butanol and 1-pentanol, are slightly less reactive towards OH radicals [117] than the aldehydes and their photolysis is also less important than for the aldehydes such that they have a minor secondary influence on ozone formation.

The formation of thermally stable organic nitrates by the reactions $\text{RO}_2\cdot + \text{NO}$, is expected to inhibit ozone formation as it is a sink for the free radicals and NO_x . The overall atmospheric lifetimes of the β , γ and δ hydroxy alkyl nitrates due to photolysis and to OH reaction are estimated to be 2-7 days [118, 119]. This implies that these compounds may be important NO_x reservoir species and can survive long range transport to regions remote from the original pollution source influencing regional and possibly global tropospheric ozone production by the subsequent NO_x release. Hydroxy nitrates are, however, minor products of the oxidation of 1-butanol and 1-pentanol, accounting for only an estimated 4% and 7%, respectively of total first generation products at high NO_x .

- **Esters.** The experimental product data of the present studies [see section 5.2 and 5.3] have helped to elucidate several aspects of the atmospheric degradation mechanisms of methyl propionate and dimethyl succinate; in particular, they have provided insight into the reaction routes of the alkoxy radicals formed during the atmospheric oxidation of these esters. The intermediate alkoxy radicals are observed to undergo, with different relative importance, reaction with oxygen, isomerisation and/or decomposition.

The bulk of the photooxidation of both esters produces multifunctional oxygenated compounds such as HC(O)C(O)OCH_3 , $\text{CH}_3\text{C(O)C(O)OCH}_3$ and $\text{CH}_3\text{CH}_2\text{C(O)OH}$ in the case of methyl propionate and $\text{CH}_3\text{OC(O)CH}_2\text{CH}_2\text{C(O)OH}$, $\text{CH}_3\text{OC(O)CH}_2\text{CH}_2\text{C(O)OC(O)H}$ and $\text{CH}_3\text{OC(O)C(O)CH}_2\text{C(O)OCH}_3$ in the case of dimethyl succinate which all have a lower reactivity towards OH radicals than the parent compounds. In particular, anhydrides and acids, especially those with lower molecular weight, are highly soluble compounds and may be rapidly incorporated into clouds droplets (where hydration of the anhydrides leads to acid formation) and rained out, contributing to the acidity of precipitation.

The formation of organic nitrates, via processes such as $\text{RO}_2\cdot + \text{NO}$, in the degradation of methyl propionate and dimethyl succinate are poorly quantified and their overall formation

yields could only be estimated. As described above, organic nitrates may play an important role in regional air chemistry due to their relatively long atmospheric lifetimes.

Finally, in order to estimate the tendency of the investigated compounds to promote ozone formation, all the aspects of their reaction mechanisms must be combined with the various characteristics of the environment into which they are emitted, in computer model simulations.

- **Alcohols.** To date, there have been only a few published studies on the ability of alcohols to generate ozone. Derwent *et al.* [13, 120] estimated the incremental change in ozone produced by an additional incremental mass emission of alcohols in a photochemical trajectory model using a realistic air mass trajectory for regional scale ozone formation across Northwest Europe. The primary alcohols show Photochemical Ozone Creation Potential values [POCP = (ozone increment with the alcohol/ozone increment with ethylene) × 100] ranging from 20 for methanol to 63 for 1-butanol. Note that ethane, regarded as unreactive species with a negligible contribution to regional scale ozone formation, has a POCP of 12.3 [120]. These results have been confirmed by recent modelling studies of Jenkin *et al.* [121] and Andersson-Sköld *et al.* [122] on the photochemical ozone creation potentials of oxygenated organic compounds in the planetary boundary layer over Northwest Europe. No specific and quantitative indications on the ozone impact were found in the literature for 1-pentanol.

- **Esters.** There are a number of different ways to define the VOC effects on ozone. Similar to the POCP concept is “incremental reactivity” criterion developed by Carter and Atkinson [123, 124]. This is defined as the amount of additional ozone formation resulting from the addition of a small amount of the compound to the system in which ozone is formed, divided by the amount of compound added. Carter [105] reported the incremental reactivities calculated for dimethyl succinate, relative to ethane, for various scenarios representing different urban ozone exceedence areas around the United States [105]. The predicted ozone impact for dimethyl succinate, relative to an equal mass of ethane, is ~ 0.65 – 0.8 [105]; the relative reactivity appeared to be only slightly affected by variations in scenarios conditions or how ozone was quantified. The estimated dimethyl succinate mechanism used by Carter [105] in these atmospheric simulations differs, in some respects significantly, in the branching ratios of competing reactions of the various alkoxy radicals from the mechanism proposed here on the basis of the experimental results of the product study.

No estimates of the potential effect of methyl propionate on ozone formation in urban atmosphere were found in the literature. Derwent *et al.* [13, 120] reported POCP values relative to ethylene for a series of esters (including methyl formate, and the acetates from methyl

acetate up to *t*-butyl acetate). Esters showed low atmospheric reactivity with POCPs which, in some cases, were lower than that of ethane regarded as unreactive species.

In general, the estimates of the potential effect on ozone formation calculated for alcohols and esters indicates that oxygenated (especially highly oxygenated) VOCs tend to be inefficient ozone producers. This is partly because there are fewer oxidation steps available before complete oxidation to CO₂ and partly because the presence of oxygen tends to decrease the reactivity towards OH per unit molecular weight. Consequently, the chemical properties which make them suitable candidates as alternative solvents and relatively harmless compounds regarding health also appear to be associated with low potential for ozone production. This is particularly the case for the esters which, in addition to being relatively unreactive itself, have also very unreactive oxidation products. These species appear, therefore, to be of some potential significance for the replacement and substitution of more reactive organic compounds in industrial or chemical processes and as solvents.

Chapter 8

Summary

The decision whether it is appropriate and beneficial for the environment to deploy specific oxygenated organic compounds as replacements for traditional solvent types requires a quantitative assessment of their potential atmospheric impacts including tropospheric ozone and other photooxidant formation. This involves developing chemical mechanisms for the gas-phase atmospheric oxidation of the compounds which can be reliably used in models to predict their atmospheric reactivity under a variety of environmental conditions. Until this study, there was very little information available concerning the atmospheric fate of alcohols and esters. The objectives of this study were to measure the atmospheric reaction rates and to define atmospheric reaction mechanisms for the following selected oxygenated volatile organic compounds: the alcohols, 1-butanol and 1-pentanol, and the esters, methyl propionate and dimethyl succinate.

The study has successfully addressed these objectives.

Relative rate coefficients have been measured for the reactions of the hydroxyl radicals with 1-butanol, 1-pentanol, methyl propionate and three dibasic esters dimethyl succinate, dimethyl glutarate and dimethyl adipate. The rate coefficients (in units of $\text{cm}^3 \text{ molecule}^{-1} \text{ s}^{-1}$) were found to be $(8.28 \pm 0.85) \times 10^{-12}$ and $(1.11 \pm 0.11) \times 10^{-11}$ for 1-butanol and 1-pentanol, respectively; $(9.29 \pm 1.13) \times 10^{-13}$ for methyl propionate; $(1.95 \pm 0.27) \times 10^{-12}$, $(2.18 \pm 0.30) \times 10^{-12}$ and $(3.73 \pm 0.59) \times 10^{-12}$ for dimethyl succinate, dimethyl glutarate and dimethyl adipate, respectively. In addition, rate coefficients have been also measured for the reactions of chlorine atoms with methyl propionate and its major degradation products – propionic formic anhydride, propionic acid and methyl pyruvate – and with the three dibasic esters. The present kinetic data improve the reliability and precision of the OH radical and Cl atom kinetic data base required to develop structure-reactivity relationships for OH and Cl reaction with VOCs, especially for oxygenated compounds, and to predict their tropospheric lifetime.

The tropospheric degradation of alcohols and esters is initiated by reaction with hydroxyl radicals. The OH radical abstracts a hydrogen from a C–H group and the alkyl radical formed

rapidly adds O_2 to generate a peroxy radical, RO_2^\cdot . In the presence of NO, peroxy radicals react with NO to produce the corresponding alkoxy radicals, RO^\cdot , and NO_2 . Alkoxy radicals are important intermediates in the atmospheric oxidation of most volatile organic compounds. Alkoxy radicals have been shown to undergo a variety of degradation pathways – reaction with oxygen, unimolecular decomposition or isomerisation – resulting in the complex behaviour exhibited in the oxidation of organic compounds under atmospheric conditions.

Product investigations of the room temperature gas-phase reaction of OH radicals with 1-butanol and 1-pentanol in the presence of NO_x have been carried out in the outdoor *EUPHORE* smog chamber facility in Valencia/Spain. The observed oxidation products and their distribution have allowed the construction of the first explicit degradation mechanism of long-chain alcohols. Several interesting general conclusions can be drawn about the atmospheric fate of primary alcohols:

- the OH radical reaction with primary alcohols proceeds principally by hydrogen atom abstraction from the $-CH_2-$ group at the α position to the $-OH$ functional group due to the activating effect of this entity. The α hydroxy alkyl radical thus formed reacts with oxygen to form the corresponding aldehyde in unit yield.
- The reaction channels involving H-atom abstraction from $-CH_2-$ groups at the β , γ etc. positions gradually decrease in importance, since the activating effect of the $-OH$ group lessens with increasing distance from the functional group.
- The dominant reaction pathway of the β , γ etc. hydroxy alkoxy radicals, RO^\cdot appears to be decomposition to form aldehydes and hydroxy carbonyl compounds.
- The first generation oxidation products are mainly aldehydes and, to a minor extent, hydroxy aldehydes and hydroxy ketones; their further reactions with OH radicals and photolysis have an important influence on ozone formation and on the chemistry and transport of NO_y in the troposphere.

Based on the results of the product studies, detailed atmospheric degradation mechanisms have been constructed for the OH radical initiated oxidation of 1-butanol and 1-pentanol.

The reaction of OH radicals with the investigated esters, methyl propionate and dimethyl succinate, is relatively slow, making photoreactor chamber studies of the oxidation products difficult and their analysis inaccurate. Thus, the faster reactions with chlorine atoms were

employed as a surrogate to mimic the OH radical reactions, allowing the first detailed elucidation of the oxidation mechanism of methyl propionate and dimethyl succinate.

In general, reactions of chlorine atoms with VOCs represent a convenient method to generate the possible alkoxy radicals and to investigate their atmospheric fates.

- Alkoxy radicals of structure $\text{RC(O)OCH}_2\text{O}^\bullet$ undergo i) α ester rearrangement resulting in the formation of the corresponding acid RC(O)OH and the formyl radical $\text{HC}(\cdot)\text{O}$; ii) bimolecular reaction with O_2 yielding the anhydride RC(O)OC(O)H .
- The other possible alkoxy radicals formed in the degradation mechanism of these esters are found to undergo, with different relative importance, reaction with oxygen, decomposition or, if possible, isomerisation to form multifunctional oxygenated products which show a lower reactivity towards OH radicals than the parents compounds.

A *Structure–Activity Relationship (SAR)* method has been used to predict the relative importance of the various alkoxy radicals formed in the gas-phase reaction of these esters with OH radicals; these estimates have been combined with the alkoxy radicals fates ascertained in Cl atoms studies to propose atmospheric degradation mechanisms for the OH radical initiated oxidation of methyl propionate and dimethyl succinate.

The investigated esters appear to exhibit low reactivity with respect to ozone and other secondary pollutant formation. These species would appear to be suitable candidates as replacements in a substitution programme for aromatic and olefinic hydrocarbon solvents.

Finally, the mechanisms constructed from the product data obtained in this work can be incorporated into models to obtain accurate estimates of the impacts of the ozone formation from these compounds. The results from the models could serve as a basis for beneficial decision making.

Annex A

Abbreviation

CFC	Chlorofluorocarbon
DBE	Dibasic ester
DBE-4	Dimethyl succinate
DBE-5	Dimethyl glutarate
DBE-6	Dimethyl adipate
EPA	Environmental protection agency
<i>EUPHORE</i>	European photoreactor
FTIR	Fourier transform infrared
GC	Gas chromatography
HPLC	High performance liquid chromatography
IR	Infrared (≥ 700 nm)
MPR	Methyl propionate
MPYR	Methyl pyruvate
NMR	Nuclear magnetic resonance
NMVOC	Non-methane volatile organic compound
NO _x	NO + NO ₂
NO _y	It consists of NO, NO ₂ , nitric acid (HNO ₃), inorganic aerosol nitrate (NO ₃ ⁻), nitrous acid (HNO ₂), nitrate radical (NO ₃), peroxy nitric acid (HOONO ₂), chlorine nitrate (ClONO ₂), dinitrogen pentoxide (N ₂ O ₅), PAN and other nitrates of various types.
OVOC	Oxygenated volatile organic compound
PAN	Peroxy acetyl nitrate
POCP	Photochemical ozone creation potential
ppb	Parts per billion (1 ppb = 2.46×10^{10} molecules cm ⁻³ at 1 bar and 298 K)
ppm	Parts per million (1 ppm = 2.46×10^{13} molecules cm ⁻³ at 1 bar and 298 K)
PRA	Propionic acid
PRFA	Propionic formic anhydride
<i>SAR</i>	Structure activity relationship

UV	Ultraviolet (200-400 nm)
VIS	Visible (400-700 nm)
VOC	Volatile organic compound

Annex B

Experimental parameters

Table B.1: Reaction rate coefficients of the employed reference compounds in $\text{cm}^3 \text{ molecule}^{-1} \text{ s}^{-1}$.

Substance		Reaction rate coefficient	
methanol	CH_3OH	$(9.32 \pm 2.33) \times 10^{-13}$	k_{OH}
ethanol	$\text{C}_2\text{H}_5\text{OH}$	$(3.27 \pm 0.65) \times 10^{-12}$	
<i>n</i> -propanol	$\text{C}_3\text{H}_7\text{OH}$	$(5.53 \pm 1.66) \times 10^{-12}$	
<i>n</i> -butane	<i>n</i> - C_4H_{10}	$(2.53 \pm 0.51) \times 10^{-12}$	
<i>c</i> -hexane	<i>c</i> - C_6H_{12}	$(7.49 \pm 1.87) \times 10^{-12}$	
Cl-methane	CH_3Cl	$(4.80 \pm 0.96) \times 10^{-13}$	k_{Cl}
Cl-ethane	$\text{C}_2\text{H}_5\text{Cl}$	$(8.04 \pm 0.57) \times 10^{-12}$	
<i>iso</i> -Cl-propane	<i>iso</i> - $\text{C}_3\text{H}_7\text{Cl}$	$(2.0 \pm 0.3) \times 10^{-11}$	
ethane	C_2H_6	$(5.74 \pm 0.46) \times 10^{-11}$	
methyl formate	$\text{CH}_3\text{OC(O)H}$	$(1.4 \pm 0.1) \times 10^{-12}$	

Table B.2: Experimental conditions used in experiments performed to measure OH and Cl reaction rate coefficients. DBE-4 = dimethyl succinate; DBE-5 = dimethyl adipate; DBE-6 = dimethyl glutarate; min = photolysis duration in minutes; c = concentration in ppm, N = number of the experiments.

	substrate	reference	min	$c_{\text{substrate}}$	$c_{\text{ref.}}$	$c_{\text{substrate}}/c_{\text{ref.}}$	N
OH	1-butanol ^a	<i>c</i> -C ₆ H ₁₂	7-15	11.1-14	2.5-4	4:1-3:1	3
	1-pentanol ^a	<i>c</i> -C ₆ H ₁₂	8-15	9-11.8	2.5-4	3:1-4:1	3
	methyl propionate ^b	CH ₃ OH	10-15	7.8-10.6	22.4-30	1:2-1:4	2
		C ₂ H ₅ OH	8-19	7.8-10.6	15.4-20.6	1:1-1:2	2
	DBE-4 ^{b, c}	<i>n</i> -C ₄ H ₁₀	24-28	8-9.2	17.3-22.2	1:2 – 1:3	6
		C ₂ H ₅ OH	25-30	8-9.2	15.3-20	1:2	4
DBE-5 ^{a, c}	C ₂ H ₅ OH	17-22	14.3-16.4	19.8-30.4	1:1-1:2	4	
	C ₃ H ₇ OH	17-25	14.3-16.4	14.5-28.2	1:1 – 1:2	4	
DBE-6 ^{b, c}	C ₃ H ₇ OH	16-19	16.6-20.3	20.1-36.2	1:1 – 1:2	4	
	<i>c</i> -C ₆ H ₁₂	16-19	12.9-20.6	5.9-7.1	2:1 – 3:1	4	
Cl	methyl propionate ^b	C ₂ H ₅ Cl	6-10	9.5-12-6	24.7-37	1:2 – 1:3	2
		C ₂ H ₆	8-11	9.5-12-6	30.2-37	1:3 – 1:4	2
	propionic formic anhydride ^b	C ₂ H ₅ Cl	10-14	8.4-22.1	16.8-25.3	1:1-1:2	2
		CH ₃ OC(O)H	10-14	8.4-22.1	9.8-14.7	1:2-2:1	2
	propionic acid ^b	C ₂ H ₅ Cl	9	12.4	24.7	1:2	1
		CH ₃ OC(O)H	9-12	12.2-20.3	2.4-5	4:1 – 5:1	2
	methyl pyruvate ^b	CH ₃ OC(O)H	9	13.1	3.9	1:3	1
		CH ₃ Cl	10-17	9.8-13.3	14.8-24.7	1:1 – 1:2	2
	DBE-4 ^{b, c}	C ₂ H ₅ Cl	10-15	6.9-9.1	24.7-41.9	1:3 – 1:6	9
		<i>iso</i> -C ₃ H ₇ Cl	10-15	6.9-9.1	6.6-16.5	1:1 – 1:2	9
	DBE-5 ^{b, c}	C ₂ H ₅ Cl	10-12	7.1-8.3	24.5-37	1:3 – 1:5	2
		<i>iso</i> -C ₃ H ₇ Cl	9-13	6.1-7.2	9.9-11.2	1:1 – 1:2	2
DBE-6 ^{b, c}	C ₂ H ₅ Cl	9-15	5.5-7.4	24.5-37	1:3 – 1:7	2	
	<i>iso</i> -C ₃ H ₇ Cl	10-14	5.5-7.4	9.9-11.2	1:1 – 1:2	2	

^a 480 ℓ reactor; 24 superactinic lamps.

^b 405 ℓ reactor; 18 fluorescent lamps.

^c Correction for wall loss according to the Eq. II.

Table B.3: Experimental conditions used in experiments for the mechanistic study of the OH radical initiated oxidation of 1-pentanol.

System	HONO
Number of experiments	4
Optical path length (m)	554.5 (EUPHORE)
Photolysis time (min)	186-315
Spectra	number
	scans
	time resolution (min)
Chromatograms	number
	time resolution (min)
Temperature (K)	298 ± 2
Pressure (mbar)	1001 ± 10
Concentration (ppb)	1-pentanol
	HONO
1-Pentanol consumption	30-40%

Table B.4: Experimental conditions used in experiments for the mechanistic study of the OH radical initiated oxidation of 1-butanol.

System	HONO
Number of experiments	4
Optical path length (m)	554.5 (EUPHORE)
Photolysis time (min)	75-160
Spectra	number
	scans
	time resolution (min)
Chromatograms	number
	time resolution (min)
Temperature (K)	298 ± 2
Pressure (mbar)	1001 ± 10
Concentration (ppb)	1-butanol
	HONO
1-Butanol consumption	20-30%

Table B.5: Experimental conditions used in experiments for the mechanistic study of the Cl atom initiated oxidation of methyl propionate.

System	Cl ₂ /NO
Number of experiments	10
Reactor (ℓ)	405
Optical path length (m)	50.4
Lamp TL05	18
Photolysis time (s)	7-20
Spectra number	7-10
scans	60-120
time resolution (s)	70-130
Temperature (K)	296 \pm 2
Pressure (mbar)	1002 \pm 10
Concentration (ppm) methyl propionate	10-15
Cl ₂	15-20
NO	15-20
Methyl propionate consumption	40-60%

Table B.6: Experimental conditions used in experiments for the mechanistic study of the Cl atom initiated oxidation of dimethyl succinate.

System	Cl ₂ /NO
Number of experiments	8
Reactor (ℓ)	405
Optical path length (m)	50.4
Lamp TL05	18
Photolysis time (s)	10-15
Spectra number	10-15
scans	40-90
time resolution (s)	50, 60, 90
Temperature (K)	298 ± 2
Pressure (mbar)	1004 ± 10
Concentration (ppm) dimethyl succinate	8-15
Cl ₂	20-30
NO	15-20
Dimethyl succinate consumption	40-60%

Annex C

Absorption cross sections

The following tables list the FTIR absorption cross sections determined in this work. Most of the calibration measurements were performed in the 405 ℓ reactor, and partly in the 480 ℓ reactor, at 1000 mbar and at 298 K.

Typically, weighed amounts of a liquid or solid-phase compound were dissolved in CH₂Cl₂ or CHCl₃, and different amounts of the solution were, then, subsequently injected into the evacuated chamber in a stream of gas. All the spectra were acquired with a resolution of 1 cm⁻¹. The absorption coefficients are indicated in ppm⁻¹ m⁻¹ units (1 ppm = 2.46 × 10¹³ molecule cm⁻³ at 1000 mbar and 298 K) and refer to the maximum IR absorption at the indicated wavelengths or to the integral of the absorption bands.

The measured values have an uncertainty of ± 10%.

<i>1-butanol</i>	
Wavelengths	σ_{10}
3704 – 3628	$2.32 \cdot 10^{-3}$
3013 – 2816	$4.45 \cdot 10^{-2}$
1504 – 1427	$1.78 \cdot 10^{-3}$
1428 – 1362	$1.55 \cdot 10^{-3}$
1114.4 – 977	$1.12 \cdot 10^{-2}$

<i>1-pentanol</i>	
Wavelengths	σ_{10}
3015 – 2851	$5.06 \cdot 10^{-2}$
1524 – 1429	$2.10 \cdot 10^{-3}$
1429 – 1353	$1.72 \cdot 10^{-3}$
1147 – 931	$1.47 \cdot 10^{-3}$

<i>pentanal</i>	
Wavelengths	σ_{10}
3017 – 2845	$2.91 \cdot 10^{-2}$
2842 – 2762	$3.64 \cdot 10^{-3}$
2758 – 2648	$7.25 \cdot 10^{-3}$
1842 – 1661	$2.00 \cdot 10^{-2}$
1506 – 1314	$4.99 \cdot 10^{-3}$
1047 – 947	$1.74 \cdot 10^{-3}$

<i>butanal</i>	
Wavelengths	σ_{10}
3020 – 2852	$2.09 \cdot 10^{-2}$
2852 – 2760	$4.14 \cdot 10^{-3}$
2760 – 2645	$7.60 \cdot 10^{-3}$
1823 – 1665	$2.04 \cdot 10^{-2}$

<i>propanal</i>	
Wavelengths	σ_{10}
3027 – 2862	$1.15 \cdot 10^{-2}$
2862 – 2764	$5.28 \cdot 10^{-3}$
2764 – 2645	$7.72 \cdot 10^{-3}$
1803 – 1708	$2.00 \cdot 10^{-2}$
1162 – 1048	$2.04 \cdot 10^{-3}$
937 – 816	$3.05 \cdot 10^{-3}$

<i>dimethyl glutarate</i>	
Wavelengths	σ_{10}
1812 – 1711	$4.53 \cdot 10^{-2}$
1492 – 1409	$9.40 \cdot 10^{-3}$
1234 – 1116	$2.94 \cdot 10^{-2}$
1108 – 955	$6.51 \cdot 10^{-3}$

<i>methyl propionate</i>	
Wavelengths	σ_{10}
3090 – 2813	$2.48 \cdot 10^{-2}$
1803 – 1721	$3.23 \cdot 10^{-2}$
1496 – 1411	$7.38 \cdot 10^{-3}$
1387 – 1312	$7.31 \cdot 10^{-3}$
1312 – 1147	$3.86 \cdot 10^{-2}$
1047 – 996	$1.54 \cdot 10^{-3}$

<i>propionic acid</i>	
Wavelengths	σ_{10}
3607 – 3553	$8.03 \cdot 10^{-3}$
3060 – 2868	$1.08 \cdot 10^{-2}$
1843 – 1718	$4.19 \cdot 10^{-2}$
1413 – 1345	$4.49 \cdot 10^{-3}$
1215 – 1100	$2.22 \cdot 10^{-2}$
1100 – 1028	$6.84 \cdot 10^{-3}$
848 – 776	$1.25 \cdot 10^{-3}$

<i>methyl pyruvate</i>	
Wavelengths	σ_{10}
1817 – 1694	$4.96 \cdot 10^{-2}$
1389 – 1237	$2.00 \cdot 10^{-2}$
1227 – 1176	$3.10 \cdot 10^{-3}$
1176 – 1086	$2.72 \cdot 10^{-2}$
1029 – 998	$2.05 \cdot 10^{-2}$

<i>propionic formic anhydride</i>	
Wavelengths	σ_{10}
3590 – 3559	$7.13 \cdot 10^{-4}$
1824 – 1762	$6.32 \cdot 10^{-2}$
1211 – 1107	$2.10 \cdot 10^{-2}$
1099 – 1007	$5.40 \cdot 10^{-2}$

<i>dimethyl succinate</i>	
Wavelengths	σ_{10}
2983 – 2819	$7.43 \cdot 10^{-3}$
1847 – 1681	$5.22 \cdot 10^{-2}$
1400 – 1308	$1.16 \cdot 10^{-2}$
1189 – 1095	not linear

<i>succinic formic anhydride</i>	
Wavelengths	σ_{10}
1808	$7.92 \cdot 10^{-4}$
1126	$8.57 \cdot 10^{-4}$
1028	$6.33 \cdot 10^{-4}$

<i>mono-methyl succinate</i>	
Wavelengths	σ_{10}
3596 – 3568	$2.63 \cdot 10^{-3}$
1844 – 1721	$2.40 \cdot 10^{-2}$
1385 – 1335	$2.92 \cdot 10^{-3}$
1234 – 1153	$3.95 \cdot 10^{-3}$
1153 – 1102	$9.05 \cdot 10^{-3}$

<i>dimethyl oxaloacetate ENOL FORM</i>	
Wavelengths	σ_{10}
1713 – 1659	$2.64 \cdot 10^{-2}$
1659 – 1633	$1.23 \cdot 10^{-2}$
1295 – 1246	$8.57 \cdot 10^{-2}$
1046 – 1015	$7.611 \cdot 10^{-3}$

<i>2-Br-methyl acetate</i>	
Wavelengths	σ_{10}
3140 – 2811	$1.02 \cdot 10^{-3}$
1830 – 1699	$3.30 \cdot 10^{-2}$
1342 – 1237	$2.70 \cdot 10^{-2}$
1237 – 1070	$1.82 \cdot 10^{-2}$
1053 – 980	$4.20 \cdot 10^{-3}$

<i>4,5-dihydro-2-methyl furan</i>	
Wavelengths	σ_{10}
3041 – 2806	$2.81 \cdot 10^{-2}$
1717 – 1639	$6.06 \cdot 10^{-3}$
1271 – 1215	$4.02 \cdot 10^{-3}$
1215 – 1136	$5.58 \cdot 10^{-3}$
1044 – 984	$5.43 \cdot 10^{-3}$
984 – 884	$6.66 \cdot 10^{-3}$

Annex D

Syntheses

All the NMR spectra were recorded using a Bruker ARX 400 at 400 MHz and the gas-phase FTIR spectra using a Nicolet Magna 550 with a total path length of 50.4 m a resolution of 1 cm^{-1} .

D.1 Methyl nitrite

Methyl nitrite was prepared following a published method [125] with some small modifications.

69 g (1 mol) of NaNO_2 and 50 ml $\text{CH}_3\text{OH}/40\text{ ml H}_2\text{O}$ solution were mixed in a 2 l two-neck flask equipped with a stirrer and a dropping funnel and cooled in an ice bath.

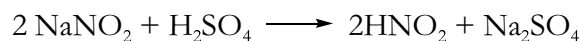
A solution of 27 ml H_2SO_4 conc. in 50 ml H_2O was added dropwise to the mixture over a period of 3 hours. The reaction products were swept out of the reaction flask, passed over an anhydrous CaCl_2 bed and collected in a trap cooled at dry-ice temperature. The pale yellow liquid methyl nitrite was stored in the dark at $-78\text{ }^\circ\text{C}$ to prevent decomposition.

Yield: not determined

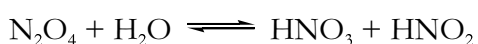
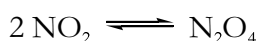
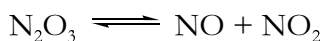
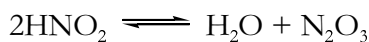
Purity: in the FTIR spectrum, CH_3OH was not detectable.

D.2 Nitrous acid

Procedure [126]: 30 ml of a 30% sulphuric acid solution were placed in a 100 ml three-neck round bottomed flask fitted with a stirrer, dropping funnel, thermometer and synthetic air inlet and outlet; the latter was directly connected to the reaction chamber. To the stirred flask 20 ml of a 1% NaNO_2 solution were added dropwise at $20\text{ }^\circ\text{C}$ over a period of 30-50 min. Nitrous acid and the side products NO and NO_2 were flushed into the reaction chamber in a stream of gas.

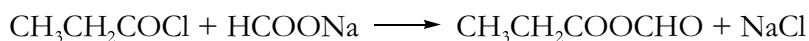


Aqueous solutions of nitrous acid are unstable and decompose when heated – slowly also at room temperature – and concentrated. NO and NO₂ are, then, formed according to the following disproportion mechanism:



D.3 Propionic formic anhydride

Propionic formic anhydride was synthesised following a procedure similar to that described in the literature for methoxymethyl formate [127, 128]:



A dry 50 ml round bottomed flask equipped with a thermometer was charged with 13.2 g (194 mmol) sodium formate (Fluka, 99.5%) finely ground to ensure better contact. To the reagent, previously heated to the temperature of 200 °C, 4.0 ml (46 mmol) of propionyl chloride (Aldrich, 97%) was rapidly added. In order to ensure complete reaction, the flask was shaken until a homogenous white mixture was obtained, while the temperature was maintained at 23-27 °C using a cooling bath. The mixture was then filtered with suction and the solid residue rinsed four times with 20 ml diethyl ether (dried over calcium chloride); the washings were added to the original filtrate. The removal of the solvent by vacuum evaporation at room temperature afforded 3.4 g of a slightly yellow and resinous product.

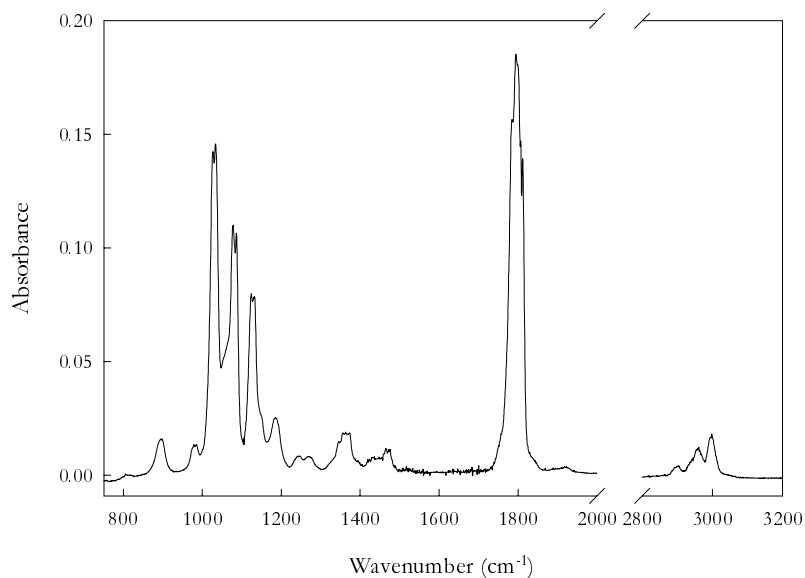
The product was vacuum distilled and 2.2 g of the colourless fraction boiling at 51-54 °C at 35 mbar was collected.

Yield: 3.4 g (72%)

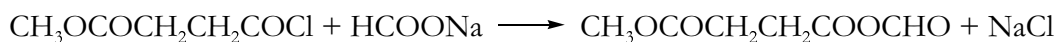
Purity: 80% (¹H-NMR)

¹H-NMR (CDCl₃): δ (ppm) = 9.03 (s, 1H, -C(O)H); 2.51 (q, 2H, -CH₂-C(O)-);
1.16 (t, 3H, -CH₃).

FTIR (gas-phase):



D.4 Succinic formic anhydride



3.25 ml (27 mmol) of methyl succinyl chloride (Fluka, 98%) was, rapidly, added to 6.8 g (100 mmol) of sodium formate (Aldrich, 99%), previously heated to a temperature of 50 °C.

The synthesis of succinic formic anhydride proceeded according to the steps described in D.3. However, in this case, the final vacuum distillation of the product reaction residue was carried out without success: the pale yellow and dense product decomposed at 30 °C at 30 mbar to a yellow resinous solid product.

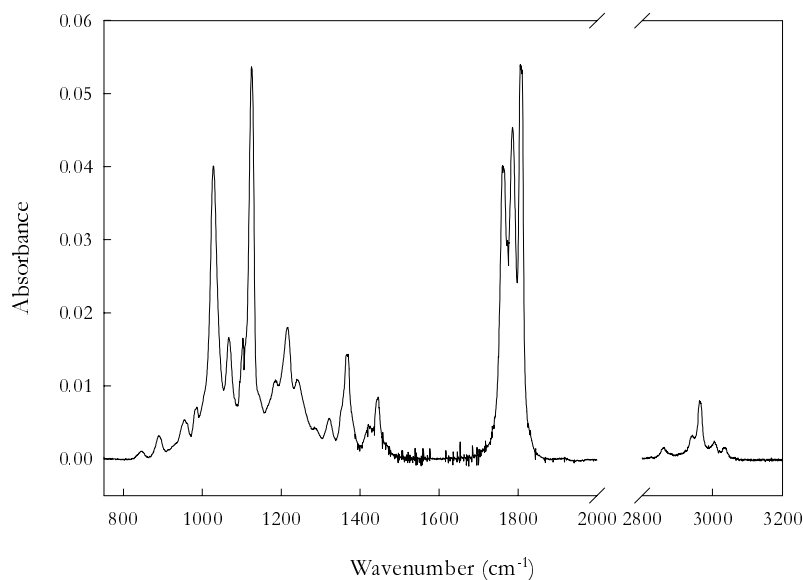
Yield: 4.3 g (100%)

Purity: 70% (¹H-NMR)

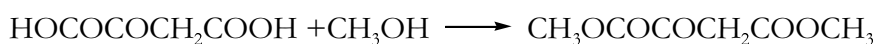
¹H-NMR (CDCl₃): δ (ppm) = 9.03 (s, 1H, -C(O)H); 3.67 (s, 3H, -CH₃); 2.80 (t, 2H, -CH₂-);
2.67 (t, 2H, -CH₂-).

¹³C-NMR (CDCl₃): δ (ppm) = 171.9 [-C(O)-O-CH₃]; 155.8 [-C(O)H];
169.6 [-C(O)-OC(O)H]; 29.1 [-CH₂-]; 27.7 [-CH₂-].

FTIR (gas-phase):



D.5 Dimethyl oxaloacetate



A 100 ml flask was charged with 2 g (15.14 mmol) of oxalacetic acid and 20 ml of methanol. To the stirred mixture, 0.5 ml of H_2SO_4 conc. was added dropwise. The mixture was heated for few hours under reflux. The solution was, then, allowed to cool at room temperature, evaporated under vacuum and redissolved in ethyl acetate. The organic layer was extracted twice with water, using a saturated aqueous solution of NaCl and dried with anhydrous Na_2SO_4 . The removal of the solvent afforded 1.8 g of a solid crystalline mass of dimethyl oxaloacetate pure to such an extent that further purification was not necessary.

As reported in the literature [104], dimethyl oxaloacetate has been shown to exist exclusively in an enol structure in the solid phase. In solution, dimethyl oxaloacetate, being a 1,3-dicarbonyl compound, exists as an equilibrium mixture of keto and enol forms. It is known that the keto-enol tautomerization is solvent dependent and that the proportion of the keto form increases with increasing solvent polarity. An NMR study of dimethyl oxaloacetate confirmed this behaviour and allowed the position of the keto-enol equilibrium in CDCl_3 to be defined as 83.5% of the enol form and 16.5% of the keto form.

Yield: 1.6 g (74%)

Purity: 100% ($^1\text{H-NMR}$)

Melting point: 74 °C

Enol form

$^1\text{H-NMR}$ (CDCl_3): δ (ppm) = 11.52 (s, 1H, $-\text{OH}$); 5.99 (s, 1H, $\text{H-C}=\text{C-OH}$);

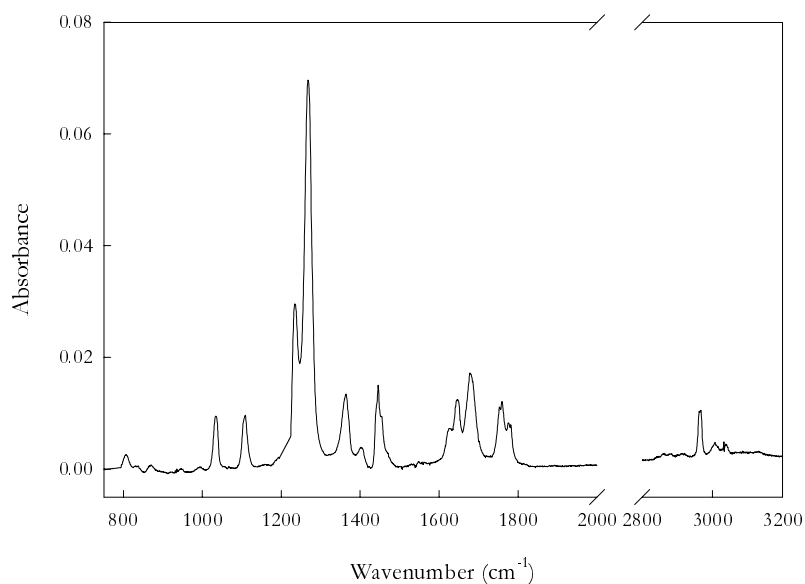
3.85 (s, 3H, $-\text{O-CH}_3$); 3.79 (s, 3H, $-\text{O-CH}_3$).

$^{13}\text{C-NMR}$ (CDCl_3): δ (ppm) = 172.14 [$-\text{C}=\text{C-OH}$]; 162.11 [$-\text{C(O)C}=\text{C}-$];

159.09 [OHCC(O)-]; 96.68 [$-\text{C}=\text{C-OH}$]; 52.98 [$\text{CH}_3-\text{O}-$];

52.07 [$\text{CH}_3-\text{O}-$].

FTIR (gas-phase):



Keto form

$^1\text{H-NMR}$ (CDCl_3): δ (ppm) = 3.86 (s, 3H, $-\text{O-CH}_3$); 3.80 (s, 3H, $-\text{O-CH}_3$);

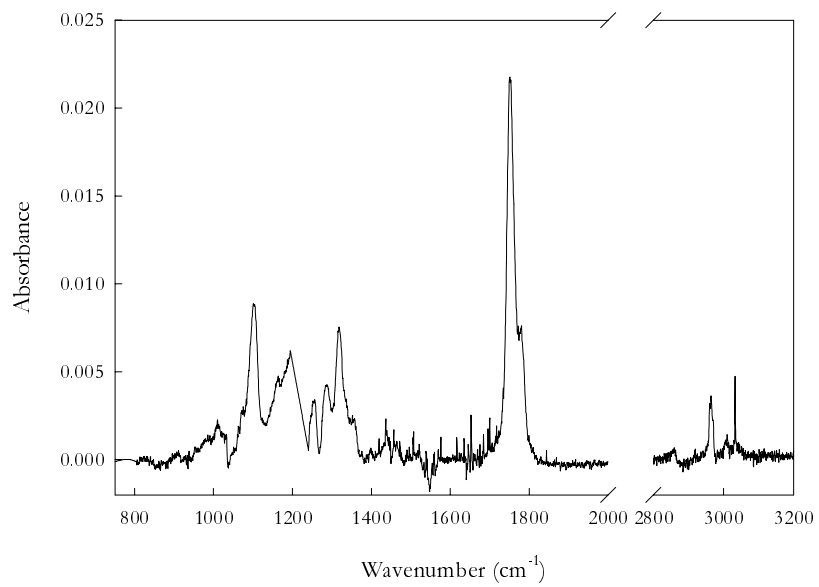
3.72 (s, 2H, $-\text{CH}_2-$).

$^{13}\text{C-NMR}$ (CDCl_3): δ (ppm) = 186.07 [$-\text{CH}_2-\text{C(O)-C(O)-}$]; 166.68 [$-\text{O-C(O)-CH}_2-$];

160.33 [$-\text{C(O)-C(O)-O-}$]; 53.34 [$\text{CH}_3-\text{O}-$];

52.57 [$\text{CH}_3-\text{O}-$]; 44.89 [$-\text{CH}_2-$].

FTIR (gas-phase):



Annex E

Gases and Chemicals

Table E. 1: Gases employed in this work. All the gases were supplied by Messer Griesheim.

Gas	Purity (Vol %)
<i>n</i> -butane	99.5
chlorine	99.8
chloroethane	99
chloromethane	99.8
ethane	99.5
nitrogen	99.999
NO	99.8
NO ₂	98
synthetic air (20.5% O ₂ in N ₂)	99.995

Table E.2: Chemicals employed in this work: stated purities and manufacturers.

Chemicals	Purity (Vol %)	Company
butanal	99.5	Aldrich
1-butanol	99	Lancaster
chloroform	99.9+	Aldrich
2-chloropropane	99 (GC)	Aldrich
dichloromethane	99+	Lancaster
4,5-dihydro-2-methylfuran	97 (GC)	Aldrich
dimethyl adipate	99+ (GC)	Aldrich
dimethyl glutarate	98	Aldrich
dimethyl succinate	98 (GC)	Aldrich
ethanol	96	Fluka
<i>n</i> -hexane	99.9+	Aldrich
4-hydroxy-2-butanone	95	Lancaster
5-hydroxy-2-pentanone	95	Aldrich
1-iodopentane	98	Fluka
3-iodopropanol	97	Aldrich
methanol	99.8	Fluka
methyl-bromo-acetate	97	Aldrich
methyl crotonate	98	Aldrich
methyl formate	97	Aldrich
methyl propionate	99 (GC)	Aldrich
methyl pyruvate	98	Aldrich
<i>mono</i> -methyl glutarate	95	Aldrich
<i>mono</i> -methyl succinate	95	Aldrich
methyl succinyl chloride	98	Fluka
oxolacetic acid	98	Aldrich
pentanal	99	Aldrich
1-pentanol	99+	Aldrich
propanal	97	Aldrich
1-propanol	99.7 (GC)	Merck
propionic acid	99	Aldrich
propionyl chloride	97	Aldrich
sodium formate	99.5	Fluka

Bibliography

- [1] P. J. Crutzen.
Introductory lecture. Overview of tropospheric chemistry: developments during the past quarter century and a look ahead.
Faraday Discussion **100** (1995) 1-21.

- [2] J. O. Nriagu and M. S. Simmons.
Environmental Oxidants.
Advances in Environmental Science and Technology. Vol 28. John Wiley & Sons, 1994.

- [3] A. J. Haagen-Smit, E. F. Darley, M. Zaitlin, H. Hull, W. Noble.
Investigation on injury to plants from air pollution in the Los Angeles area.
Plant Physiology **27** (1952) 18-34.

- [4] B. J. Finlayson-Pitts and J. N. Pitts, Jr.
Atmospheric Chemistry: Fundamentals and Experimental Techniques.
John Wiley & Sons, New York, 1986.

- [5] J. H. Seinfeld and S. N. Pandis.
Atmospheric Chemistry and Physics, from Air Pollution to Climate Change.
John Wiley & Sons, New York, 1998.

- [6] M. Ritter (ed.).
CORINAIR 1994 inventory.
European Topic Centre on Air Emissions. European Environmental Agency, Copenhagen, 1998.

- [7] Environmental data in Germany, 1998
Umweltbundesamt, Berlin, 1998.

- [8] Ullmann's Encyclopaedia of Industrial Chemistry.
VCH Verlagsgesellschaft, Weinheim, 1985.

- [9] P. J. Crutzen.
Mein Leben mit O₃, NO_x und anderen YZO_x-Verbindungen (Nobel-Vortrag).
Angewante Chemie **108** (1996) 1878-1898.
- [10] M. J. Molina.
Die Abnahme des Ozongehalts in der Polaratmosphäre (Nobel-Vortrag).
Angewante Chemie **108** (1996) 1900-1907.
- [11] F. S. Rowland.
Der Abbau des stratosphärischen Ozons durch Fluorchlorkohlenwasserstoffe (Nobel-Vortrag).
Angewante Chemie **108** (1996) 1908-1923.
- [12] E. Browing.
Toxicity and Metabolism of Industrial Solvents.
Elsevier Publishing Company, New York, 1965.
- [13] R. G. Derwent, M. E. Jenkin, S. M. Saunders.
Photochemical ozone potentials for a large number of reactive hydrocarbons under European conditions.
Atmospheric Environment **30** (1996) 181-199.
- [14] T. J. Kelly, R. Mukund, C. W. Spicer, A. J. Pollack.
Concentrations and transformations of hazardous air pollutants.
Environmental Science and Technology **28** (1994) 378A-386A.
- [15] Montreal Protocol on the Protection of the Ozone Layer.
United Nations Environment Programme, Nairobi, Kenya, 1992.
- [16] C. M. Cooney.
California struggles with the presence of MTBE in public drinking water wells.
Environmental Science and Technology **31** (1997) 269A.
- [17] D. A. Schwartz.
MTBE health assessment may loosen California's drinking water standard.
Environmental Science and Technology **33** (1999) 60A-61A.

- [18] V. Leclaire.
MTBE water contamination raises concerns, research questions.
Environmental Science and Technology **31** (1997) 176A-177A.
- [19] J. F. Pankow, N. R. Thomson, R. L. Johnson, A. I. Baehr, J. S. Zogorski.
The urban atmosphere as a non-point source for transport of MTBE and other volatile organic compounds (VOCs) to shallow groundwater.
Environmental Science and Technology **31** (1997) 2821-2828.
- [20] US state orders fuel additive ban.
Chemistry & Industry (1999) 247.
- [21] R. Atkinson.
Gas-Phase Tropospheric Chemistry of Organic Compounds.
Journal of Physical and Chemical Reference Data, Monograph No. 2, 1994.
- [22] T. J. Wallington and M. J. Kurylo.
The gas phase reactions of hydroxyl radicals with a series of aliphatic alcohols over the temperature range 240-440 K.
International Journal of Chemical Kinetics **19** (1987) 1015-1023.
- [23] L. Nelson, O. Rattigan, R. Neavyn, H. Sidebottom.
Absolute and relative rate constants for the reaction of hydroxyl radicals and chlorine atoms with a series of aliphatic alcohols and ethers at 298 K.
International Journal of Chemical Kinetics **22** (1990) 1111-1126.
- [24] T. J. Wallington, P. Dagaut, R. Liu, M. J. Kurylo.
Rate constants for the gas phase reactions of OH with C₅ through C₇ aliphatic alcohols and ethers: predicted and experimental values.
International Journal of Chemical Kinetics **20** (1988) 541-547.
- [25] T. J. Wallington, P. Dagaut, R. Liu, M. J. Kurylo.
The gas phase reactions of hydroxyl radicals with a series of esters over the temperature range of 240-440 K.
International Journal of Chemical Kinetics **20** (1988) 177-186.
- [26] S. Le Calvé, G. Le Bras, A. Mellouki.
Kinetic studies of OH reactions with a series of methyl esters.
Journal of Physical Chemistry A **101** (1997) 9137-9141.

- [27] S. M. Aschmann and R. Atkinson.
Rate constants for the gas phase reactions of selected dibasic esters with OH radical.
International Journal of Chemical Kinetics **30** (1998) 471-474.
- [28] R. Atkinson.
A structure-activity relationship for the estimation of rate constants for the gas-phase reaction of OH radicals with organic compounds.
International Journal of Chemical Kinetics **19** (1987) 799-828.
- [29] E. S. C. Kwok and R. Atkinson.
Estimation of hydroxyl radical reaction rate constants for gas-phase organic compounds using a structure-reactivity relationship: an update.
Atmospheric Environment **29** (1995) 1685-1695.
- [30] K. Azad and J. M. Andino.
Products of the gas-phase photooxidation reactions of 1-propanol with OH radicals.
International Journal of Chemical Kinetics **31** (1999) 810-818.
- [31] J. S. Baxley and J. R. Wells.
The hydroxyl radical reaction rate constant and atmospheric transformation products of 2-butanol and 2-pentanol.
International Journal of Chemical Kinetics **30** (1998) 745-752.
- [32] R. Atkinson and S. M. Aschmann.
Alkoxy radical isomerisation products from the gas-phase OH radical-initiated reactions of 2,4-dimethyl-2-pentanol and 3,5-dimethyl-3-hexanol.
Environmental Science and Technology **29** (1995) 528-536.
- [33] Y. Rudich, R. Talukdar, J. B. Burkholder, A. R. Ravishankara.
Reaction of methylbutenol with hydroxyl radical: mechanism and atmospheric implications.
Journal of Physical Chemistry **99** (1995) 12188-12194.
- [34] G. Fantechi, N. R. Jensen, J. Hjorth, J. Peeters.
Mechanistic studies of the atmospheric oxidation of methyl butenol by OH radicals, ozone and NO₃ radicals.
Atmospheric Environment **32** (1998) 3547-3556.

- [35] E. C. Tuazon, S. M. Aschmann, R. Atkinson, W. P. L. Carter.
The reactions of selected acetates with OH radical in the presence of NO: novel rearrangement of alkoxy radical of structure $RC(O)OCH(O)R$.
Journal of Physical Chemistry **102** (1998) 2316-2321.
- [36] L. K. Christensen, J. C. Ball, T. J. Wallington.
Atmospheric oxidation mechanism of methyl acetate.
Journal of Physical Chemistry A **104** (2000) 345-351.
- [37] E. C. Tuazon, S. M. Aschmann, R. Atkinson.
Products of the gas-phase reaction of the OH radical with the dibasic ester $CH_3OC(O)CH_2CH_2CH_2C(O)OCH_3$.
Environmental Science and Technology **33** (1999) 2885-2890.
- [38] S. E. Wyatt, J. S. Baxley, J. R. Wells.
The hydroxyl radical reaction rate constant and products of methyl isobutyrate.
International Journal of Chemical Kinetics **31** (1999) 551-557.
- [39] D. A. Good, J. Hansen, M. Kamoboures, R. Santiono, J. S. Fransisco.
An experimental and computational study of the kinetics and mechanism of the reaction of methyl formate with Cl atoms.
Journal of Physical Chemistry A **104** (2000) 1505-1511.
- [40] E. C. Tuazon, W. P. L. Carter, S. M. Aschmann, R. Atkinson.
Products of the gas-phase reaction of methyl *tert*-butyl ether with OH radical in the presence of NO_x .
International Journal of Chemical Kinetics **23** (1991) 1003-1015.
- [41] D. F. Smith, T. E. Kleinidienst, E. E. Hudgens, C. D. McIver, J. J. Bufalini.
Kinetics and mechanism of the atmospheric oxidation of ethyl *tertiary* butyl ether.
International Journal of Chemical Kinetics **24** (1992) 199-215.
- [42] D. F. Smith, C. D. McIver, T. E. Kleinidienst.
Kinetics and mechanism of the atmospheric oxidation of tertiary amyl methyl ether.
International Journal of Chemical Kinetics **25** (1995) 453-472.
- [43] ALDRICH Katalog/Handbuch Feinchemikalien 1999-2000.
SIGMA-ALDRICH Chemie GmbH, Postfach, D-82039 Deisenhofen, FRG.

- [44] K. H. Becker.
The European Photoreactor EUPHORE.
Final Report of the EC-Project, Contract EV5V-CT92-0059. FB9-Physikalische Chemie,
Bergische Universität Wuppertal, Wuppertal, FRG (1996).
- [45] R. Atkinson.
Kinetics and mechanism of the gas-phase reactions of the hydroxyl radical with organic
compounds under atmospheric conditions.
Chemical Reviews **86** (1986) 69-201.
- [46] I. Barnes, V. Bastian, K. H. Becker, E. H. Fink, F. Zabel.
Reactivity studies of organic substances towards hydroxyl radicals under atmospheric
conditions.
Atmospheric Environment **16** (1982) 545-550.
- [47] R. Atkinson, S. M. Aschmann, W. P. L. Carter, A. M. Winer, J. N. Pitts, Jr.
Alkyl nitrate formation from the NO_x-air photooxidations of C₂-C₈ *n*-alkanes.
Journal of Physical Chemistry **86** (1982) 4563-4569.
- [48] E. C. Tuazon, H. Mac Leod, R. Atkinson, W. L. P. Carter.
 α -Dicarbonyl yields form the NO_x-air photooxidations of a series of aromatic
hydrocarbons in air.
Environmental Science and Technology **20** (1986) 383-387.
- [49] F. Cavalli, I. Barnes, K. H. Becker.
FT-IR kinetic and product study of the OH radical-initiated oxidation of 1-pentanol.
Environmental Science and Technology **34** (2000) 4111-4116.
- [50] F. Cavalli, I. Barnes, K. H. Becker, T. J. Wallington.
Atmospheric oxidation mechanism of methyl propionate.
Journal of Physical Chemistry A, in press (2000).
- [51] A. Notario, G. Le Bras, A. Mellouki.
Absolute rate constants for the reactions of Cl atoms with a series of esters.
Journal of Physical Chemistry A **102** (1998) 3112-3117.
- [52] T. J. Wallington, L. M. Skewes, W. O. Siegl, C. Wu, S. M. Japar.
Gas phase reaction of Cl atoms with a series of oxygenated organic species at 295 K.
International Journal of Chemical Kinetics **20** (1988) 867-875.

- [53] R. Atkinson and W. P. L. Carter.
Kinetics and mechanism of the gas-phase reactions of ozone with organic compounds under atmospheric conditions.
Chemical Review **84**(1984) 437-470.
- [54] J. G. Calvert and J. N. Pitts, Jr.
Photochemistry.
John Wiley and Sons, New York, 1966.
- [55] R. G. Prinn, R. F. Weiss, B. R. Miller, J. Huang, F. N. Alyea, D. M. Cunnold, P. J. Fraser, D. E. Hartley, P. G. Simmonds.
Atmospheric trends and lifetime of CH_3CCl_3 and global OH concentrations.
Science **269** (1995) 187-192.
- [56] J. R. Snider and G. A. Dawson.
Tropospheric light alcohols, carbonyl, and acetonitrile: concentrations in the southwestern United States and Henry's law data.
Journal of Geophysical Research **90D** (1985) 3797-3805.
- [57] C. L. Yaws and H. C. Yang.
Henry's law constant for compounds in water, 181-206.
In *Thermodynamic and Physical Property Data*.
Gulf Publishing Company, Houston, 1992.
- [58] J. Hine and P. K. Mookerjee.
The intrinsic hydrophilic character of organic compounds. Correlations in terms of structural contributions.
Journal of Organic Chemistry **40** (1975) 292-298.
- [59] E. S. C. Kwok, S. M. Aschmann, R. Atkinson.
Rate constants for the gas-phase reactions of the OH radical with selected carbamates and lactates.
Environmental Science and Technology **30** (1996) 329-334.
- [60] S. Langer, E. Ljungstrom, I. Wangberg, T. J. Wallington, M. D. Hurley, O. J. Nielsen.
Atmospheric chemistry of di-*tert*-butyl ether: rates and products of the reactions with chlorine atoms, hydroxyl radicals and nitrate radicals.
International Journal of Chemical Kinetics **28** (1986) 299-306.

- [61] T. J. Wallington, M. D. Hurley, J. C. Ball, M. E. Jenkin.
FTIR product study of the reaction of $\text{CH}_3\text{OCH}_2\text{O}_2 + \text{HO}_2$.
Chemical Physics Letters **211** (1993) 41-47.
- [62] R. Atkinson and S. M. Aschmann.
Kinetic of the gas phase reaction of Cl atoms with a series of organics at 296 ± 2 K and atmospheric pressure.
International Journal of Chemical Kinetics **17** (1985) 33-41.
- [63] R. Atkinson, D. L. Baulch, R. A. Cox, R. F. Hampson, Jr., J. A. Kerr, M. J. Rossi, J. Troe.
Evaluated kinetic and photochemical data for atmospheric chemistry, Organic species. Supplement VII.
Journal of Physical and Chemical Reference Data **28** (1999) 391-393.
- [64] K. Stemmler, W. Mengon, J. A. Kerr
OH radical initiated photooxidation of 2-ethoxyethanol under laboratory conditions related to the troposphere: product studies and proposed mechanism.
Environmental Science and Technology **30** (1996) 3385-3391.
- [65] K. Stemmler, W. Mengon, J. A. Kerr
OH radical initiated photooxidation of 2-butoxyethanol under laboratory conditions related to the troposphere: product studies and proposed mechanism.
Environmental Science and Technology **31** (1997) 1496-1504.
- [66] A. C. Baldwin, J. R. Barker, D. M. Golden, D. G. Hendry.
Photochemical smog. Rate parameter estimates and computer simulations.
Journal of Physical Chemistry **81** (1977) 2483-2492.
- [67] R. Atkinson, E. C. Tuazon, W. P. L. Carter.
Extent of H-atom abstraction from the reaction of the OH radical with 1-butene under atmospheric conditions.
International Journal of Chemical Kinetics **17** (1985) 725-734.
- [68] R. Atkinson, E. C. Tuazon, S. M. Aschmann.
Products of the gas-phase reactions of a series of 1-alkenes and 1-methylcyclohexene with the OH radical in the presence of NO.
Environmental Science and Technology **29** (1995) 1674-1680.

- [69] E. S. C. Kwok, R. Atkinson, J. Arey.
Isomerisation of β -hydroxyalkoxy radicals formed from the OH radical-initiated reactions of C₄-C₈ 1-alkenes.
Environmental Science and Technology **30** (1996) 1048-1052.
- [70] R. Atkinson, D. L. Baulch, R. A. Cox, R. F. Hampson, Jr., J. A. Kerr, M. J. Rossi, J. Troe.
Evaluated kinetic, photochemical, and heterogeneous data for atmospheric chemistry. Supplement V.
Journal of Physical and Chemical Reference Data **26** (1997) 521-1011.
- [71] R. Atkinson, D. L. Baulch, R. A. Cox, R. F. Hampson, Jr., J. A. Kerr, M. J. Rossi, J. Troe.
Evaluated kinetic and photochemical data for atmospheric chemistry. Supplement VI.
Journal of Physical and Chemical Reference Data **26** (1997) 1329-1499.
- [72] R. Atkinson.
Gas-phase tropospheric chemistry of volatile organic compounds: 1. Alkanes and alkenes.
Journal of Physical and Chemical Reference Data **26** (1997) 215-290.
- [73] D. H. Semmes, A. R. Ravishankara, C. A. Gump-Perkins, P. H. Wine.
Kinetics of the reactions of hydroxyl radical with aliphatic aldehydes.
International Journal of Chemical Kinetics **17** (1985) 303-313.
- [74] G. K. Moortgat.
Evaluation of radical sources in atmospheric chemistry through chamber and laboratory studies.
In First Annual Report on the EU-Project, RADICAL, Contract ENV4-CT97-0419. Atmospheric Chemistry Division, Max-Planck-Institut für Chemie, Mainz, Germany (1998).
- [75] R. Atkinson, S. M. Aschmann, W. P. L. Carter, A. M. Winer, J. N. Pitts, Jr.
Alkyl nitrate formation from the NO_x-air photooxidations of C₂-C₈ *n*-alkane.
Journal of Physical Chemistry **86** (1982) 4563-4569.
- [76] R. Atkinson.
Atmospheric reactions of alkoxy and β -hydroxyalkoxy radicals.
International Journal of Chemical Kinetics **29** (1997) 99-111.

- [77] J. J. Orlando, G. S. Tyndall, M. Bilde, C. Ferronato, T. J. Wallington, L. Vereecken, J. Peeters.
Laboratory and theoretical study of the oxy radicals in the OH- and Cl-initiated oxidation of ethene.
Journal of Physical Chemistry A **102** (1998) 8116-8123.
- [78] R. Atkinson and W. P. L. Carter.
Reactions of alkoxy radicals under atmospheric conditions: the relative importance of decomposition versus reaction with O₂.
Journal of Atmospheric Chemistry **13** (1991) 195-210.
- [79] K. Y. Choo and S. W. Benson.
Arrhenius parameters for the alkoxy radical decomposition reactions.
International Journal of Chemical Kinetics **13** (1981) 833-844.
- [80] S. M. Aschmann and R. Atkinson.
Products of the gas-phase reactions of the OH radical with n-butyl methyl ether and 2-isopropoxyethanol: reactions of ROC(O) < radicals.
International Journal of Chemical Kinetics **31** (1999) 501-513.
- [81] H. Somnitz and R. Zellner.
Theoretical studies of unimolecular reactions of C₂-C₅ alkoxy radicals. Part I. *Ab initio* molecular orbital calculations.
Physical Chemistry Chemical Physics **2** (2000) 1899-1905.
- [82] H. Somnitz and R. Zellner.
Theoretical studies of unimolecular reactions of C₂-C₅ alkoxy radicals. Part II. RRKM dynamical calculations.
Physical Chemistry Chemical Physics **2** (2000) 1907-1918.
- [83] H. Hein, A. Hoffmann, R. Zellner.
Direct investigations of reactions of 1-butoxy and 1-pentoxy radicals using laser pulse initiated oxidation: reaction with O₂ and isomerisation at 293 K and 50 mbar.
Physical Chemistry Chemical Physics **1** (1999) 3743-3752.
- [84] R. Atkinson, E. S. C. Kwok, J. Arey, S. M. Aschmann.
Reactions of alkoxy radicals in the atmosphere.
Faraday Discussion **100** (1995) 23-37.

- [85] E. S. C. Kwok, J. Arey, R. Atkinson.
Alkoxy radical isomerisation in the OH radical-initiated reactions of C₄-C₈ *n*-alkanes.
Journal of Physical Chemistry **100** (1996) 214-219.
- [86] D. F. McMillen and D. M. Golden.
Hydrocarbon bond dissociation energies.
Annual Review of Physical Chemistry **33** (1982) 493-532.
- [87] C. Papagni, J. Arey, R. Atkinson.
Rate constants for the gas-phase reactions of a series of C₃-C₆ aldehydes with OH and NO₃ radicals.
International Journal of Chemical Kinetics **32** (2000) 79-84.
- [88] R. Atkinson, S. M. Aschmann, W. P. L. Carter, A. M. Winer, J. N. Pitts, Jr.
Alkyl nitrate formation from the NO_x-air photooxidations of C₂-C₈ *n*-alkane.
Journal of Physical Chemistry **86** (1982) 4563-4569.
- [89] M. H. Baghal-Vayjooee, A. J. Colussi, S. W. Benson.
The very-low-pressure study of the kinetics and equilibrium : Cl + CH₄ → CH₃ + HCl at 298 K. The heat of formation of the CH₃ radical.
International Journal of Chemical Kinetics **11** (1979) 147-154.
- [90] B. J. Finlayson-Pitts and J. N. Pitts, Jr.
Chemistry of the Upper and Lower Atmosphere.
Academic Press, New York, 2000.
- [91] G. P. Brasseur, J. J. Orlando, G. S. Tyndall.
Atmospheric Chemistry and Global Change.
Oxford University Press, Oxford, 1999.
- [92] S. W. Benson.
Thermochemical Kinetics. 2nd Ed.
Wiley, New York, 1976.
- [93] J. G. Calvert, R. Atkinson, J. A. Kerr, S. Madronich, G. K. Moortgat, T. J. Wallington, G. Yarwood.
The Mechanisms of the Atmospheric Oxidation of the Alkenes.
Oxford University Press, Oxford, 2000.

- [94] F. Kirchner, L. P. Thüner, I. Barnes, K. H. Becker, B. Donner, F. Zabel.
Thermal lifetimes of peroxy nitrates occurring in the atmospheric degradation of oxygenated fuel additives.
Environmental Science and Technology **31** (1997) 1801-1804.
- [95] L. K. Christensen, T. J. Wallington, A. Guschin, M. D. Hurley.
Atmospheric degradation mechanism of CF_3OCH_3 .
Journal of Physical Chemistry A **103** (1999) 4202-4208.
- [96] N. Tsalkani and G. Toupance.
Infrared absorptivities and integrated band intensities for gaseous peroxyacetyl nitrate (PAN).
Atmospheric Environmental **23** (1988) 1849-1854.
- [97] R. Atkinson, W. P. L. Carter, A. M. Winer.
Effect of temperature and pressure on alkyl nitrate yields in the NO_x photooxidations of *n*-pentane and *n*-heptane.
Journal of Physical Chemistry **87** (1983) 2012-2018.
- [98] C. T. Pate, B. J. Finlayson, J. N. Pitts, Jr.
A long path infrared spectroscopic study of the reaction of methyl peroxy free radicals with nitric oxide.
Journal of the American Chemical Society **96** (1974) 6554-6558.
- [99] F. Flocke, E. Atlas, S. Madronich, S. M. Schauffler, K. Aikin, J. J. Margitan, T. P. Bui.
Observations of methyl nitrate in the lower stratosphere during STRAT: implications for its gas phase production mechanisms.
Geophysical Research Letters **25** (1998) 1891-1894.
- [100] K. H. Becker, H. Geiger, P. Wiesen.
Kinetic study of the OH radical chain in the reaction system $\text{OH} + \text{C}_2\text{H}_4 + \text{NO} + \text{air}$.
Chemical Physics Letters **184** (1991) 256-261.
- [101] T. J. Wallington, W. F. Schneider, J. Sehested, M. Bilde, O. J. Nielsen, L. K. Christensen, M. J. Molina, L. T. Molina, P. W. Wooldridge.
Atmospheric chemistry of HFE-7100 ($\text{C}_4\text{F}_9\text{OCH}_3$): reaction with OH radicals, UV spectra and kinetic data for $\text{C}_4\text{F}_9\text{OCH}_2\cdot$ and $\text{C}_4\text{F}_9\text{OCH}_2\text{O}_2\cdot$ radicals, and the atmospheric fate of $\text{C}_4\text{F}_9\text{OCH}_2\text{O}\cdot$ radicals.
Journal of Physical Chemistry A **101** (1997) 8264-8274.

- [102] G. S. Tyndall, J. J. Orlando, C. S. Kegly-Owen, T. J. Wallington, M. D. Hurley.
Rate coefficients for the reactions of chlorine atoms with methanol and acetaldehyde.
International Journal of Chemical Kinetics **31** (1999) 776-784.
- [103] T. Maurer.
Troposphärische Oxidation ausgewählter Ethylenglykoldiether und Formaldehydacetale.
Dissertation, Bergische Universität-Gesamthochschule Wuppertal, FB9-Physikalische
Chemie, February 2000.
- [104] D. W. Schiering and J. E. Katon.
The vibrational spectra and structures of dimethyl oxaloacetate and dimethyl
oxaloacetate- d_2^* .
Spectrochimica Acta **42A** (1986) 487-498.
- [105] W. P. L. Carter, D. Luo, I. L. Malkina, S. M. Aschmann, R. Atkinson.
Investigation of the Atmospheric Ozone Formation Potential of Selected Dibasic Esters.
Final Report to the Dibasic Ester Group, SOCMA. University of California, Riverside,
California (1997).
- [106] W. P. Hess and F. P. Tully.
Hydrogen-atom abstraction from methanol by OH.
Journal of Physical Chemistry **93** (1989) 1944-1947.
- [107] J. A. McCaulley, N. Kelly, M. F. Golde, F. Kaufman.
Kinetic studies of the reactions of F and OH with CH_3OH .
Journal of Physical Chemistry **93** (1989) 1014-1018.
- [108] E. Porter, J. C. Wenger, J. Treacy, H. W. Sidebottom, A. Mellouki, S. Téton, G. Le Bras.
Kinetic studies on the reactions of hydroxyl radicals with diethers and hydroxyethers.
Journal of Physical Chemistry A **101** (1997) 5770-5775.
- [109] S. Téton, A. Mellouki, G. Le Bras, H. W. Sidebottom.
Rate constants for reactions of OH radicals with a series of asymmetrical ethers and *tert*-
butyl alcohol.
Journal of Physical Chemistry **28** (1996) 291-297.
- [110] A. Mellouki, S. Teton, G. Le Bras.
Kinetics of OH radical reactions with a series of ethers.
International Journal of Chemical Kinetics **27** (1995) 7919-805.

- [111] J. A. Kerr.
Strengths of chemical bonds, 9-123-9-145.
In Handbook of chemistry and physics.
CRC press, INC, 1995-1996.
- [112] S. Carr, C. E. Canosa-Mas, J. C. Wenger, H. W. Sidebottom, R. P. Wayne, D. E. Shallcross.
A kinetic and mechanistic study of the reaction of OH and Cl with some halogenated acetones and their atmospheric implications.
Journal of Physical Chemistry A. To be published.
- [113] T. J. Wallington and M. J. Kurylo.
Flash photolysis resonance fluorescence investigation of the gas-phase reactions of OH radicals with a series of aliphatic ketones over the temperature range 240-440 K.
Journal of Physical Chemistry **91** (1987) 5050-5054.
- [114] A. J. Haagen-Smit, C. E. Bradley, M. M. Fox.
Ozone formation in photochemical oxidation of organic substances.
Industrial and Engineering Chemistry **45** (1953) 2086-2089.
- [115] UN ECE. Protocol to the 1979 convention on long-range transboundary air pollution concerning the control of emissions of volatile organic compounds or their transboundary fluxes.
ECE/EB.AIR/30. United Nations Economic Commission for Europe, Geneva, Switzerland, 1991.
- [116] F. Zabel.
Unimolecular decomposition of peroxy nitrates.
Zeitschrift für Physikalische Chemie **188** (1995) 119-142.
- [117] S. M. Aschamann, J. Arey, R. Atkinson.
Atmospheric chemistry of selected hydrocarbons.
Journal of Physical Chemistry A **104** (2000) 3998-4003.
- [118] K. Treves, L. Shragina, Y. Rudich.
Henry's law constants of some β -, γ -, and δ -hydroxy alkyl nitrates of atmospheric interest.
Environmental Science and Technology **34** (2000) 1197-1203.

- [119] R. K. Talukdar, J. B. Burkholder, M. Hunter, M. K. Gilles, J. M. Roberts, A. R. Ravishankara.
Atmospheric fate of several alkyl nitrates.
Part 1: rate coefficients of the reactions of the alkyl nitrates with isotopically labelled hydroxyl radicals.
Part 2: UV absorption cross-sections and photodissociation quantum yields.
Journal of Chemical Society, Faraday Discussion **93** (1997) 2787-2805.
- [120] R. G. Derwent, M. E. Jenkin, S. M. Saunders, M. J. Pilling.
Photochemical ozone potentials for organic compounds in Northwest Europe calculated with a master chemical mechanism.
Atmospheric Environment **32** (1998) 2429-2441.
- [121] M. E. Jenkin and G. D. Hayman.
Photochemical ozone creation potentials for oxygenated volatile organic compounds: sensitivity to variations in kinetic and mechanistic parameters.
Atmospheric Environmental **33** (1999) 1275-1293.
- [122] Y. Andersson-Sköld and L. Holmberg.
Photochemical ozone creation potentials (POCP) and replacement of solvents in Europe.
Atmospheric Environmental **34** (2000) 3159-3169.
- [123] W. P. L. Carter and R. Atkinson.
An experimental study of incremental hydrocarbon reactivity.
Environmental Science and Technology **21** (1987) 670-679.
- [124] W. P. L. Carter and R. Atkinson.
An computer modeling study of incremental hydrocarbon reactivity.
Environmental Science and Technology **23** (1989) 864-880.
- [125] W. D. Taylor, T. D. Allston, M. J. Moscato, G. B. Fazekas, R. Kozlowski, G. A. Takacs.
Atmospheric photodissociation lifetimes for nitromethane, methyl nitrite, and methyl nitrate.
International Journal of Chemical Kinetics **12** (1980) 231-240.
- [126] K. Wirtz (CEAM, Spain).
Private communication (1999).

- [127] K. Pihlaja and A. Lampi.
¹³C NMR Chemical shifts – a conformational probe for 1-alkoxyalkyl esters.
Acta Chemica Scandinavica B **40** (1986) 196-199.
- [128] D. P. Weeks and F. H. Field.
Chemical ionization mass spectrometry. XI. Reactions of methoxymethyl formate and methoxymethyl acetate with methane and isobutane.
Journal of the American Chemical Society **92** (1970) 1600-1605.